8-2019

A distinct pattern of sterile inflammation induced by zinc oxide nanowires.

Ruqaih Salem Alghsham
University of Louisville

A DISTINCT PATTERN OF STERILE INFLAMMATION INDUCED BY ZINC

OXIDE NANOWIRES

By

Ruqaih Salem Alghsham

B.S. King Abdul-Aziz University, 2008

M.S. University of Louisville, 2016

A Dissertation Submitted to the Faculty of the School of Medicine of the

University of Louisville

in Partial Fulfillment of the Requirements

for the Degree of

Doctor of Philosophy in Microbiology and Immunology

Department of Microbiology and Immunology

University of Louisville

Louisville, Kentucky

August, 2019

A DISTINCT PATTERN OF STERILE INFLAMMATION INDUCED BY ZINC

OXIDE NANOWIRES

By

Ruqaih Salem Alghsham

B.S. King Abdul-Aziz University, 2008

M.S. University of Louisville, 2016

A Dissertation Approved on:

August 2, 2019

by the following Dissertation Committee:

_____

Dr. Haribabu Bodduluri (Chair)

_____

Dr. Pascale Alard

_____

Dr. Venkatakrishna Rao Jala

_____

Dr. Russell D. Salter

_____

Dr. Mahendra Sunkara

DEDICATION

I dedicate this dissertation to the memory of a very special person that left us too

soon, my mother, Lulwa Aldawway. I will always love you and remember you.

You are deeply missed!

ACKNOWLEDGEMENTS

you did to help me start and finish my PhD. Thanks for giving up your work and career for me. Thanks for all your sacrifice and your efforts to make us happy and comfortable. Thanks for taking care of me and our lovely daughters. Your tremendous, sustained support made possible my success in this graduate program.

ABSTRACT

A DISTINCT PATTERN OF STERILE INFLAMMATION INDUCED BY ZINC OXIDE NANOWIRES

Ruqaih Salem Alghsham

August 2, 2019

In recent years, there has been an increasing interest in nanotechnology. Engineered nanomaterials (ENMs) become an increasingly important area in nanotechnology. Recent developments in ENMs have drawn commercial and research attention in many areas such as agriculture, medicine, and Industry. High-aspect ratio zinc oxide nanowires (ZnONWs) have become one of the most significant ENMs due to their remarkable physical properties which makes them useful in a wide-range of applications. However, questions have been raised about ZnONW safety uses and biological consequences.

In this dissertation, we investigated the inflammatory potential of ZnONWs in mouse models. C57BL/6 mice were exposed to ZnONW via intra-tracheal route. Two days post-instillation, the broncho-alveolar lavage fluid (BALF) was analyzed for inflammatory cells and for presence of pro-inflammatory cytokines.

We found that the intratracheal instillation of ZnONW in C57BL/6 mice induced a significant increase in the total numbers of immune cells in BALFs two days after instillation. Macrophages and eosinophils were the predominant cellular infiltrates of ZnONW-exposed mouse lungs. In an air-pouch mouse model that simulates local exposure to ZnONW, similar cellular infiltrates were observed. Analysis of lavage fluids revealed that pro-inflammatory cytokines IL-6 and TNF-α as well as chemokines CCL11 and CCL2 were increased both in BALFs and air-pouch lavage fluids. The cellular basis of inflammatory mediators that were induced by ZnONW were investigated in cultured cells. ZnONW exposure induced both IL-6 and TNF-α production only in macrophages but not in lung epithelial cells (LKR13). Exposure of macrophages to ZnONW induced the production of CCL11 only while LKR13 cells induced both CCL11 and CCL2. Confocal microscopy showed rapid phagocytic uptake of FITC-ZnONW aggregates by macrophages. The phagocytosis of ZnONW particles is essential for the production of both IL-6 and TNF-α. These results suggest that exposure to ZnONW may induce distinct inflammatory mediators through phagocytic uptake.

TABLE OF CONTENTS

LIST OF TABLE

LIST OF FIGURES

CHAPTER 1

INTRODUCTION

Engineered nanomaterials (ENMs)

Material with a one or more dimensional shape in the size range from 1 to 100 nanometers (nm) are referred to as nanomaterials [1, 2]. There are two types of nanomaterials: naturally occurring nanoparticles, which are also referred to as ultrafine nanoparticles, and engineered nanoparticles (ENPs). The naturally occurring nanoparticles include volcanic ash soot from forest fires or diesel engines [3-6]. These naturally occurring nanomaterials are usually physically and chemically heterogeneous [7]. On the other hand, engineered nano-materials (ENMs) are created by the manipulation of matter at the nano-scale to produce new materials and structures [8, 9]. A myriad of new ENMs are being rapidly developed and introduced into many different sectors, such as commerce, agriculture, and medicine [10-12].

ENMs are designed with very specific properties related to chemistry, shape, size, and surface area. Their novel physicochemical properties facilitate wide-range of applications in consumer products, such as food additives, batteries, cosmetics, drug delivery system, and sunscreens [12]. ENMs are being produced in large-scale quantities, thereby posing unknown environmental, human, and occupational exposure hazards. The tiny size and light weight of these ENMs make control, such as filtration or dampening, difficult.

Types of engineered nanomaterials

There are different types of ENMs exist; however, for the purpose of this dissertation, the focus is on two types of ENMs: metal-based ENMs and carbon-based ENMs. Metal-based ENMs are defined by particles that are made of metal precursors while carbon-based ENMs contain predominantly carbon atoms that are arranged in a unique way.

Commonly used ENMs

❖ **Metal-based ENMs**

- Silicon dioxide nanoparticles (SiONP): SiONP is the main component for the manufacturing of several consumer products, such as glass, paints, plastics, cosmetics, food additives, and rubber [13, 14].

- Titanium oxide nanoparticles (TiONP): TiONP has applications in the manufacturing of cosmetics, food, and sunscreen products. The unique properties and the size of TiONPs allow them to form a protective layer on the skin without being completely absorbed [13].

- Zinc oxide nanoparticles (ZnONP): With the significant advancement in the alternative energy market, ZnONP has become one of the leading metal oxide ENMs used in electronics, optical devices. ZnONP is also used in battery storage due to its photocatalytic activity [15].

- Aluminum oxide nanoparticles (AlONP): AlONP is commonly used in making cement, paints, and aircrafts.

  ❖ **Carbon-based ENMs**

- Graphene: Graphene is a nanomaterial composed of an allotropic, two-dimensional hexagonal structure of carbon atoms, which was first described in the 1970s; however, nano-scale graphene was introduced in 2004 with different structures, such as single layers, nanotubes, and fibers. Recently, graphene has become a promising nanomaterial for many bio-technological applications, in the field of environmental engineering and biomedicine [16].

- Single or multi-walled carbon nanotubes (CNTs): CNTs are derived from graphene, which is considered one of the oldest and most widely used natural nanomaterial. CNTs are used in many applications, such as biomedical and electronic devices [17, 18].

ENMs market dynamics

In 2015, the global market for nanotechnology was predicted to grow and to employ up to two million workers [19]. By 2022, the anticipated benefits from

the ENMs market will be $55 Billion (Fig1) [20]. The US and Japan have over a half of the world's demand for ENMs. The U.S. leads the global market and the recent developments in the field of ENMs by 46%, especially in the global health sector [20]. Hence, in the U.S. alone, 800,000 workers face a high probability for occupational exposure hazards to ENMs [21]. According to Nanowerk, there are more than 1,000 consumer products containing ENMs. Approximately 2,500 commercial ENMs are used, that including 27% metal oxide nanoparticles, such as ZnONP and SiONP [.http://www.nanowerk.com/ phpscripts/ndbsearch.php]. The growing production of ENMs has raised concerns related to their potential effects on the environment and biological health. In addition, ENMs are synthesized in and with varying shapes, sizes, coatings, surface charges, and surface areas, which makes both biological and environmental potential hazards unpredictable. Hence, the biological and environmental impacts of ENMs must be determined.

Dynamics of the global nanomaterials demand by regions bases is listed below from the highest to the lower demand

• North America includes the U.S., Canada, and Mexico.

• Europe includes the UK, Germany, France, and Italy.

• The Asian Pacific region includes China, India, and Japan.

• Central and South America (Brazil).

• The Middle East includes Saudi Arabia and Turkey.
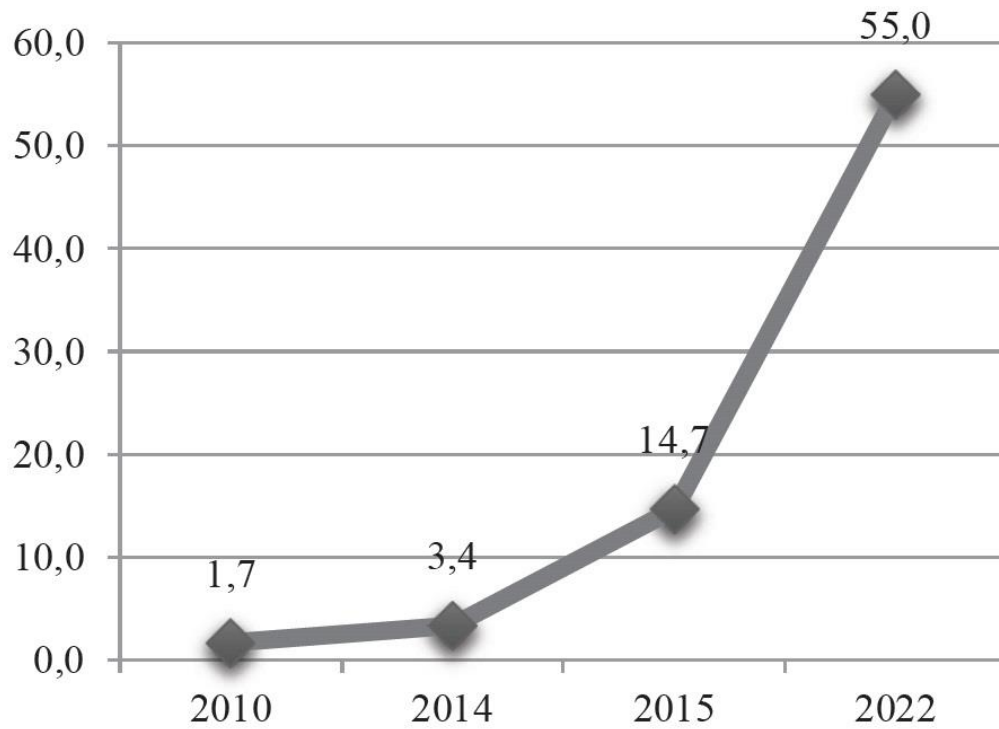
Figure 1: The ENMs market growth from the base year 2010 to 2022 in terms of revenue (USD billion) [20].

The environmental and biological impacts of ENMs

In the past two decades, nano-toxicology has become a highly important field in science due to an increase in the utilization of ENMs. This has increased the need for studying the potential side effects of ENMs in biological and ecological systems, which will ultimately contribute to understanding and generating rules and safety measurements when using and synthesizing ENMs. In this section, the implications of ENMs for environmental and biological systems are discussed.

The environmental impacts

Without doubt, the volume of ENMs released into the environment will increase due to the widespread use of products containing ENMs either during manufacture, transport, use, or disposal [22]. Consequently, the entire environmental compartment will be affected. The eco-toxicological effects of ENMs are not well-defined and require further investigation [23] for several reasons. First, the current data on the actual volume release of ENMs and the accumulated concentration into the environment are poorly understood and limited [24-26]. This is because the lack of data on the production volumes of ENMs creates a fundamental obstacle to future investigations into their release [27, 28]. Another challenge is that different ENMs accumulate at different sizes and rates in the environment depending on the variable abiotic factors in the environment (pH soil, ionic composition, and soil texture), which leads to differences in eco-toxicological outcomes. Furthermore, there is a lack of suitable tools, analytical approaches, and methods to study the environmental impact of

ENMs. Another important question that needs to be addressed is what is the fate of the end-of-life product of ENMs and their proper safe disposal methods? Therefore, there is a compelling need to study and to investigate the actual release and distributions of ENMs in the environment to better understand their impacts [29-32]. Previous studies have shown that soluble metal oxide ENMs, such as TiO_2 and ZnO, might accumulate in environmental components (soils, soil's organisms, and freshwater) as particulates in concentrations that exceed the sub-toxic levels [27, 33-35]. Furthermore, some metal oxide materials, such as TiO_2 and ZnO, which are essential elements in many consumer products, have antimicrobial properties that may pose a direct or indirect impact, triggering alterations in the ecosystem, including fish, bacteria, and plants [36]. Table 1 presents the environmental concentrations of some ENMs in three main pathways into the environment.

ENMs	Surface water	WWTP Sludge	WWTP Waste and Sewage
ZnONP	1−10 000 ng/L	13.6−64.7 mg/kg,	0.22−1.42 µg/L,
TiONP	21−10 000 ng/L	100−2000 mg/kg	1−100 µg/L
CNP	0.001−0.8 ng/L	0.0093−0.147 mg/kg	3.69−32.66 ng/L
AgNP	0.088−10 000 ng/L	1.29−39 mg/kg	0.0164−17 µg/L

Table 1: Predicted environmental concentrations of highly used ENMs in three main pathways into the environment (modified and reproduced from Ref [37]).

The biological impacts

The potential consequences of ENMs on biological systems strongly depend on the physical and chemical properties as well as the route of exposure [38]. Several studies have reported the toxicity of ENMs in both *in vitro* and *in vivo* experimental models [39-52]; however, the biological effects of many of the ENMs are not well-defined. The small sizes of ENMs allow them to infiltrate epithelial barriers, causing their accumulation and deposition into vital organs and tissues, including the kidneys, heart, and liver [53-57]. In addition, some forms of ENMs may cross blood-brain barriers, leading to brain damage and neurological side effects [55]. Furthermore, studies have shown that exposure to ENMs via several routes, such as inhalation, ingestion, or dermal contact, could lead to a variety of disorders, such as myocardial infarction, stroke, thrombosis caused by platelet enhanced aggregation by ENMs [58-60], and lung injury or inflammation [61, 62]. Moreover, at the cellular level, ENMs may induce cell death, mitochondrial damages, and genotoxicity (DNA damage and mutation) [53, 63, 64]. The leakage of ENMs ions from their core may elicit biological consequences, especially if the metal ion released has biological and physiological functions. Earlier studies have suggested that the production of reactive oxygen species (ROS) and free radicals are the underlying mechanisms of ENMs cytotoxicity. Cell death and cell damage could result from ROS or ENMs' physical damage of cell membranes. In addition to oxidative stress, inflammation, DNA damage, and apoptosis have also been suggested to be mechanisms of ENMs toxicity [65-71]. Other proposed mechanisms in which

ENMs induce toxicity have been suggested, such as the disruption of intracellular transport and cell division, a disturbance in DNA transcription, mitochondrial damage and dysfunction, and lysosomal destabilization, leading to autophagy and cell death [72]. Moreover, genotoxicity is one of the biological side effects of ENMs exposure, and ENMs genotoxicity is defined by the damage of the intracellular DNA that could result from direct ENM interactions with DNA or indirect interactions via ROS production after ENM exposure; however, long-term secondary adverse effects, such as chronic respiratory distress syndrome, of ENMs are overlooked and require further investigation.

OSHA's exposure limit recommendations

• Respirable carbon nanotubes and carbon nanofibers should not exceed 1.0 (µg/m3) as an eight-hour time-weighted average (TWA).

• TiONPs (particle size less than 100 nm) should not exceed 0.3 (mg/m3).

• TiONPs (particle size greater than 100 nm) should be 2.4 mg/m3.

OSHA's permissible exposure limits to zinc oxide fumes

• 5 mg/m3 (TWA).

• 10 mg/m3 short-term exposure limit (STEL).

Exposure limits for other nanomaterials do not exist yet.
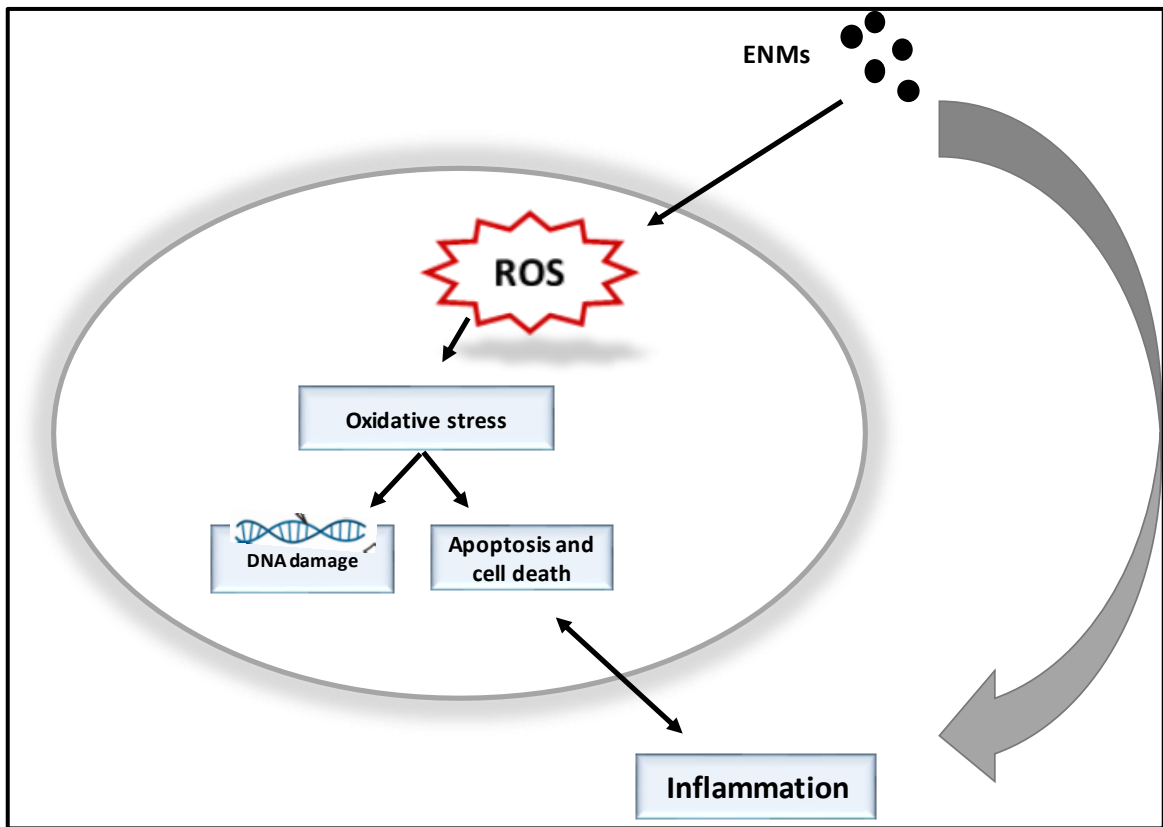
Figure 2: The schematic model illustrates the mechanisms in which ENM induces cytotoxicity: ENMs induce ROS generation, which leads to oxidative stress. Oxidative stress could either be induced cell death or DNA damage that could lead to an inflammatory response. ENMs could also prompt inflammation through damage-associated molecular patterns (DAMP).

Factors influence ENMs toxicity

The physicochemical properties of ENMs, including dissolution, size, shape, chemical composition, surface area, and charge, influence the biological-interaction of ENMs. Thus, for a complete understanding of the biological impacts of ENMs, it is important to evaluate the physicochemical properties of ENMs and to understand the interaction between these properties to determine the toxic potential of ENMs in the biological system. There are underlying factors that contribute to ENMs toxicity: size, shape, surface area, charge, and chemical composition.

Size

Size is an important factor that determines the effective interaction mechanism between ENMs and biological systems, especially the immune system. It has been suggested that the smaller the particles, the more toxic they are [73]. ENMs with a size less than 20 nm can easily traverse through epithelium and endothelium barriers and enter cells. The small size of ENMs, which is similar to the size of spheroproteins (2-10 nm), not only enable their translocation through cellular membranes but also allows them to enter the nuclei and other cell organelles [74]. According to Huo et al., six nm gold NPs were found in the nucleus, while 16 nm gold NPs were only found in the cytoplasm [75]. Furthermore, size controls the recognition, uptake, and clearance of ENMs by immune cells, such as macrophages. ENMs with a size less than five nm enter the cell membrane via nonspecific transport mechanisms, whereas 10 to 25 nm

ENMs are taken up by immune cells through pinocytosis. Larger particles are believed to be prime for the phagocytosis mechanisms, such as micropinocytosis [76, 77]. Due to the small size, ENMs of 5-10 nm will be not cleared effectively by immune cells, which leads to the accumulation and translocation of ENMs in vital organs [78-80]. Aggregation and agglomeration also contribute to the size and toxicity of ENMs. Once ENMs interact with biological media, they can aggregate or agglomerate[1], which can influence the particle size and can lead to different biological effects.

Shape

ENMs have different shapes, such as spheres, sheets, cubes, rods, and ellipsoids. The shape as well as the aspect ratio are the two essential elements that influence the toxicity of ENMs. Several studies have investigated shape-dependent toxicity [81-84]. According to Holian et al., the clearance of TiONPs, either spherical or nano-belts, was affected by particle shape after pulmonary lung exposure in mice. TiONP spheres were cleared more effectively than TiONP nano-belts [85]. Moreover, rod-like or needle-like ENMs induced more cell death and damage compared to spherical ENMs [86]. Overall, shape controls the uptake and clearance of ENMs by phagocytes and could lead to cell death and damage.

---

[1]*Aggregation is different from agglomeration: aggregation cannot be reversible under any certain conditions, while in agglomeration, under some chemical/biological conditions, the release of the actual primary individual particles is possible [21].*

Surface area and charge

ENMs are characterized by a large surface area, which provide them with a high reaction capacity and a high catalytic activity compared to micro-particle of the same material. Because the first interactions between ENMs and biological systems begin at the surface of the ENMs, the surface area plays a role in toxicity. The smaller the size, the more surface area they have and the higher toxicity [73]. The surface charge significantly contributes to the toxicity of ENMs [87, 88]. Surface charges affects the interaction and translocation of ENMs. Positively charged ENMs were found to be more toxic than negative or neutral ENMs [89]. The electrostatic attraction between the negative charges of the cell membrane (glycoprotein) and the positive charge of ENMs allows them to enter the cell easily compared to neutral or negatively charged ENMs [90]. Moreover, positively charged ENMs adsorb protein more efficiently than those with a negative charge. The adsorption with serum protein and other proteins allows ENMs to form a protein corona. This formation has a direct effect on the uptake and recognition of ENMs by immune cells [91].

Chemical composition

Particle chemistry is a crucial aspect of cell molecular mechanisms and oxidative stress. The chemical stability of ENMs is affected by the environmental conditions inside the cells, e.g., the pH level. Therefore, chemical composition is another factor that affects ENMs toxicity. Some

ENMs, such as ZnONP, is known to have a high dissolution rate with a low pH [92]. Although Zn and other metal ions have biological benefits for the cell, studies have shown that ZnONP induces toxicity and cell death due to the dissolution of ZnONP inside the acidic vacuoles of cells, leading to an increase in the Zn ions inside the cells [92]. The type of metal also contributes to the toxicity and has different toxic effects. A comparison study was performed to study the toxicity effect of SiONPs and ZnONP. SiONP induce toxicity by altering the DNA structure of the cells, whereas toxicity induced by ZnONP is caused by the production of ROS and oxidative stress [93], indicating that particle chemical composition played a primary role in the cytotoxic function.

In summary, shape, size, chemical composition, surface charge, and area are major factors that determine and influence the toxicity of ENMs; however, other factors must be investigated, such as coating and surface roughness.

Sterile inflammation

The immune system plays a vital role in host defense against intrusion, including by pathogens, through the process of inflammation. For microbial infections, an inflammatory cascade promotes the recruitment and activation of innate immune cells, such as macrophages and neutrophils [94]. These cells have a role-clearing microbe though phagocytosis and the production of pro-inflammatory cytokines and chemokines to activate an adaptive immune response. Inflammation can also be triggered in response to non-microbial agents. This type of inflammation is known as sterile inflammation, which is an inflammation triggered by pathogen-free agents, such as physical, chemical, or metabolic insults, including environmental particles, such as asbestos and silicon dioxide crystals [94, 95]. Sterile inflammation is considered one of the underlying factors that lead to many inflammatory diseases. ENMs, such as metal-oxide and carbon-based nanoparticles, may initiate sterile inflammation [96]. Similar to pathogen-induced inflammation, ENMs may prompt sterile inflammation and may induce the recruitment of inflammatory cells, such as macrophages and neutrophils, and the production of pro-inflammatory cytokines because they can function as danger signals (DAMP) [96]. The inflammation cascade may be induced by damage-associated molecular patterns (DAMP) [97]; Previous studies reported that ENMs promote the secretion of chromatin associates protein high-mobility group box-1 (HMGB-1) which considered as highly active danger signal that initiate inflammatory cascade [98]. However, the process of

inflammation induced by ENMs is not fully understood, and the possible biological consequences of ENMs-induced sterile inflammation requires further investigation [96]. Table 2 provides a list of *in vitro* studies that investigated the signaling pathway of sterile nanoparticles-induced sterile inflammation. [96, 99-103].

Type of nanomaterial	Cell type	Signaling pathways	Biological effect
MWCNT	A549 lung epithelial cells	NLRP-3 inflammasome activation	Activation of the inflammasome –caspase-1 related pathway leading to IL-β and IL-18 release
TiO2-NP	Human intestinal epithelial cells, human epithelial, colorectal adenocarcinoma Caco-2 cells, and THP-1macrophages	NLRP-3 inflammasome activation	Exposure to TiO2-NPs induces NLRP-3-ASC-caspase-1 assembly and caspase-1cleavage; The activation of NLRP-3 complex causes the release of functionally active IL-1β.
SiONP	Murine bone marrow-derived dendritic cells, murine bone marrow derived macrophages, human macrophage cell lineTHP1, and primary human keratinocytes	NLRP-3 inflammasome activation	Induced caspase-1 cleavage and IL-1β secretion via the NLRP-3 inflammasome
ZnO-NP	Macrophages and A549 cells	NF-kB; NLRP-3 inflammasome activation	Activation of the inflammasome – caspase-1 related pathway leading to IL-β and IL-18 release.

Table 2: In vitro studies that investigated the signaling pathway of sterile nano-particles induced inflammation.

Zinc oxide nanoparticle (ZnONP)

ZnONP applications

Zinc oxide nanoparticles (ZnONP) have become one of the most important and promising metal oxide nanoparticles that are commonly used in many different areas due to their unique physical and chemical properties [104, 105]. ZnONP have been used in many industrial products. In 2015, worldwide production was estimated to be about one million tons per year. The rubber industry was the first known to use ZnONP based on their waterproof function and enhancement of the performance of high polymers in rubber [106, 107]. Later, due to ZnONP' UV absorption properties, they were used in many personal consumer products, such as cosmetics and sunscreen [108]. Moreover, ZnO has an antimicrobial activity, and thus ZnONP is commonly used as food additives as well as in the textile industry and for deodorants and antibacterial products [109]. ZnONP has a promising application in the field of electro, opto, and photo technology, electronic/electrical devices, and batteries [110-112]. Apart from these applications, ZnONP have attracted considerable attention in the medical field and are used in drug delivery systems and anticancer treatments, and they have the potential to enhance other drugs' activities, such as insulin [110, 113, 114]. The tremendous increase in production and the use of ZnONP poses a large risk of exposure to both the public and workers, who could be exposed through different routes, such as ingestion, inhalation, or skin contact [21]; however, the biological effect of ZnONP remains controversial in recent studies. Previous studies have shown that ZnONP has anti-inflammatory

properties due to the suppression of the mRNA expression of many inflammatory cytokines, such as IL-1β and TNF-α [115-121]. Moreover, the U.S. Food and Drug Administration (FDA) categorized the use of ZnO in micron sizes as safe, "GRAS" (generally recognized as safe), for use as food additives but not ZnONP. On the other hand, many other studies have suggested that ZnONP indeed exhibit inflammatory potential both *in vivo* and *in vitro*.

Potential exposure hazards and side effects of ZnONP

It has been known for some time that metal fume fever syndrome is caused by the inhalation of ZnO fumes among foundry workers [122-125]. Exposure to ZnONP may also lead to health complication. Consequently, there is a need for an evaluation of the health consequences of ZnONP exposure. ZnONP could be recognized by the immune system as danger signals. Consequently, inflammatory responses to ZnONP could lead to a wide range of disorders. Several studies have demonstrated that ZnONP have the ability to induce toxicity both *in vivo* and *in vitro*.

In vitro toxicity of ZnONP

Extensive studies have investigated the toxicity effect of ZnONP in different cell lines.

Production of reactive oxygen species (ROS)

ROS is formed as a result of mitochondrial oxidative metabolism and cellular responses to bacterial infections. It is composed of different oxidative species, which include superoxide anion, hydrogen peroxide,

20

singlet oxygen, and hydroxyl radicals. ROS is known for its regulatory role in cell signaling and homeostasis [126]. There are two types of sources that induce ROS formation within the cells: endogenous and exogenous. Mitochondrial respiration and inflammatory responses are some of endogenous sources for ROS generation, while bacterial invasion, pollution, and ENMs act as exogenous sources. Several studies have shown that ZnONP induce a substantial increase in the ROS level *in vitro* after ZnONP exposure [127-131]. Thus, ROS production leads to oxidative stress and mitochondrial damage [132].

Oxidative stress

Upon ZnONP exposure, the intracellular levels of ROS increases. This triggers the enzymatic and non-enzymatic antioxidant system in cells. When the antioxidant system in the cell is exhausted, the cells fail to reduce the intracellular ROS level, leading to ROS accumulation and a disturbance in the cellular homeostasis. As a result, oxidative stress occurs. Oxidative stress contributes to cell damage, mitochondrial damage, and autophagy [132-137].

Another cellular response to ZnONP is the production of pro-inflammatory cytokines. The interaction of ENMs with cell surface receptors leads to the activation of intracellular signaling pathways. According to Roy et al., Toll-like receptor 6 (TLR6) mediates the inflammatory responses of ZnONP in peritoneal macrophages [138]. The production of pro-inflammatory cytokines, such as IL-8 and TNF-α, is

mediated through the activation and upregulation of inflammatory pathways, including nuclear factor kappa-light-chain enhancer of activated Bcells (NF-κβ), mitogen-activated protein kinase (MAPK), and other pathways involved in Myeloid differentiation primary response 88 (myD88) [139-141].

Genotoxicity

Genotoxicity is a potential biological response to ZnONP exposure. It has been shown that high doses of ZnONP leads to cellular toxicity and cell death; however, the effect of a low dose of ZnONP exposure has been overlooked. Low doses of ZnONP could lead to genetic alterations, causing DNA damage [142-145]. According to Heim et al., ZnONP induces a DNA double strand break [146]. These genetic alterations could lead to mutations and carcinogenesis. The genotoxicity of ZnONP was investigated in kidney epithelial cells and other cell types [147]. ZnONP induces DNA damage due to an increase in ROS generation, which results from an increase in intracellular Zn^{2+} ion concentrations. ZnONP also induces dysregulation in cardiac functions and vascular homeostasis. Intra-tracheal instillation of ZnONP to Wistar rats induced systemic inflammation, dyslipidemia, increase levels of serum biomarkers of atheroslcerogenesis (heme oxygenase-1 [HO-1] and platelet endothelial cell adhesion molecules-1 ,and aortic pathological damage [148].

The underlying factor that leads to ZnONP toxicity is the solubility of ZnONP in the acidic vacuole of the cells, such as phagolysosome. This leads to

an increase in the intracellular Zn^{2+} ions concentration [149-152]. The Zn2+ ion is an essential element in many biological reactions. It is important for enzyme activity and many nuclear proteins, such as zinc finger nucleases [113].

In vivo ZnONP toxicity

Several studies have investigated the toxicological effect of ZnONP *in vivo* [153-156]. The intra-tracheal instillation of ZnONP in mice induced acute lung inflammation and lung injury with a significant increase in the LDH level detected in bronchial alveolar lavage fluids (BALF) [157, 158]. Moreover, ZnONP induced the recruitment of macrophages and neutrophils with high levels of pro-inflammatory cytokines, such as IL-6 in BALF, after pulmonary exposure in mice [159-161]. Furthermore, ZnONP appears to have an adjuvant-like response to allergen ovalbumin (OVA) and induce Th2 responses in mice [154]. Oral exposure to ZnONP in rats for five days revealed significant hepatic damage and severe nephrotoxicity [162, 163]. According to Attia et al., neurotoxicity in rats was observed after oral exposure to ZnONP resulting in oxidative stress and genotoxicity, inflammation, and apoptosis [133]. In addition, a study conducted with human volunteers showed that the inhalation of ZnONP induces flu-like symptoms and a significant increase in serum amyloid A (SAA), and two acute phase proteins C-reactive protein (CRP) [164]. It has been suggested that the toxicity of ZnONP *in vivo* is similar to the *in vitro* finding of the solubility of ZnONP in the acidic pH of cell vacuoles [165]; however, a study conducted by Xia et al. showed that dietary ZnONP improved intestinal microbiota and inflammation responses in weaned piglets [166].

23

ZnONP and the innate immune cells

The innate immune system (nonspecific) is the first line of defense against foreign insults, including ENMs. The interaction of ENMs with innate immune cells may induce an immunomodulatory response either by the activation or the suppression of the innate immune system (Fig3) [98, 167]. The key mechanism of the innate immune system is the process of phagocytosis. Phagocytic cells, such as macrophages, and other phagocyte cells mediate the phagocytosis process through pattern recognition receptors (PRPs) on phagocytic cells, (e.g. toll-like receptors (TLR)), that recognize a wide variety of pathogens' molecular patterns referred to as pathogen-associated molecular patterns (PAMPs) such as lipopolysaccharides (LPS) on the bacterial cell wall [168]. Similarly, macrophages could recognize ENMs. ENMs may interfere with It has been suggested that ENMs may serve as DAMP signals that could induce innate immune reactions [96].Several studies have shown that ZnONP induces the activation and recruitment of innate immune cells upon exposure either *in vitro* or *in vivo* correspondingly.

Macrophages and ZnONP

Macrophages are the first responders to danger signals. They are professional phagocytic cells that mediate recognition and phagocytosis via different reporters, including scavenger receptors (SR), mannose receptors (MR), and complement receptors (CR) [169]. Furthermore, receptors on macrophage such as TLRs play a vital role in the early recognition of ZnONP and subsequently induce a pro-inflammatory response [141, 170]. According to Roy

24

et al., the inflammatory responses of activated macrophages triggered by ZnONP depend on TLR6, which induces the expression of genes involved in inflammation. Briefly, ZnONP promoted the expression of CD1d, MHC-II, CD86, and CD71, which are activation and maturation markers, on macrophages as well as the production of pro-inflammatory cytokines, such as IL-6, IL-1β, and TNF-α. The production of these pro-inflammatory cytokines was suppressed after inhibiting MAPKs pathways and TLR6 signaling using siRNA [138]. Moreover, the downstream signaling of TLRs mediates the activation of many inflammatory pathways, such as MAPK, ERK1/2, JNK, p38, and NF-κB. The activation of these pathways leads to the production of pro-inflammatory cytokines and chemokines by the recruitment of a specific set of adaptor molecules, such as MyD88 and TRIF [171]. It has been suggested that ZnONP induces inflammatory responses through the activation of MyD88, NF-κB, and MAPK [139]. Furthermore, the activation of TLR signaling not only induces inflammation and the production of pro-inflammatory cytokines but also increases the phagocytosis process by macrophages such as TLR6 [169].

Macrophages have the ability to infiltrate tissues during inflammation [172]. Alveolar macrophages play a major role in the onset and progression of pulmonary diseases, such as asthma, chronic obstructive pulmonary disease (COPD), and pulmonary fibrosis [173]. Because inhalation is the common exposure route of ZnONP, alveolar macrophages are one of the first cells to come in contact with ZnONP in the lungs [159, 174]. The interaction between these cells and ZnONP is not well-understood. Some researchers have proposed

that the interaction between alveolar macrophages and ZnONP is mediated by non-specific binding, and some believe that it is mediated via scavenger receptors, such as the B1 scavenger receptor [134]. Moreover, ZnONP inhalation in mice infected with *Haemophilus influenza* (NTHi) reduced the bacterial clearance in BALF and in lung tissues by impairing alveolar macrophage activation [175].

Lung epithelial cells and ZnONP

Lung epithelial cells play an important role in immune responses upon ZnONP exposure. *In vitro*, ZnONP exhibited the highest toxicity to lung epithelial cells compared to other ENMs, such as TiO2, CeO2, and Al$_2$O$_3$NP [176]. The toxicity was linked to oxidative stress and DNA damage after ZnONP exposure [177, 178]. According to Wu et al., ZnONP induced IL-8 expression in bronchial epithelial cells through the phosphorylation of the proteins p65 and IkB-α, which are both part of the NF-κB signaling pathway [140]. A previous study showed that challenged mice with ZnONP after ovalbumin (OVA) administration, lead to induce Th2 responses in the lungs. These results indicated that ZnONP could act as adjuvants to OVA, [179].

Eosinophils

Eosinophils were first discovered in 1879 by Paul Ehrlich. Eosinophils account for around 3% of the leukocyte sub-population in human circulation with a half-life ranging from 8-18 hours, while in the tissues, the half-life could extend up to six days [180]. Eosinophils are characterized by a distinctive dark pink intracellular granule in standard hematoxylin and eosin (H&E) staining.

Eosinophils' granules contain hydrolytic enzymes, such as the major basic protein (MBP), eosinophil peroxidase (EPO), eosinophil-derived neurotoxin (EDN), and cationic granule proteins [181]. Moreover, it has been acknowledged that eosinophilic granules not only contain hydrolytic enzymes but also contain various cytokines and chemokines. These pre-made cytokines and chemokines have many diverse biological functions and are available for rapid release upon stimulation [182-184]. Initially, it was believed that eosinophils only play a major role in controlling parasitic infections (helminth) and are involved in allergy diseases, such as asthma [185-188]. Later, eosinophils' functions were found to be involved in many physiological processes, such as organ development [189, 190], tissue repair and degradation [191-193], maintaining and recruiting lymphocytes [194-196], anti-microbial activity [197-199], fungal immunity [200, 201], and tumor immunity [202].

Previous studies have suggested that ZnONP may promote eosinophilic airway inflammation in rodents. In OVA, challenged mice models, ZnONP exposure was found to increase the eosinophilic inflammation in the broncho alveolar lavage fluid (BALF) at seven days after oropharyngeal aspiration [154]. In another study, the intra-tracheal instillation of ZnONP induced the recruitment of eosinophils in the alveolar interstitium in C57BL/6 mice [153]. In contrast, according to Silva et al., ZnONP provides anti-apoptotic properties to human eosinophils by preventing caspase activation and Bcl-xL degradation, leading to delayed human eosinophils apoptosis [203]. In addition, ZnONP did not induce the production of ROS in human eosinophils [203].

Cellular mediators induced by ZnONP (cytokines and chemokines)

Interlukins-6 (IL-6) and Tumor necrosis factor alpha (TNF-α)

For most acute inflammatory conditions, both IL-6 and TNF-α are elevated. IL-6 induces fever reactions, while TNF-α promotes hypertension through endothelia cell activation [204]. Furthermore, IL-6 and TNF-α activate immune cells and are involved in the progression of many inflammatory diseases, such as rheumatoid arthritis [205]. IL-6 is a cytokine involved in many physiological processes, such as inflammation, infection, and regulation of metabolic, regenerative, and neural processes [206]. TNF-α is a pleotropic cytokine with diverse biological functions, including acute and chronic inflammation and the regulation of cell growth and proliferation [207]. As mentioned above, ZnONP induce toxicity in the cells via oxidative stress. The overwhelming oxidative stress response by the cells promotes the activation of several signaling pathways, such as MAPK and NF-κB, triggering cell signaling cascades that lead to an increase in cytokine expression, such as interleukins and TNF-α [208]. Several studies showed that ZnONP exposure induces the production of IL-6 and TNF-α both *in vivo* and *in vitro* [123, 138, 178, 209, 210]. Once ZnONP are engulfed by macrophages or exposed to epithelial cells, a variety of pro-inflammatory cytokines, such as IL-6 and TNF-α, and chemokines, such as CCL2, CCL3, CXCL1, and CCL11, are secreted; however, the exact sequence of the events that occur in these cells that result in the production of these cytokines/chemokines is not defined.

Monocyte chemoattractant protein 1

Monocyte chemoattractant protein 1(MCP-1), also known as CCL2, is a potent macrophage chemoattractant involved in the polarization and recruitment of murine macrophages during inflammation [211]. Previous data suggest that elevated levels of CCL2 are linked to chronic inflammatory diseases, such as obesity associated-type 2 diabetes and cardiovascular diseases [212, 213]. Regarding ZnONP exposure, earlier studies reported a significant increase in CCL2 levels after ZnONP exposure either *in vivo (lung)* or *in vitro* [158, 179, 214]. According to Sahu et al., ZnONP promote the expression of the MCP-1 mRNA level in THP-1 cells in vitro after exposure [215]. Moreover, in Balb/c mice, exposure to ZnONPs induced the production of CCL2 in lung, leading to a T helper cell (T_h2) response.

Eotaxin (CCL11)

Eotaxin (CCL11) is an eosinophils chemoattractant that was first defined in the BALF of OVA-sensitized guinea pigs to promote eosinophils recruitment [216]. In asthma and animal pulmonary allergic inflammation models, there is a positive correlation between the number of eosinophils recruited to the lungs and the local CCL11 level [217-220]. As stated, ZnONP promotes lung inflammation and induce the accumulation of eosinophils in BALF or the alveolar interstitium in rodent inflammation models with or without OVA sensitization, respectively. Saptarshi et al. reported the upregulation of CCL11 mRNA in the lung tissue after ZnONP exposure in mice. Furthermore, the CCL11 level was significantly elevated in BALF within 24 hours of ZnONPs exposure in mice [153, 221].
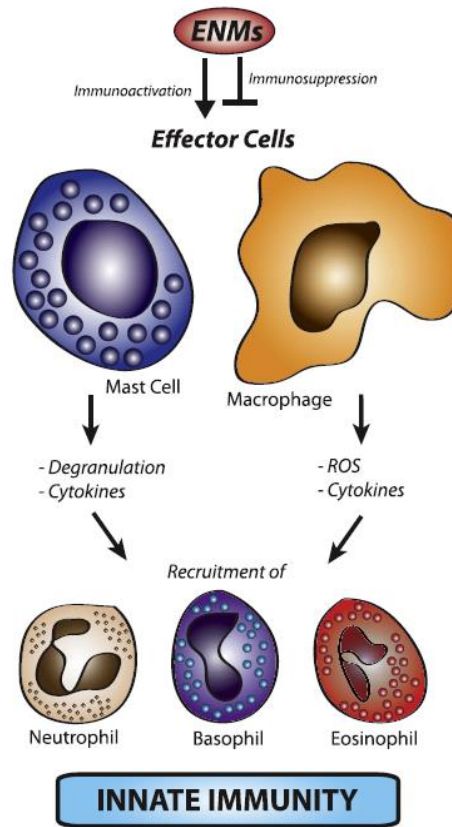
Figure 3: Schematic model illustrating ENMs inducing an immunomodulatory response in the innate immune system: ENMs could induce an innate immune response by a direct interaction with innate immune cells, such as macrophage and mast cells, or by recruiting the innate immune cells to the site of exposure through cellular mediators, such as through cytokines and cell-specific chemokines, leading to the recruitment of more immune cells, such as neutrophils, basophiles, and eosinophils. Figure adopted from [95].

Zinc oxide nanowires (ZnONWs)

Zinc oxide nanowires (ZnONWs) with a one-dimensional (1D) shape have recently been synthesized by Advanced Energy Materials, LLC. (Fig 4). They have developed novel vapor-phase methods for generating these nanowires, which have numerous potential industrial applications; however, finite information is available regarding the potential biological effects of these novel nanowires. ZnONW share the same chemical composition as the commercial spherical ZnONP, which induce toxicity both *in vivo* and *in vitro*. The toxicity is mainly due to the solubility of ZnO particles in the acidic pH inside the phagolysosomal compartment of the cell. On the other hand, the change in the physical form of ZnONW to 1D may elicit different biological responses, especially an immune response [38, 92]. In addition, there are other ENMs that have a 1D shape, such as a carbon nanotube (CNT). Carbon nanotubes have been widely used in many areas such as biomedical and electronic devices [18, 19]. Due to the unique 1D shape and small size of CNT, it has been linked to many pulmonary diseases, such as lung fibrosis and asthma [222]. According to Rydman et al., CNTs induce inflammation in mice lungs by recruiting macrophages and eosinophils [223]. Furthermore, CNTs lead to inflammation and progressive fibrosis on the parietal pleura in mice. The cellular mechanism of CNTs inducing inflammation is ROS generation, which leads to activation in AP-1, NF-κB, p38, and Akt signaling pathways [68]. Due to the large-scale production and increasing utilization of ZnONWs, concerns regarding ZnONW toxicity and whether ZnONWs are safe

are increasing. Thus, it would be highly beneficial to study and to investigate the safety of these ZnONWs.
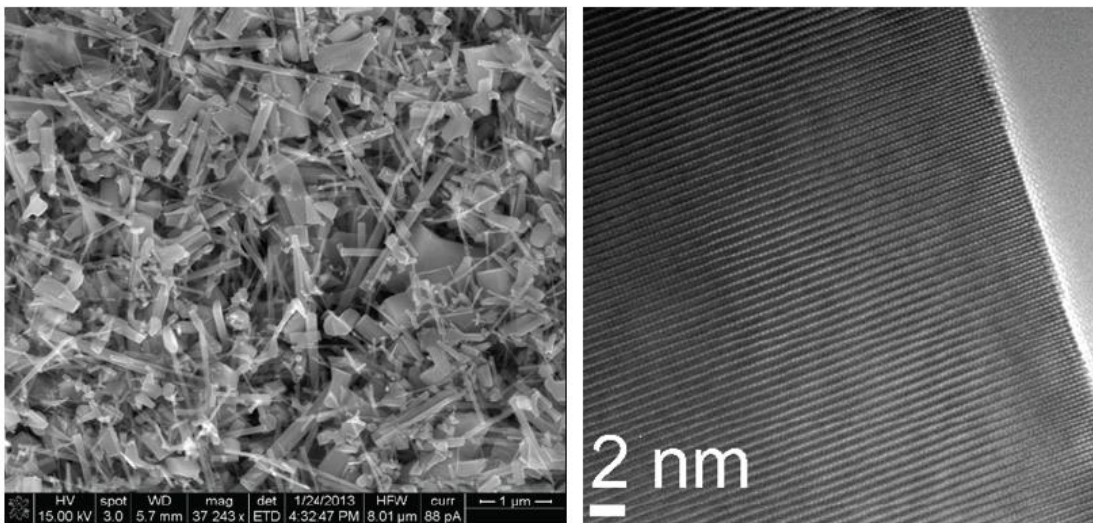
Figure 4: Scan electron microscopy (SEM) image of ZnONWs (left); transmission electron microscopy (TEM) of ZnONWs (right).

Significance and Aim of the study

ZnONW has become one of the most important products in optical and electronic applications. They are being produced in large-scale quantities using different methods, such as vapor-phase, solution-phase, and hydrothermal methods, which could lead to occupational health risks. The potential exposure routes of these ZnONWs may vary depending on both occupational and environmental exposure. Human exposure to ZnONW and under acidic conditions in the cells (ZnO has a sensitive dissolution point) eventually trigger the release of Zn ions within the cells, leading to cell toxicity and death. Therefore, for this dissertation, the biological effect of ZnONW was assessed. First, the way such cellular and molecular responses are integrated into an inflammatory response *in* mouse models was determined. In addition, the cell types involved in the production of pro-inflammatory cytokines and chemokines were delineated. Therefore, the specific aims were as follows.

AIM I: Investigate the potential of ZnONW to induce sterile inflammation in a mouse model. The large-scale production and ZnONW may lead to environmental pollution which increased risk of human exposure to ZnONW. Since the common exposure routes for these particles are skin contact, and lung, the inflammatory response in the following models. The consequences of local/systemic inflammatory responses to ZnONW were investigated.

Because the common exposure routes for these particles are skin contact (local) and inhalation, the inflammatory responses in the following models were

examined. First, local inflammation in the air pouch was used as a skin exposure model. Second, to simulate airway exposure, lung inflammation following the intra-tracheal instillation of ZnONW was analyzed. Lavage fluids were analyzed for inflammatory infiltrates as well as cytokines and chemokines were measured to identify the cellular mediators responsible for inducing inflammation.

AIM II: Defining the cellular mediators and cell types activated by ZnONW exposure.

The specific pathways that could lead to the sterile inflammation *in vitro* were assessed. Previous studies showed that macrophage-specific (CCL2) and eosinophil-specific (CCL11) chemokines and TNF-α and IL-6 cytokines are induced upon ZnONP exposure, and because ZnONW share the same chemical composition of ZnONP, it was important to explore whether ZnONW induce the production of these chemokines and cytokines as well as to investigate the cellular and molecular basis for the production of these cytokines and chemokines by ZnONW. Using murine primary macrophages (BMDM), macrophage cell lines (RAW-264.7 cells), and lung epithelial cell lines (LKR-13), ZnONW was exposed to these cell lines, and the chemokine and cytokine production in culture supernatants was determined. The results were further confirmed using the qRT-PCR. Next to investigate the cellular uptake of ZnONW in BMDMs cells, FITC labeled ZnONWs were generated. Confocal microscopy, various staining techniques and pharmacological inhibitors were used to define the cellular uptake of ZnONW. Lastly, In-vitro toxicity experiments were

performed in bone marrow-derived macrophages, RAW-264.7, and LKR13 cells to evaluate the cell viability upon ZnONW exposure.
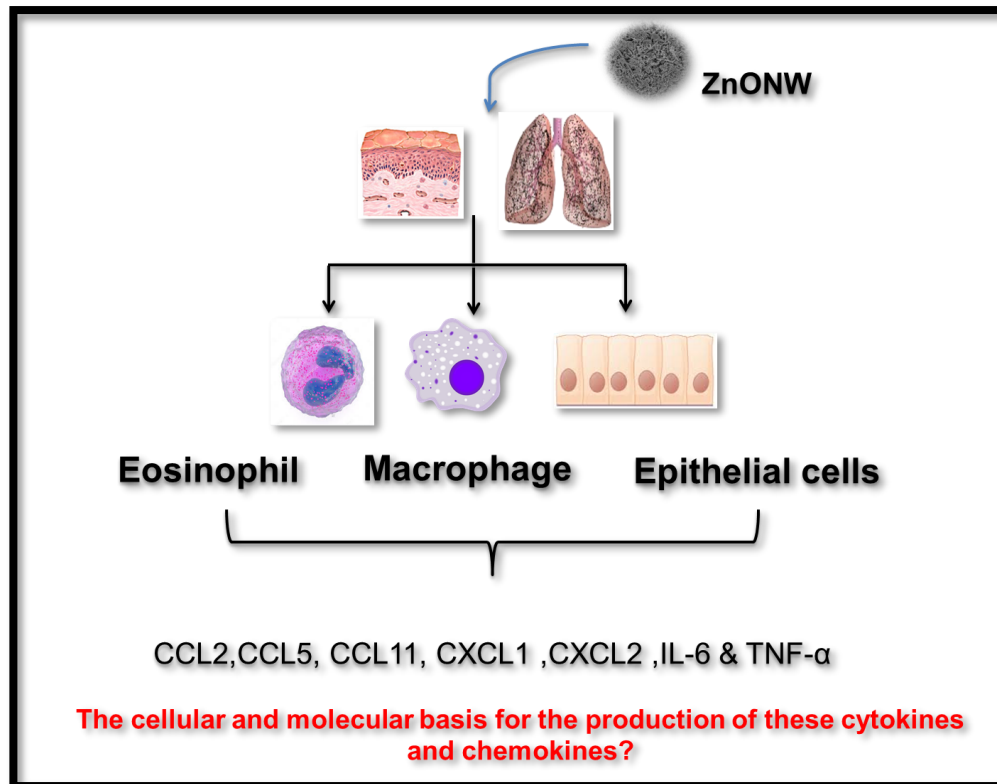
Figure 5: Schematic model of ZnONWs-induced sterile inflammation: ZnONWs induce inflammation in the lungs and the Air-pouch by recruiting immune cells, such as macrophages and eosinophils. The inflammatory exudates contain IL-6, TNF-α, CXC, and CCL. The cell types responsible for the production of these chemokines and cytokines and the pathways need to be identified.

CHAPTER 2

MATERIALS AND METHODS

Nanoparticles and Reagents

Zinc Oxide nanoparticles ZnONPs (10-30 nm) and ZnONWs (100 nm) were provided by Advanced Energy Materials, LLC, a nanowire powder manufacturing company in Louisville, KY. Silicon dioxide nanoparticles (SiO2NPs 7nm &200 nm) was obtained from sigma Aldrich. All particles were made endotoxin-free by baking at 200°C overnight. The following pharmacological inhibitors were used in the study: Cytocholasin D, (from Sigma-Aldrich) Bafilomycin-A1 (Santa Cruz). E.coli, LPS (LPS-EK; InvivoGen).

Mice

C57BL/6 mice were purchased from Jackson laboratories and bred at the University of Louisville. All mice were used in ex-vivo and in-vivo experiments were sex and age matched 6-8 weeks. All mice were maintained in a specific pathogen free facility and cared for in accordance with the institutional and National Institutes of Health (NIH) guidelines. The University of Louisville Institutional Animal Care and Use Committee (IACUC) approved all the procedures.

Fluorescein isothiocyanate (FITC) labeling of ZnONWs

Four mg of ZnONWs were dispersed in 3 ml anhydrous dimethylformamide (DMF). Then a diluted solution of 0.5 µl of amino-propyl-triethoxy-silane (APTS) in 25 µl DMF was added to the ZnONWs suspensions, which was followed by sonication, and stirring under nitrogen at room temperature for 20 h. ZnONWs were collected by centrifugation and removing the supernatant. After washing, ZnONWs were re-suspended in 0.5 ml DMF and mixed with a solution of 1 mg FITC and 0.5 ml DMF. The suspension was stirred for 4 h, and the FITC-labeled ZnONWs were collected by centrifugation. FITC-labeled. ZnONWs were thoroughly washed with DMF, dried under vacuum and stored as dry powders [224].

Bone marrow derived macrophages

Six to eight-week-old C57BL/6 mice were euthanized by using CO_2. The hind legs were dissected and the bone marrow cells were flushed out with cold Dulbeco's Modified Eagle Medium (DMEM). The bone marrow cells were cultured in DMEM containing 10% FBS,100 units/ml penicillin, 100 mg/ml streptomycin, 2 mM L-glutamine and 50 mM β -mercaptoethanol supplemented with 25 ng/ml recombinant mouse macrophage colony stimulating factor (BioLegend; San Diego, CA). The cells were plated at a density of 1 million cells per 100-mm tissue culture dishes containing 10 ml of medium. After 3 days, 10 ml of fresh growth medium was added to replace the medium. The cells were

maintained for another 3 days before the experiments. The purity of the cells (>99%) was confirmed using flow cytometry by surface staining for F4/80 and CD11b.

Cell culture

Raw 264.7, mouse macrophage cell line (American Type Culture Collection (ATCC), Manassas, VA, USA) and LKR13 cells, murine K-ras mutant lung adenocarcinoma cell line were maintained in Dulbecco's Modified Eagle's Medium (DMEM; Hyclone Laboratories, Inc., South Logan, UT, USA) supplemented with 10% heat-activated fetal bovine serum (FBS, Hyclone Laboratories Inc.) and 100 units/ml penicillin, 100 µg/ml streptomycin, 2 µM L-Glutamine and 50 µM β - mercaptoethanol (Gibco®, Invitrogen Corporation, Carlsbad, CA, USA) at 37°C in a 5% CO_2 incubator. Cells were seeded at $0.5x10^6$ cells/ well density into six well plates.

In vitro ZnONWs, ZnONP and SiONP Stimulation Assay

BMDMs were plated at a density of $0.5x10^6$ cells per well in a six well culture dish in 2 ml of DMEM containing 10% FBS and allowed to attach overnight. BMDMs were primed with or without 10 ng/ml of LPS (LPS-EK; InvivoGen, San Diego, CA) for 3 hours. Cells were washed with pre-wormed PBS three times. Then the media was changed to 1% FBS media with final volume of 1000µl in 6 well plate. The cells were then pre-treated with or

without the pharmacological inhibitors Baf-A1 or CytD at the indicated concentrations for 1 hour prior to stimulation with 10 or 20 µg/ml of particles for 3-6 hours.

RAW 264.7 cells were plated at a density of $0.5x\ 10^6$ cells per well in a six well culture dish in 2 ml of Hyclone DMEM containing 10% FBS and allowed to attach overnight. The cells were primed with or without 10 ng/ml of LPS for 3 hours. Cells were washed 3 times with pre-wormed PBS. Then the media was changed to 1% FBS media with final volume of 1000 µl in 6 well plate. The cells were then treated with 10 or 20 µg/ml of particles for 6-18 hours.

LKR13 cells were plated at a density of $0.5\ x10^6$ cells per well in a six well culture plate in 2 ml of Hyclone DMEM containing 10% FBS and allowed to attach overnight. Cells were washed 3 times with pre-wormed PBS. Then the media was changed to 1% FBS media with final volume of 1000 µl in 6 well plate. The cells were then treated with 10 or 20 µg/ml of particles for 6 hours.

Enzyme-Linked Immunosorbent Assay (ELISA)

IL-6, TNF-α and IL-1β in the cell culture supernatants were measured using mouse IL-6, TNF-α and IL-1β ELISA MAX Standard Kit (Biolegend). LTB₄ in the cell culture supernatants was measured using LTB₄ EIA Kit (Cayman Chemicals). Briefly, Polyvinyl chloride (PVC) microtiter plates were coated with anti-cytokine antibody overnight at 4°C. The next day, the plates were washed using washing buffer, and non-specific binding blocked using blocking buffer

provided by the manufacturer. The standard dilution and the required dilutions were made for the following step. Cell culture supernatants were added to the coated plates, and plates were incubated for 2 hours at room temperature. The secondary antibodies (detection antibody) for IL-6, IL-1β and TNFα were added to the respective plates. Then plates were washed. The assay was developed according to the manufacturer's instruction and the intensity of the signal was detected using ELISA plate reader at recommended wavelength (405 nm for IL-6, TNF-α, or IL-1β and at 450nm for LTB_4). The data was calculated by extrapolating the absorbance of each protein (cytokine) and the standard curve.

RT-PCR Assay

Cells (BMDMS, RAW 264.7 and LKR13) were lysed using TRIzol reagent and total RNA was isolated using an RNeasy Mini Kit (Qiagen) using manufacturer's protocol. RNA samples were treated with DNase (Qiagen) to remove any trace of DNA from the samples before reverse transcription with TaqMan reverse transcription reagents (Applied Biosystems) using random hexamer primers. Quantitative PCR was performed using 'power SYBR-green master mix' Applied Biosystems). Expression of the target genes was normalized to GAPDH and the relative fold changes relative to the PBS were calculated using the delta delta CT method. Data were representative of triplicate cell cultures. GAPDH, CXCL1, CXCL2, CCL2, CCL3, CCL4, CCL5, CCL11, TNFα and IL-6 primers obtained from Real Time Primers.

MTT assay

The MTT assay is a colorimetric assay for assessing cell metabolic activity. BMDM, LKR13 and RAW264.7 cells were treated with ZnONWs for different time points 2, 4, 6, 18 hours. Then 3-[4, 5-dimethyltiazol-2-yl] 2, 5-diphenyl-tetrazolium bromide (MTT) was added to the cells at the end of each time point. After 2h incubation with MTT, DMSO was added for 10 min. absorbance was measured at 562 nm using a BioTek microplate reader.

Immunofluorescence

BMDMs cells (0.7×10^6) were plated in a 35 mm cover-glass bottom dish (World precision Instruments, Sarasota, FL) in DMEM with 10% FBS and grown overnight. The media was changed to DMEM with 1% FBS and the cells were primed with 10ng/ml LPS for 3 hours. Then cells were treated with 1μM Baf-A1 for 1h. Then cells were stimulated with 25 μg/ml FITC ZnONW for 3hrs. next cells were washed 3X with PBS and fixed with 10% formalin for 15 min. after fixation, cells were washed three times with 1X PBS, cells were stained with 1:500 dilution 594-Cholera toxin Subunit B and 1:1000 dilution DAPI (ThermoFisher Scientific) and washed again before analyzing with confocal microscopy. The confocal images were captured using Nikon A1R confocal microscope at 60 x magnification with appropriate lasers as indicated. A minimum of five to six fields were captured for each sample.

Acridine orange staining

Acridine orange is a fluorescence dye that is easily crosses the cell membrane. It used to stain acidic vacuoles (lysosomes, endosomes, and phagolysosome), with red to orange color and RNA, and DNA with green color in living cells. BMDMs were treated with or without Baf-A1 for one hour followed by FITC-ZnONWs. Next cells were washed and loaded with 5 µg/ml acridine orange (Sigma- Aldrich) for 30 minutes. Cells were washed with Hank's balanced salt solution (HBSS) before imaging using confocal microscopy.

Antibody staining

BMDMs were treated with 1Mm BafA-1 for 1 hour followed by 25µg/ml FITC-ZnONWs treatment for 3 hours. Then, cells were fixed with 10% formalin for 15 min and permeabilized with 0.1% saponin. Non-specific binding was blocked using with 1% BSA for 1 hour. Next, cells were incubated with LAMP-1 antibodies (a rat anti-mouse (1D4B) (abcam) at 1:500 dilution overnight at 4^0C. Later, cells were washed three times with 1X PBS and followed by an Alexa 594-labeled secondary (rat anti-mouse IgG A-11032: ThermoFisher Scientific) at 1:500 dilution for 1-2 hours. Cells were washed three times with 1X PBS and stained with DAPI. Cells were washed with HBSS before imaging by confocal microscopy.

Air pouch experiment

Five ml of sterile air was injected into the back of mice subcutaneously to generate an air pouch. Three days later another 3 ml of sterile air was injected into the pouch to maintain the air-pouch. After 3 days, 2 mg of particles in 500 μl of endotoxin-free PBS was injected into the air pouch. Control animals received 500 μl of endotoxin-free PBS. After 6 hours of injection, mice were euthanized and the air pouch was lavaged with 3 ml of cold PBS.

Particles installation in mouse lungs

Mice were treated with antibiotics for one-week prior to surgery. Mice were surgically instilled (intratracheal) with endotoxin-free PBS (negative control) or 0.67 mg of endotoxin-free SiONPs (positive control) or 0.67mg of ZnONWs suspended in endotoxin-free PBS. Previous studies have reported the use of 0.2 μg/mouse [225] and 0.168 μg/mouse of ZnONPs [226]. Particles suspension was vortexed before instillation to avoid settling of the particles. Mice were continuously maintained on antibiotics until euthanasia two days after instillation. Lungs were lavaged with 2 ml of cold PBS and BALF were obtained.

Flow Cytometry

Cells from air-pouch and BALFs were stained with various cell surface marker antibodies from BD Biosciences (San Diego, CA) or Biolegend (San Diego, CA). Data were acquired on FACS Calibur or FACS Canto (BD Biosciences) and analyzed using Flowjo software (Tree Star). Leukocytes were identified as CD45+ cells, lung macrophages as CD45+ FSChi CD11chi F4/80+ cells, neutrophils as CD45+ CD11c− Ly6Ghi Siglec-F− cells, eosinophil as CD11b, CD193, F4/80, Siglec-F, B cells as CD45+ FSClo B220+ cells, CD4 cells as CD45+ FSClo CD4+ and CD8 cells as CD45+ FSClo CD8+. In air-pouch lavage fluids, leukocytes were identified as CD45+ cells, macrophages as CD45+ FSChi F4/80+ CD11bhi Ly6Glocells and neutrophils as CD45+ SSChi Ly6Ghicells, eosinophil as CD11b, CD193, F4/80, and Siglec-F.

Cytospin

The cytospin is a high speed centrifuge to concentrate the cells in a sample on a slide. It used to analyze the cell morphology and type. The air pouch lavage fluid cells and BALFs cells were spun down using Shandon Cytospin centrifuge (Shandon Lipshaw) followed by staining with Hema-3 reagents (ThermoFisher Scientific) according to the manufacturer's recommendations.

Multiplex analysis

Lung lavage fluids and Air-pouch lavage from PBS or particles treated mice were measured for various levels of inflammatory proteins including TNF-α, CXCL1, CXCL2, CCL2, CCL4 and CCL5, CCL11, IL-1β & IL-1α. The analysis was accomplished following standard protocols at the Proteomics core facility of Medical University of South Carolina.

Statistical Analysis

Graph Pad Prism4 Software San Diego, CA was used to analyze the Data; Data were expressed as the means ± S.E from at least three independent samples. Statistical difference among groups was analyzed using the Mann–Whitney U-test (in vivo) or Unpaired Student's t-test (in vitro/ex-vivo, RNA analysis). Two-tailed P values of <0.05 were considered as significant.

CHAPTER 3

ZnONWs INDUCE STERILE INFLMMATION

IN DIFFERENTMOUSE MODELS

Introduction:

Physicochemical properties, such as size and shape, determine the interaction between ENMs and immune systems. The morphology of ENMs is one of the most important aspects for nano-toxicology. A novel class of a ZnO nanomaterials, called ZnONW, are being produced recently in high tonnage. They have a unique shape and size that differ from spherical ZnONP, which have been on the market for decades. The rapid production rate and enormous quantities substantially increase the risk exposure to ZnONW through different exposure routes that may vary depending on occupational and environmental exposure. During the production of ZnONW, workers could be exposed to free ZnONW in the air.

On the other hand, public exposure to ZnONW could occur through using products that contain ZnONW or through the release of ZnONW into the environment. The general exposure routes to ZnONW are inhalation, skin contact, and ingestion. The small size and unique shape make their exposure unavoidable, and a change in the shape could elicit different immune responses and could impact their uptake and recognition by the immune system. Moreover, limited data are available related to ZnONW toxicity as well as their acute inflammatory potential. In addition, long-term consequences of exposure to ZnONW are unknown.

Therefore, the aim was to assess the adverse effects of ZnONW and their ability to induce inflammation. Such studies are required to ensure the safe production and use of ZnONW.

The consequences of local /systemic inflammatory responses to ZnONW were investigated. First, the local inflammation in the air pouch was evaluated. The air-pouch provides a localized inflammatory setting that mimics skin exposure. Also, different cytokines and chemokines responsible for any cellular infiltration to the site of exposure were examined. Next, the consequences of systemic inflammatory responses to ZnONW were assessed using a lung inflammation model. Finally, the cellular mediators involved in the recruitment of inflammatory cells into the lungs were analyzed.

Results:

ZnONWs induce inflammation in a murine air-pouch model

One way that exposure to ZnONW can occur is through dermal contact; however, to the best of our knowledge, the possibility for ZnONW to be considered inflammatory irritants or to penetrate the skin have not been studied yet. Thus, whether exposure to ZnONW could lead to any local inflammatory response was explored. A murine air pouch model was used to assess the potential localized inflammation caused by ZnONW. The air pouch provides a localized environment allowing to study infiltration of immune cells in response to any inflammatory agent or irritant. In this experiment, the air pouch was established by injecting 5 ml of sterile air subcutaneously into the back of the mice. After three days, another 3 ml of sterile air was injected into the pouch. Three days later, 2 mg of ZnONW in 500µl of endotoxin-free PBS was injected into the air pouch. As controls, PBS alone (negative) or SiONP (2 mg each) were injected into the air pouch. The mice were euthanized six hours after particle or PBS administration, and air pouch lavage was collected with 3 ml of PBS (Fig. 6). A flow cytometry analysis and the cytospin of the air-pouch lavage revealed, as expected from our previous study, that in SiONP-treated mice, there was induced neutrophilic inflammation but no significant infiltration of macrophages or eosinophils (Fig.7a&b). In contrast, ZnONW showed a significant increase in both macrophages and eosinophils. Although a neutrophil influx was observed from ZnONW, it was relatively weaker compared to SiONP-exposed mice. These

results suggest that ZnONW-induced inflammation is both qualitatively and quantitatively different from that induced by SiONP.

Inflammatory mediators induced by ZnONW exposure in an air pouch

Because ZnONW induce inflammation by the recruitment of eosinophils and macrophages into the air pouch, which cellular mediators contribute to this distinct pattern of inflammation in the air-pouch was explored. Therefore, a multiplex analysis for the air pouch lavage from PBS or particle-treated mice was conducted. The analysis was performed in collaboration with Dr. Twal from the Medical University of South Carolina to test the levels of various inflammatory proteins. The following cytokines and chemokines were selected based on the cells detected in the air pouch: IL-1α, IL-1β, and TNF-α, IL-6, CXCL1, CCL2, CCL3, CCL4, and GM-CSF for macrophages; CXCL1-specific neutrophilic chemokine; CCL5 and CCL11 for eosinophils; and CCL2, CCL4, and CCL3 macrophage-specific chemokines. The multiplex analysis showed that in the air pouch, there was a significant increase in CCL11, CCL2, and CXCL1 (Fig. 8a) and IL-6 and TNF-α, while for IL-1β, it was only detected with SiONPs (Fig. 8b), which is consistent with cells types recruited in the air pouch. These findings indicate that macrophages and eosinophils are the major cell types that contribute to inflammation induced by ZnONW in the air pouch; however, the actual events and pathways involved in the inflammation are not yet identified.

Lung inflammation induced by ZnONWs

Inhalation is one of the most common exposure routes for ZnONW. Previous studies investigated inflammation induced by ZnONP in lung inflammation models; however, ZnONW has different physical properties than ZnONP but similar chemical compositions. Thus, whether ZnONW promote lung inflammation was examined using an acute two-day lung inflammation model. The mice were treated with antibiotics for a week before surgery to avoid infection after surgery, and after one week, the mice were surgically instilled (intra-tracheal) with endotoxin-free PBS (negative control) or 0.67 mg of endotoxin-free SiONP (positive control) or 0.67 mg of ZnONWs suspended in PBS without sonication. Particle suspension was vortexed before instillation to avoid the settling of the particles. The mice were continuously administered antibiotics until euthanized two days later. The lungs were lavaged, and bronchial alveolar lavage fluids (BALFs) were obtained. Both SiONP and ZnONW led to a massive influx of leukocytes in the lungs. Both the flow cytometry analysis and the cytospin of BALFs showed that macrophages and eosinophils were the predominant cells infiltrating the lungs with ZnONW, while SiONP only recruited neutrophils (Fig 9a). These data indicate that ZnONW have the ability to induce sterile inflammation that is distinct from the inflammation induced by other sterile nanoparticles, such as SiONP.

Inflammatory mediators induced by ZnONW exposure in the lungs

Similar to the air pouch model, the mediators that contribute to this distinct pattern of a sterile inflammatory response in the lungs were assessed. A

multiplex analysis for BALFs from PBS or particle-treated mice was performed to measure various inflammatory proteins. The following cytokines and chemokines were selected based on the cells detected in the lungs: IL-1α, IL-1β, TNF-α, IL-6, CXCL1, CCL2, CCL3, CCL4, and GM-CSF. For macrophage-specific chemokines, CCL2, CCL3, and CCL4 were selected. CXCL1 was selected for neutrophils, and CCL5 and CCL11 were selected for eosinophils. In the lungs, the levels of IL-6, TNF-α, CCL2, and CCL11 were elevated in ZnONW-treated mice; however, significant levels of IL-1β and CXCL1 were detected in BALF, which is consistent with neutrophilic inflammation that was induced by the SiONP administrated mice. These findings indicate that macrophages and eosinophils are the major cell types that contribute to inflammation induced by ZnONW in the lungs; however, the actual events and pathways involved in inflammation require further investigation.

Discussion:

ZnONW has been introduced as part of everyday consumer products. It is important to protect workers and end users from the inhalation of potentially innocuous ENMs. To the best knowledge, inadequate data are available in the literature regarding the biological effects of ZnONW *in vivo*. To address this gap in knowledge, in this chapter, the consequences of local and systemic inflammatory responses to ZnONW investigated using in a mouse model have been discussed. Such studies are required to ensure the safe production and use of ZnONW.

Local exposure such as dermal contact is considered a possible common exposure mode to ZnONW. Previous studies investigated dermal exposure to sunscreens containing ZnONP in both human and animal experimental models [227, 228]. ZnONP from sunscreen penetrate only the epidermis outer layer (stratum corneum) and were found in skin fold areas though not beyond them. These data suggested that skin exposure hazards of ZnONP are minimal and limited, and thus it is safe to use ZnONP in sunscreens [229-231]; however, most of these studies were done using healthy contact skin. Therefore, the skin exposure hazard of ZnONP for compromised and damaged skin is unknown. Further studies are necessary to elucidate this issue.

In this study, and for the first time, a murine air pouch model was used to simulate local exposure to ZnONW. Earlier studies from the laboratory showed that crystalline silica exposure (CS) induced neutrophilic inflammation in the air pouch model with a significant increase in the levels of IL-1β and LTB4 [232].

This type of inflammation observed with CS is linked to lipidosome activation and LTB4 production as well as to the NLRP3 inflammasome pathway, leading to caspase-1 activation [232, 233]. In this study, ZnONWs-induced inflammation resulted in the infiltration of macrophages and eosinophils and the production of CCL11, CCL2, IL-6, and TNF-α but not IL-β or LTB4. This is in contrast with significant neutrophilic inflammation induced by SiONPs treatment at the site of exposure (Fig. 7a, b) and significant levels of IL-β and LTB4 in the air pouch lavage (data not shown), as expected. Because IL-6 and TNF-α are produced after ZnONWs exposure, it appears that inflammation induced by ZnONWs is mediated via the NF-Kβ pathway.

In addition to skin contact, inhalation is a general exposure route to ZnONW. Previous studies with ZnONP revealed that lung inflammation was detected in mice and rats exposed to ZnONP [153, 154, 234]. Most ZnONP animal studies were performed using allergic airway inflammation models that are prone to eosinophilic inflammation [153, 155, 158, 234]. It has been suggested that Zn^{2+} ions dissolved from ZnONP might be involved in ZnONP-induced lung inflammation [92]. Nevertheless, the change in the morphology of ZnONW may influence the cellular uptake mechanisms and may cause a different immune response *in vivo*. Currently, workers are exposed to ZnONW, among other ENMs, without any permissible exposure limits. Respiratory diseases, such as fibrosis, asbestosis, and lung cancer, have been linked to inhalation exposure to fiber materials, such as carbon nanotubes and asbestos [235-237]. ZnONW has similar geometry properties as carbon nanotubes and

asbestos fibers. The intratracheal instillation of a 50mg/kg dose of CNTs induces pulmonary inflammation in mice through the recruitment of neutrophils and the activation of B cells [238]. Thus, ZnONW may need to be treated with the same caution as known inflammatory and carcinogenic materials, such as carbon nanotubes and asbestos. Based on the data from the murine inflammatory model, ZnONW induce a significant permeation of eosinophils and macrophages in BALFs, which was observed two days after ZnONW instillation without any prior sensitization (Fig. 9a, b). Furthermore, CCL11 (Eotaxin) and CCL2 chemokines were identified as cellular mediators that are responsible for recruiting eosinophils and macrophages into the lungs after ZnONW exposure. In addition, elevated levels of IL-6 and TNF-α were detected in BALF. Previous studies with other ENMs, such as TiO2NP and NiONP, reported eosinophilic inflammation in mice with OVA sensitization or at day 4 post-lung instillation, respectively [239, 240]. The exposure of rod-like carbon nanotubes (rCNT) also triggered eosinophilic inflammation in wild-type mice after 4 h/day for four consecutive days of exposure, while tangled CNT (tCNT) did not elicit any inflammatory response [241]. The results suggest that the sterile inflammation induced by ZnONW is distinct from other ENMs-induced inflammation, and the major difference is related to the recruitment of eosinophils at the site of exposure by ZnONW compared to neutrophilic inflammation with SiONP.
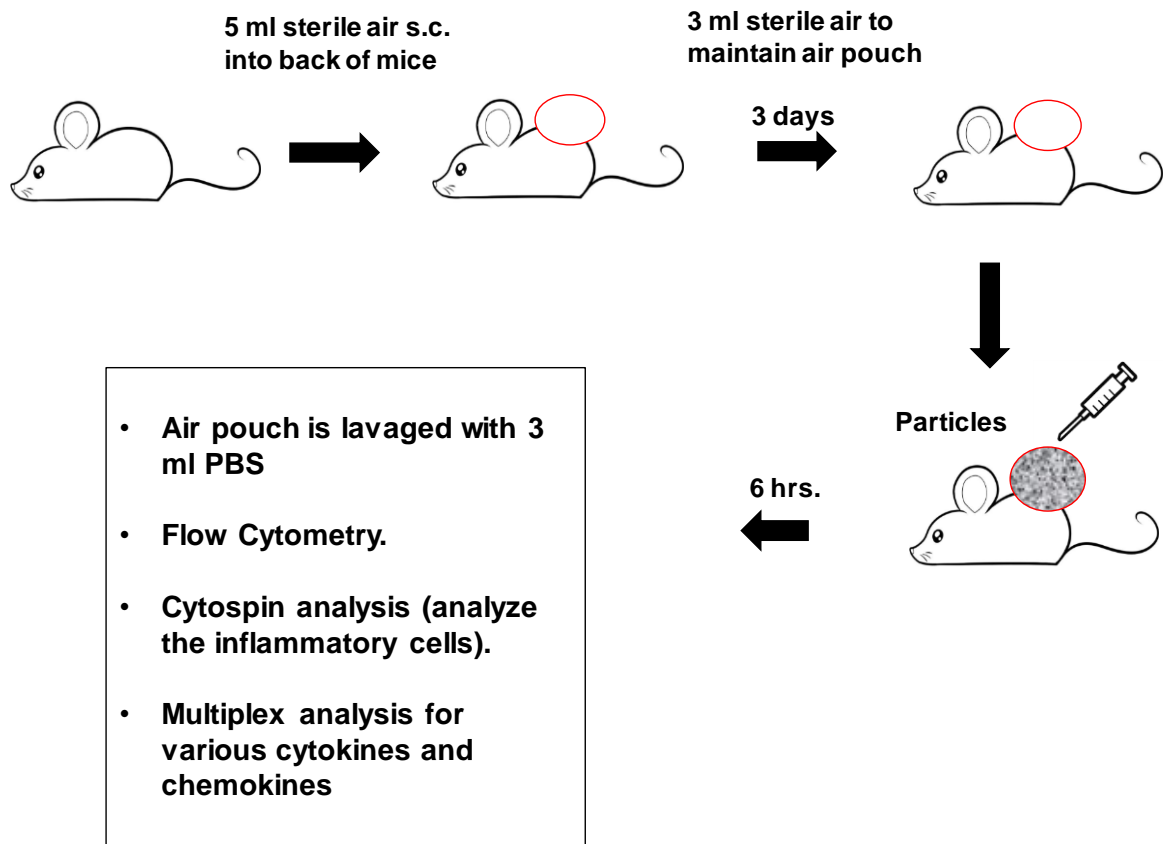
Figure 6: Air pouch Model Experimental set-up.

Five ml of sterile air was injected into the back of mice subcutaneously to generate an air pouch. To maintain the air pouch 3 ml of sterile air was injected into the pouch Three days later. After 3 days, 2 mg of particles in 500 μl of endotoxin-free PBS was injected into the air pouch. Control animals received 500 μl of endotoxin-free PBS. After 6 hours of injection, mice were euthanized and the air pouch was lavaged with 3ml of cold PBS.
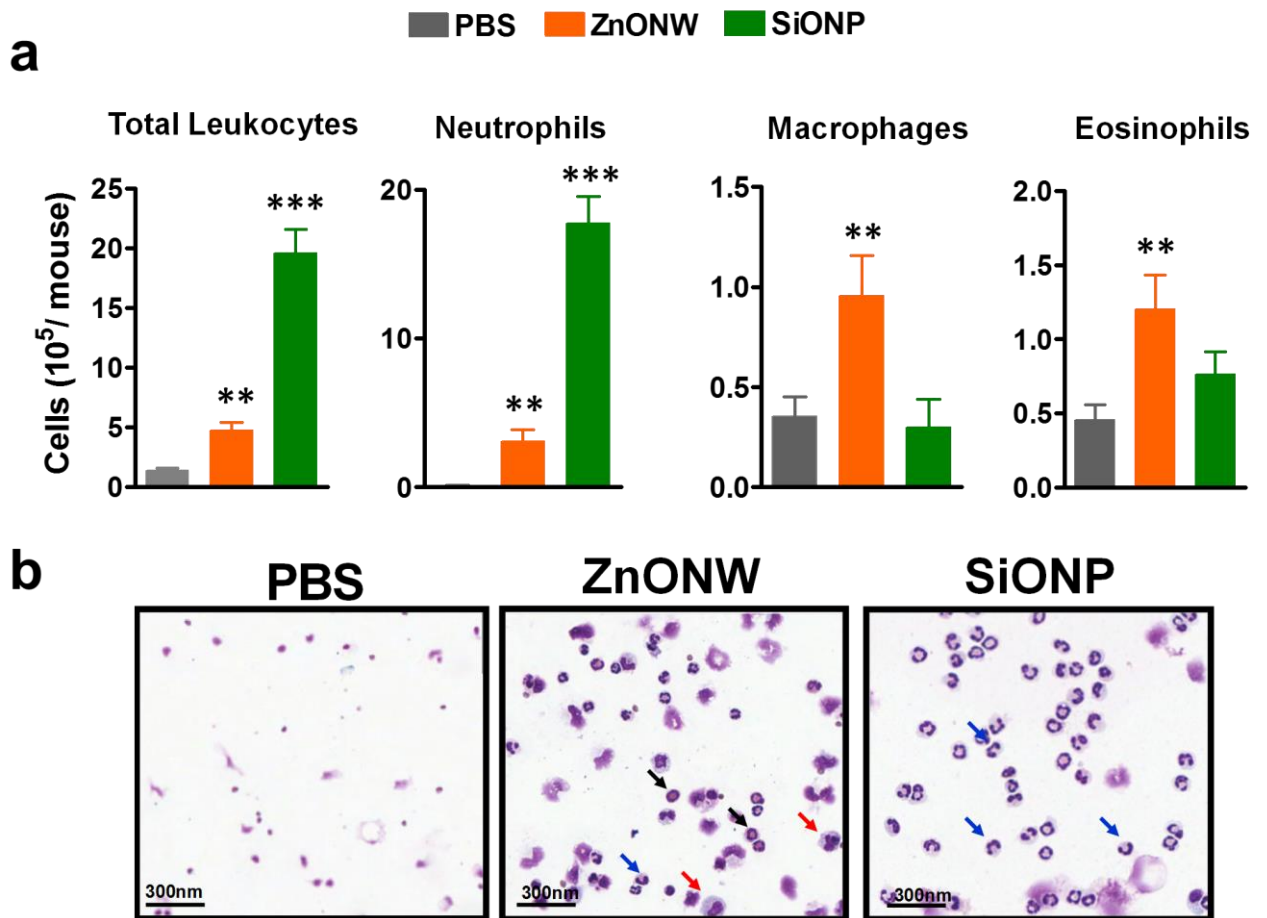
Figure 7: Local inflammation induced by ZnONWs in the air pouch.

Sterile air was injected s.c. on the back of the wild-type (WT) mice to form an air pouch and exposed to nanoparticles (ZnONWs or SiONP) or PBS as described in methods. Six hours post particle exposure the air pouch was lavaged with 3ml of buffer to assess infiltrating immune cells. The total number of leukocytes and differential count for cell types recruited in the air-pouch are indicated (a). Cytosine slides showing macrophage (red arrow), neutrophils (blue arrow) and eosinophils (black arrow) (b). Data are expressed as mean ± SE. *p<0.05, ***p< 0.001 non-parametric t-test. Data are representative of at least five mice per group.
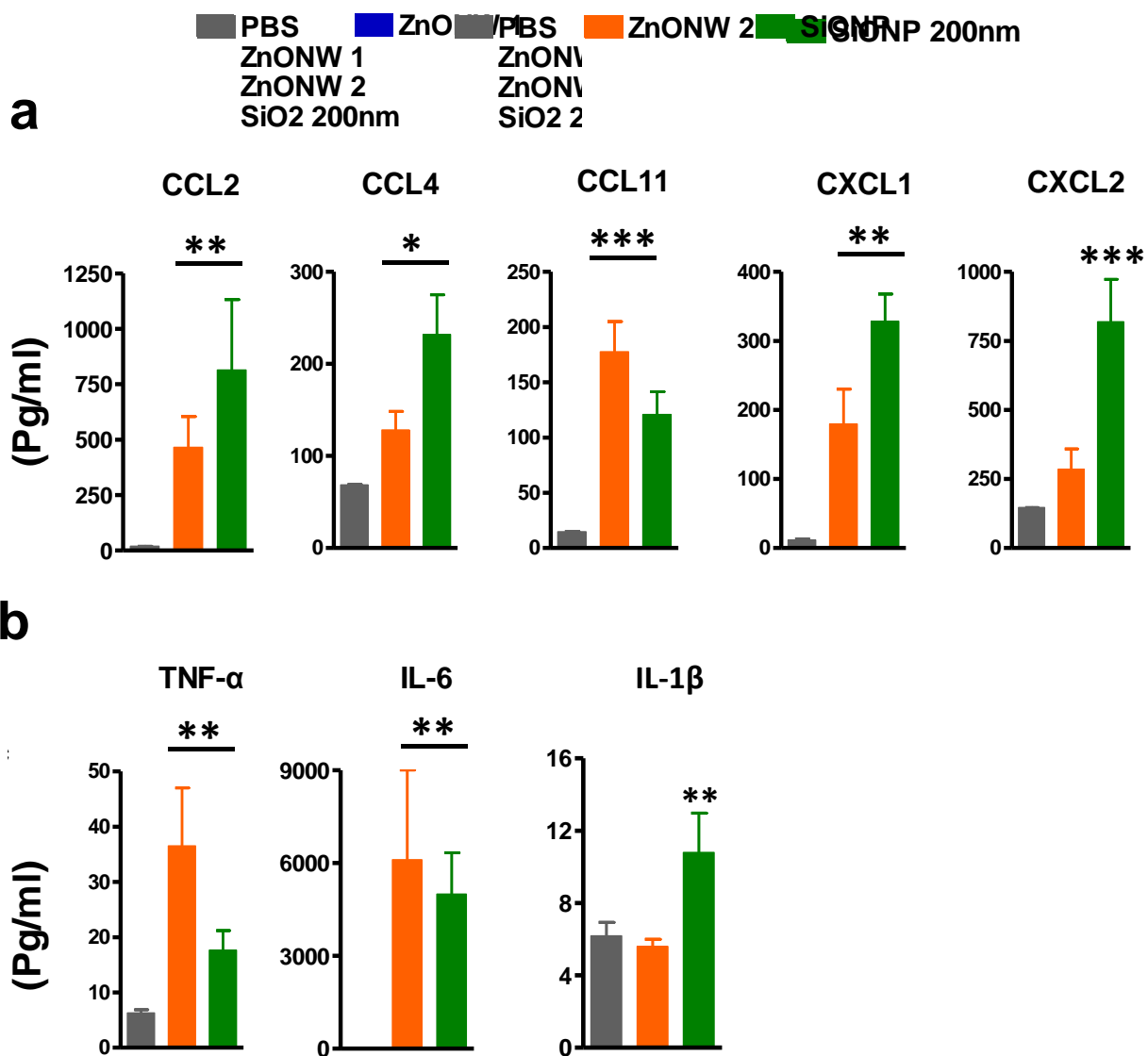
Figure 8: Inflammatory mediators induced by ZnONWs exposure in lung.
Cytokines and chemokines levels were analyzed in air-pouch lavage from PBS or particles treated mice using Multiplex analysis. Levels of various inflammatory proteins CCL2, CCL4, CCL11, CXCL1 and CXCL2 levels (a). IL-6, TNF-α and IL-1β levels (b). Data represent at least 5 mice 656 per group; error bars denote mean ± SEM. *P < 0.03, **P < 0.009, ***P < 0.0007; 657 Unpaired t-test.
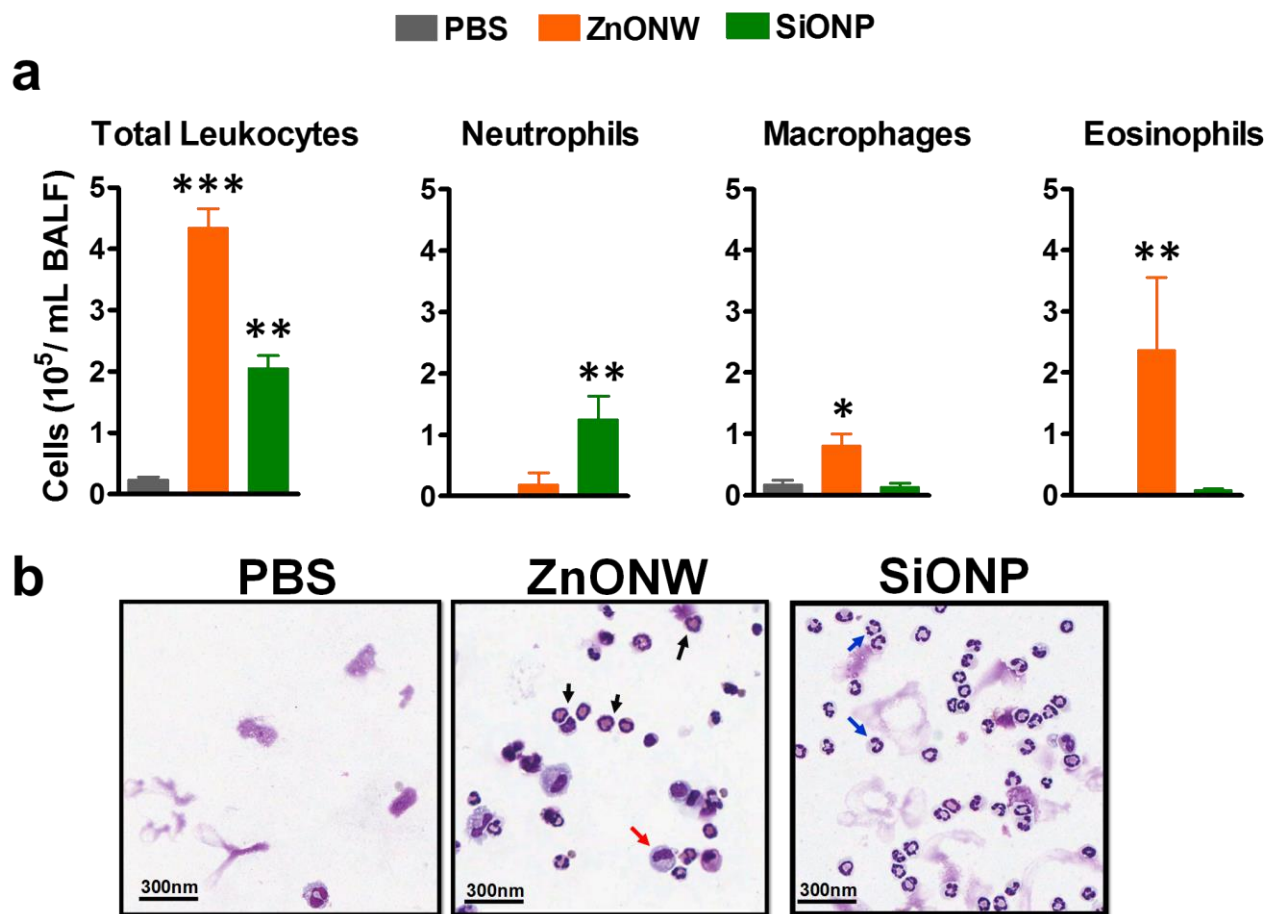
Figure 9: Nano-particle induced acute lung inflammation.

WT mice were intratracheal instilled with nanoparticles (ZnONW or SiONP) or PBS as described in methods. Lungs were lavaged with 3ml of buffer to assess infiltrating immune cells as identified by flow cytometry of BALFs (a). Total number of leukocytes and differential count for cell types recruited in the lung are indicated above. Representative cytospin slides showing macrophages (red arrow), neutrophils (blue arrow) and eosinophils (black arrow) (b). Data are expressed as mean ± SE. *p<0.05, ***p< 0.001 non-parametric t-test. Data are representative of at least five mice per group.
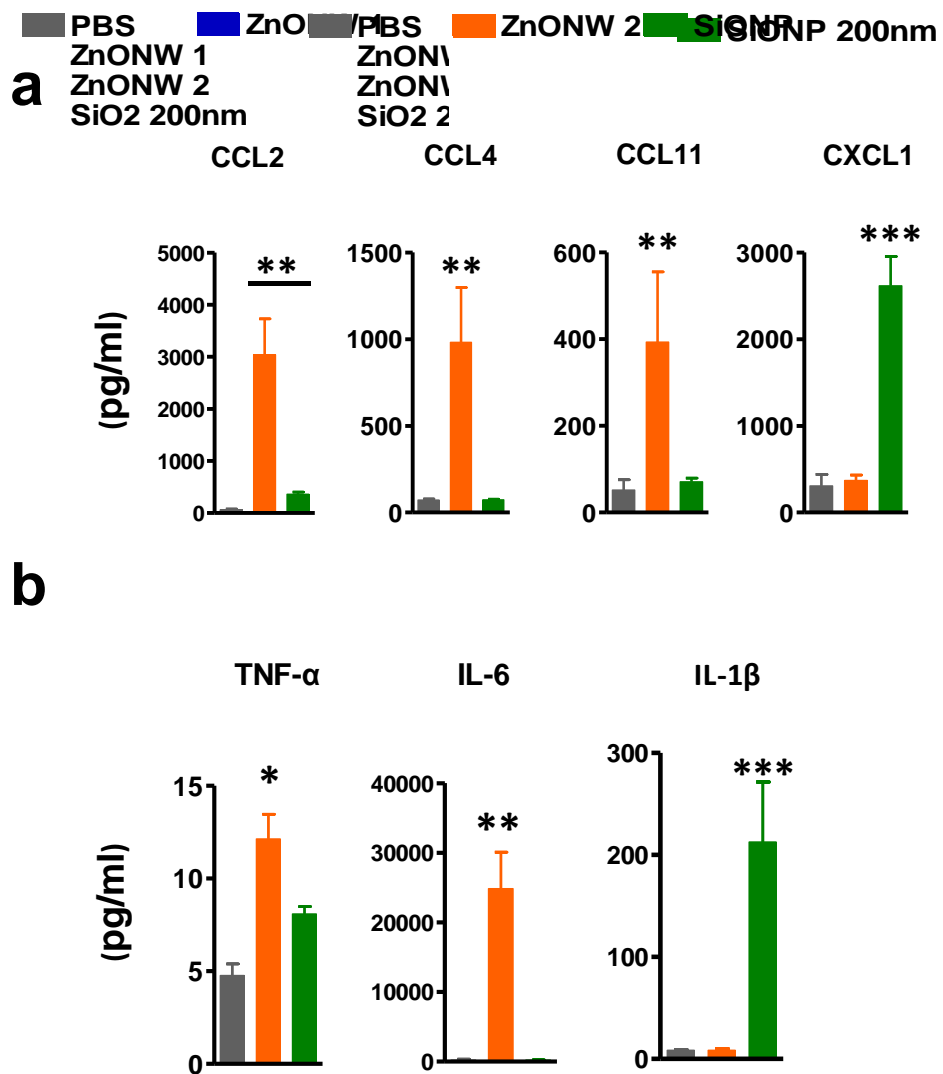
Figure 10: Inflammatory mediators induced by ZnONWs exposure in lung.
Cytokines and chemokines levels were analyzed in BALFs from PBS or particles treated mice using Multiplex analysis. Levels of various inflammatory proteins CCL2, CCL4, CCL11 and CXCL1 levels (a). IL-6, TNF-α and IL-1β levels (b). Data represent at least 5 mice 656 per group; error bars denote mean ± SEM. *P < 0.03, **P < 0.009, ***P < 0.0007; 657 Unpaired t-test.

CHAPTER 4

CELLULAR AND MOLECULAR MEDIATORS INDUCED BY

ZNONWs EXPOSURE

Introduction:

ZnONP toxicity has been extensity studies in a different mammalian cell lines [242]. The uptake mechanism and biological effect of ZnONP has also been studied in several *in vivo* and *in vitro* studies; however, novel ZnONW, which have a one-dimensional shape, were investigated in this study. The uptake and recognition mechanisms of these nanowires have not yet been identified. Moreover, most toxicity studies conducted with ZnONP showed that their toxicity is due to the solubility of ZnONP to zinc ions [52, 92, 93, 243, 244]. Still, the change in the physical properties of ZnONW may actually alter their interactions with immune cells. Subsequently, this could impact the uptake pathways of ZnONW, leading to differences in biological responses to ZnONW.

Very limited data are available related to ZnONW toxicity and translocation within the cells. ZnO nano-rods were found to be more toxic than ZnONP in Hela cells [243]. Exposure to rod-shaped ZnONP (100-200 nm) induces toxicity in human aortic endothelial cells at 10 and 50 µg/mL concentrations [244]. Furthermore, ZnONW were found to be toxic to HMMs at a concentration of 20µg/ml after 24 hours of exposure [92]. Pathogen uptake and degradation occur through the phagosomal maturation pathway such as endocytic pathway, and particles undergo the same process. It is a well-organized process that allows for particle transition into the intracellular compartments of the cell. First, it begins with early endocytic vesicles that contain the particles in the peripheral cytoplasm. Then, the particles within the early endocytic content are delivered to early endosomes (EE) that have a 6.2 pH level. EEs receive cargo from differed pathways, such as the clathrin and caveolar mediated pathways or the EEC and ARF6-dependent pathways. The content of EE is carried to large vesicles called late endosomes (LE), where the pH level is gradually reduced to 5.5. Next, in the perinuclear region, the plasma membrane and other compartments are recycled and sent back to the cell surface through recycling endosomes. Lastly, LEs fuse to the lysosomes with a final pH level equal to 4.5, and the contents are digested by the lysosomal hydrolases [245].

Under acidic conditions, such as the lysosomal vacuoles of the cells, ZnO has a highly sensitive dissolution point. The release of the zinc cation from ZnONP induces phagosomal membrane destabilization, leading to autophagy

and cell death [246]. Furthermore, the production of lysosomal proteases promotes ROS generation and induces the activation of inflammatory pathways. According to Roy et al., ZnONP triggers the production of ROS and enhance inflammatory signaling pathways, such as the MAPK kinases and NF-κB cascades, as well as the production of pro-inflammatory cytokines, such as IL-8, IL-6, and TNF-α [141]. Furthermore, they found that caveolae-mediated endocytosis is the primary mechanism in which ZnONP is taken up by peritoneal macrophage.

In chapter three, it has been demonstrated that ZnONW induced sterile inflammation by recruiting macrophages and eosinophils both in lung and air-pouch mouse models. In addition, ZnONW induced macrophage-specific (CCL2) and eosinophil-specific (CCL11) chemokines and cytokines, such as IL-6 and TNF-α, in the air pouch and lungs because tissue-resident macrophages and epithelial cells coordinate the inflammatory response. Thus, it is imperative to determine which cell types produce these chemokines and cytokines in response to ZnONW. The identification and understanding of the cellular mediators that are involved in inflammation induced by ZnONW would help in defining the underlying inflammatory mechanisms activated by ZnONW. This understanding might also provide useful insights into and knowledge of the inflammatory potential of other ENMs with similar shapes and sizes as ZnONW.

In this study, the cellular uptake, subcellular localization, and inflammatory and toxic effects of ZnONW on cellular models were investigated. To represent phagocytic cells, BMDMs and RAW 264.7 cells were chosen, while

LKR13 cells were chosen to represent bronchial epithelial cells. First, to track ZnONW' cellular uptake and localization, it was necessary to generate fluorescent-labeled ZnONW (FITC-ZnONW). BMDM was exposed to FITC-ZnONW, and the uptake and localization of these particles in the lysosomes was detected using confocal microscopy. To prevent the solubilization of ZnONW, Bafilomycin-A1 (Baf-A1), a macrolide antibiotic isolated from the streptomyces species that inhibits the vacuolar H^+ATPase (V-ATPase), was used to inhibit the acidification of phagosomes. Next, the cell types that are involved in the production of IL-6 and TNF-α cytokines and chemokines CCL11 and CCL2, which were integrated into the inflammatory response *in vivo* in mouse models, were identified. BMDM, RWA264.7, and LKR13 cell supernatants were used to measure the levels of TNF-α, IL-6, IL-1β, and LTB4 and CCL11 and CCL2. Then, the requirement of phagocytosis for IL-6 and TNF-α production was investigated using CytD. Cell lysate was used to measure the fold changes in the expression levels of mRNA of TNF-α, IL-6, CCL2, CCL3, CCL4, CXCL1, and CCL11 in BMDMs, RAW 264.7 cells, and LKR13 cells.

Results:

Preparation and characterization

ZnONWs were synthesized using downstream microwave plasma reactor methods with a rapid oxidation of zinc powders in a gas phase [23]. The dimensions of ZnONWs as determined by Scanning Electron Microscopy (SEM) were around 20-120 nm in diameter and 5000 nm in length (Figure 11).

Cytotoxicity of ZnONWs for BMDM, LKR13, and RAW 264.7 cells

Previous studies showed the toxicity of ZnONP for mammalian cells *in vitro* [13, 25-27]. ZnONP induced toxicity in a variety of cells, such as kidney, liver, and lung cell lines [12, 13, and 26]. To investigate whether ZnONW exhibit distinct cytotoxicity profiles, both dose response and time course studies were conducted. The MTT assay was used to measure the metabolic activity of cells. First, macrophage cell lines (RAW-264.7 cells) were stimulated with different doses of ZnONW of 5, 10, 20, and 100 µg/ml for six hours. It was observed that at 5, 10, and 20 µg/ml, and the cells were 95% viable, whereas 100 µg/ml reduced the cells' viability by approximately 20% (Fig. 12a). As a result, 20 µg/ml and 100 µg/ml doses were selected to perform the time course studies. As shown (Fig. 12b), nearly 100% of the cells were viable after 18 hours of treatment with 20 µg/ml dose of ZnONW, whereas more than a 50% cell death was observed at 100 µg/ml. The cytotoxicity of ZnONW was also determined in other cell types, such as BMDM and LKR13 cells. In LKR13, a similar toxicity trend as RAW-264.7 cells was observed, as shown in Fig. 13a. In BMDM, a 20

µg/ml concentration of ZnONW induced significant toxicity after 18 hours of exposure by a reduction in cell viability up to 30%, whereas 100 µg/ml induced toxicity after only 4 hours of ZnONWs stimulation (Fig. 13b). Thus, all further studies with different cell types were performed with 20 µg/ml or less doses of ZnONW for 6 hours of treatment.

Cellular uptake and translocation of ZnONWs

To investigate the cellular uptake of ZnONW in BMDMs cells, FITC-labeled ZnONW was generated as previously described [20]. Since ZnONW tend to dissolve in the acidic condition, we used Baf-A1 to block the acidification and to facilitate the visualization of ZnONWs in the cells. In order to investigate the effect of Baf-A1 on blocking the acidification of the phagolysosome Acridine orange staining was used. Cells were primed with LPS for three hours followed by a one-hour pre-treatment with or without Baf-A1. Then, cells were exposed to 25 µg/ml FITC-labeled ZnONW for three hours and washed. Followed by Acridine orange staining and examined by confocal microscopy. As shown in Fig 14 ZnONWs treated cells showed enlarged lysosomal compartments whereas in Baf-A1 treated ZnONWs exposed cells no lysosomal staining was observed. These data suggested that Baf-A1 prevent block the acidification of the phagolysosome. To evaluate the uptake of the ZnONWs, cells were primed with LPS for three hours followed by a one-hour pre-treatment with Baf-A1. Then, cells were exposed to 25 µg/ml FITC-labeled ZnONW for three hours and washed and examined by confocal microscopy. As shown in Fig 15, intracellular

ZnONW was detected only in cells pre-treated with Baf-A1, whereas cells that were not treated with Baf-A1 did not show an intracellular accumulation of ZnONW particle. These results suggest that the inhibition of phagolysosome formation prevents the dissolution of intracellular ZnONWs in the cells.

Next, to track the trans-location of FITC-ZnONW in the cells, LAMP-1 staining, LAMP-1 stains late endosomal and lysosomal compartments in the cell, was used. Baf-A1-treated BMDMs were stimulated with FITC-ZnONW followed by LAMP-1 staining. The ZnONW treatments exhibited lysosomal clumping (Fig.16a). The LAMP-1 staining was overlapped by the FITC- ZnONW (Fig.16b).

ZnONW induces the release of pro-inflammatory mediators by macrophages *in vitro*

To examine the inflammatory potential of ZnONW, BMDMs were treated with ZnONW, and the levels of pro-inflammatory cytokines, such as IL-1β, IL-6, and TNF-α, as well as the lipid chemokine LTB_4 were measured in culture supernatants. Our previous study showed that SiONP induce the production of IL-1β and LTB4. Thus SiONP was used as positive controls for the production of IL-1β and LTB_4 [19, 28]. The treatment of BMDMs with ZnONW or ZnONP did not result in any significant accumulation of IL-1β or LTB4 (Fig. 17a). As expected, SiONP treatments induced the production of IL-1β and LTB_4 in BMDMs (Fig. 17a). ZnONW induced a dose-dependent increase in the production of the cytokines IL-6 and TNF-α (Fig. 17b). Furthermore, treatment with Baf-A1 significantly reduced the ZnONW-induced production of these

cytokines (Fig. 17b). A similar dose-dependent cytokine induction profile was observed in RAW 264.7 cells treated with ZnONW (Fig 18); however, the exposure of lung epithelial cell line LKR13 to ZnONW did not result in either IL-6 or TNF-α production. These results suggest that ZnONW could induce the synthesis of pro-inflammatory cytokines IL-6 and TNF-α but not IL-1β or LTB$_4$. The soluble Zn ions are mediating the toxicity of ZnONWs. However, did Zn ions induce the production of these cytokines? In order to investigate the ability of soluble zinc induce the induction of IL-6 and TNF-α. BMDMs were treated with ZnCl$_2$ for six hours. Then IL-6 and TNF-α were measured in culture supernatants supernatant. Interestingly, treatment of cells with ZnCl$_2$ did not induce the production of these cytokines (Fig 19).

ZnONWs upregulate TNF-α, IL-6, CCL11, and CCL2 at mRNA expression level

Previous studies showed that CS exposure in the lungs leads to an increase in LTB$_4$, IL-1β, and many CXC chemokines [232]. Because ZnONW-induced inflammation is significantly different from that of CS-induced inflammation, the mediators that contribute to this distinct pattern of inflammatory responses were examined. The mRNA levels of various cytokines and chemokines that regulate macrophage and eosinophilic inflammation were measured based on the cell types detected in *in vivo* studies. In BMDMs (Fig 20) and RAW 246.7 cells (Fig 21), the ZnONW and ZnONP resulted in significantly increased CCL4 and CCL11 and IL-6 and TNF-α expression. In addition, in the

culture supernatant, the CCL11 level was significantly increased, whereas CCL2 was not significant (Fig 20). In contrast, the exposure of the lung epithelial cell line LKR-13 led to an enhanced expression of CCL2 and CCL11 mRNAs and protein levels in cell supernatants by ZnONW and ZnONP (Fig 22). The CCL11 protein was upregulated in culture supernatants of ZnONWs exposed BMDMs and LKR13 cells (Fig 23). Whereas CCL2 were levels increased only in supernatants from LKR13 cells but not in BMDMs (Fig 23).These findings suggest a basis for the recruitment of macrophages and eosinophils due to the exposure of ZnONW.

Phagocytosis is required for ZnONWs-induced TNF-α and IL-6 production

To assess the cellular uptake mechanisms of ZnONW, cells were pre-treated with cytochalasin D (CytD) (phagocytosis inhibitor) and Baf-A1 [19, 24]. CytD treated cells did not show intracellular FITC-ZnONW, suggesting that phagocytosis is required for their uptake (Fig 24a).Furthermore, treatment with CytD significantly reduced the ZnONWs induced production of IL-6 and TNF-α (Fig 24b).

Discussion:

ZnONP has been known to induce toxicity and cell death to different mammalian cell lines [12, 32, 40-42]. It has been suggested that the solubility of ZnO in the acidic vacuoles is the underlying cause of ZnONP toxicity; however, the physical properties play a major role in ENPs toxicity. Thus, whether the change in the shape of high aspect ZnONW elicits a different toxicity behavior than ZnONP was investigated. It was found that ZnONW induced toxicity in different cell types, including BMDM, RAW 267.4, and LKR13 cells (Fig. 12, 13). Significant cell death was observed at 20 µg/ml of ZnONW after 18 hours of exposure; however, at 100 µg/ml, the cell viability was further reduced even at four hours of ZnONW exposure (Fig. 12). These results are in agreement with other previous studies, which suggested that ZnONW induce toxicity in cultured cells [4, 43]. Thus, all further studies with different cell types were performed at 20 µg/ml or less doses of ZnONW for six hours of exposure.

Macrophages play an important role in innate immune responses against ENMs [32]. The uptake mechanisms of the ENMs largely depend on the physiochemical properties of the particles, such as shape and size. Previous studies showed that the cellular uptake of ENMs, such as ZnONP, gold nanoparticles, sliver nanoparticles, iron oxide nanoparticles, and carbon nanotubes, is facilitated via clathrin, caveolae, and/or scavenger receptor-mediated endocytic pathways [141, 247-252]. In addition, very little free Zn ions exist in the cytosol of healthy cells, and they are mostly found to be bounded to proteins, such as metallothionins, or to be sequestered in cellular organelles,

70

such as mitochondria and lysosomes [253]. According to Xia et al., only small faint particles remnants were detected in RAW 264.7 after exposure to FITC-labeled ZnONP [224]. This could be explained by the dissolution of ZnONP inside the acidic vacuoles of the cells. Therefore, Baf-A1 was used to block the acidification of the acidic compartment of the cells (lysosome). To assess the effect of Baf-A1 on lysosomal acidification, acridine orange staining was used. Acridine orange emits green fluorescence in nuclear and cytoplasmic compartments, while acidic lysosomes or phagolysosome are stained orange to red. ZnONW-treated cells showed red enlarged lysosomal compartments. Acridine orange staining in the lysosomal compartments was completely absent in Baf-A1-treated cells exposed to ZnONW (Fig. 14). This indicated that Baf-A1 inhibited the acidification of the acidic compartment in the cells.

ZnONW was detected in intracellular compartments only in the presence of Baf-A1 (Fig. 15 a and b), an inhibitor of vacuolar acidification. It was concluded that in the absence of Baf-A1, the ZnONW taken up by these cells are readily solubilized to generate Zn ions.

The inflammatory pathways triggered by ENMs, such as SiONP, titanium dioxide nanoparticles (TiONP), and carbon nanotubes (CNT), were all linked to the activation of the inflammasome –caspase-1 related pathway (NLRP3) and the release of the cytokine IL-1 β [95, 96]. The current studies showed that the stimulation of BMDMs and RAW 267.4 cells with ZnONW did not induce IL- β or LTB$_4$ production, whereas SiONP induced both IL- β and LTB$_4$ (Fig. 17a), as expected. These results suggest that ZnONW do not activate the NLRP3

inflammasome pathway; however, ZnONP is known to induce the production of IL-6 and TNF-α [138, 254, 255]. The results also showed that ZnONW exposure leads to a significant increase in the production of both IL-6 and TNF-α in a dose-dependent manner in RAW267.4 (Fig. 18) and BMDM but not in LKR13 (Fig.17b) cells; however, in the presence of Baf-A1, exposure to ZnONW did not result in any IL-6 or TNF-α production, suggesting that soluble Zn ions mediate the induction of these cytokines (Fig.17b). Interestingly, the treatment of cells with ZnCl$_2$ did not induce the production of these cytokines (data not shown). Thus, the uptake of the particles as well as their dissolution within the phagolysosomeal compartment appears essential for the induction of cytokines, and the externally provided ZnCl$_2$ is not sufficient for activating the production of pro-inflammatory cytokines. Furthermore, both ZnONP [138, 254, 255] and ZnONW (current study) induced a similar cytokine profile, which suggests that it is the chemical nature rather than the shape of the ZnO ENMs that is the primary cause of the observed cytokine profile. Together, these results suggest that ZnONW induce a distinct inflammatory pathway from SiONP and other ENMs.

The molecular basis for the *in vivo* ZnONW-mediated cellular infiltration was further analyzed *in vitro* in different cell types. The CCL11, CCL2, IL-6, and TNF-α expression levels in BMDM (Fig. 19), RAW 267.4 (Fig. 20), and LKR13 cells (Fig. 21) stimulated with ZnONW was examined. The data suggested that lung epithelial cells and resident macrophages could be the primary responders to ZnONW, producing CCL2 and CCL11 and leading to macrophage and eosinophil recruitment to the site of exposure. Moreover, macrophages are

considered one of the major sources for TNF-α production upon activation. When cells are exposed to TNF-α, NF-kβ is activated, leading to the expression of many pro-inflammatory cytokines genes, such as IL-6 [256]. Furthermore, the upregulation of CCL11 and CCL2 mRNA expression is mediated via the intracellular signaling of TNF-α through the NF-Kβ pathway [257]. Because NF-Kβ is a transcription factor known to regulate both CCL11 and CCL2 promoters and to signal downstream of both the IL-6 and TNF receptors [257-259], further studies are needed to define the NF-Kβ signaling pathways that are activated upon ZnONW exposure and therefore involved in the production of CCL11, CLL2, IL-6, and TNF-α.

Phagocytosis typically involves the uptake of larger particles (>250nm). Aggregates of the FITC-ZnONW in the vacuoles (Fig. 15a) were consistently observed, suggesting that they may be taken up by the actin-dependent endocytic pathways. Consistent with this notion, treatment with CytD completely blocked the uptake of FITC-ZnONW (Fig. 23a). Moreover, CytD exposure to ZnONW did not result in any IL-6 or TNF-α production (Fig. 23b), suggesting that phagocytosis is required for the uptake and the production of IL-6 and TNF-α.

In summary, ZnONW induced the production of pro-inflammatory cytokines IL-6 and TNF-α and and eosinophil-specific CCL11 in BMDMs. In contrast LKE13 cells induce the production of CCL2 and CCL11 only but not IL-6 and TNF-α. These results suggest that lung epithelial cells could be the primary source for CLL2 and CLL11 which lead to recruitment of macrophage and

eosinophils to the site of exposure. And macrophages as the secondary

responder that in turn produce the IL-6, TNF-α and CCL11.
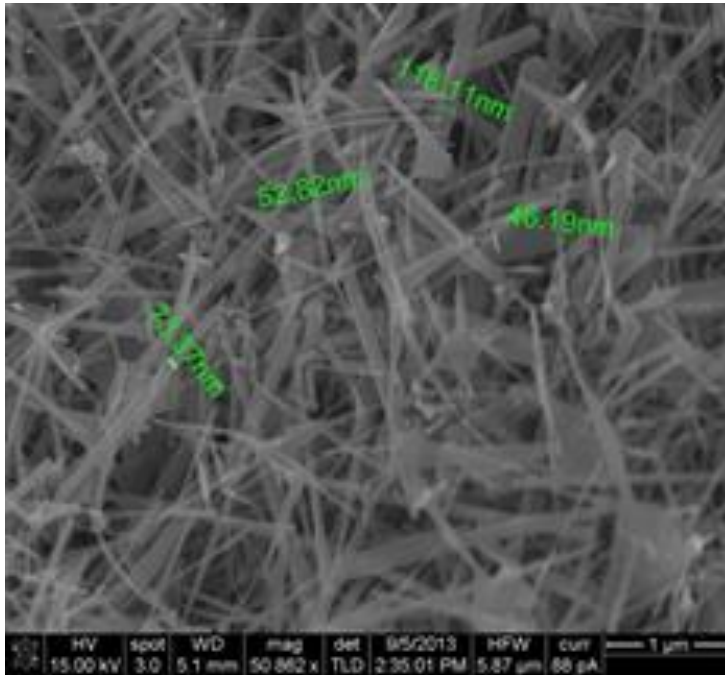
Figure 11: Scanning Electron Microscopy (SEM) of ZnONWs.

Scanning Electron Microscopy (SEM) image of ZnONWs indicating size of individual nanowires. The dimensions of ZnONWs as determined by Scanning Electron Microscopy (SEM) were around 20-120 nm in diameter with 5000 nm in length.

RAW 264.7
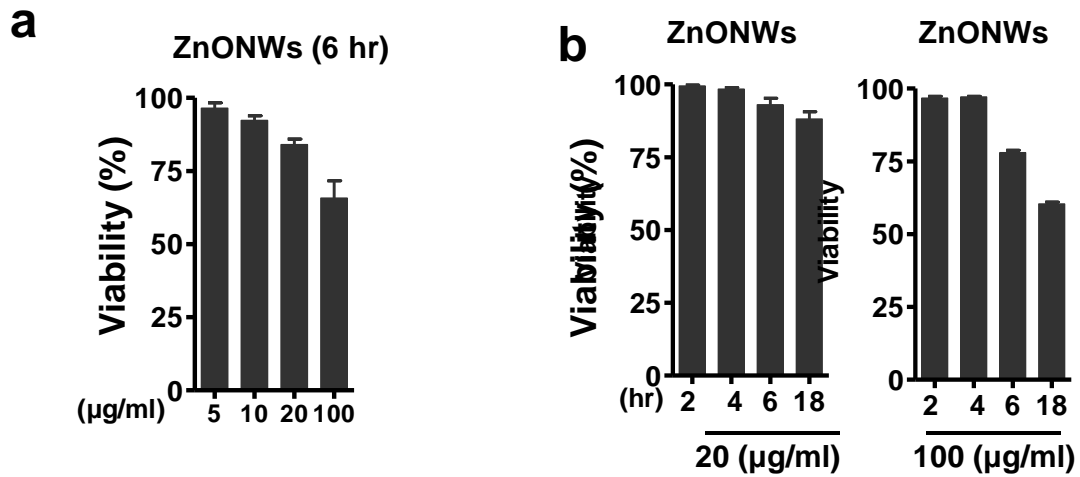
Figure 12: Cytotoxicity assessment of ZnONW.

0.5x106 cells /ml of RAW-264.7 cells were stimulated with different concentrations for different times with ZnONW as indicated or with PBS as negative control. Cell viability was assessed using MTT test. RAW-264.7 cells were stimulated with ZnONW 5, 10, 20 and 100 µg/ml for 6 hours (a). Time course study for RAW-264.7 cells, cells were stimulated with ZnONW 20µg/ml & 100µg/ml concentrations for 2, 4, 6 & 18 hours (b). Data represented is from one of the three experiments. Data are expressed as mean ± SE. **p< 0.01, ***p< 0.001 non-parametric-test.

Figure 13: Cytotoxicity assessment of ZnONW.

0.5×10^6 cells /ml of BMDMs from WT mice, LKR13 cells were stimulated with different concentrations for different times points with ZnONW as indicated or with PBS as negative control. Cell viability was assessed using MTT test. LKR13 cells were stimulated with ZnONW 20µg/ml & 100µg/ml concentrations for 2, 4, 6 & 18 hours (a). BMDMs were stimulated with ZnONW 20µg/ml & 100µg/ml concentrations for 2, 4, 6 & 18 hours (b). Data represented is from one of the three experiments. Data are expressed as mean ± SE. **p< 0.01, ***p< 0.001 non-parametric-test.
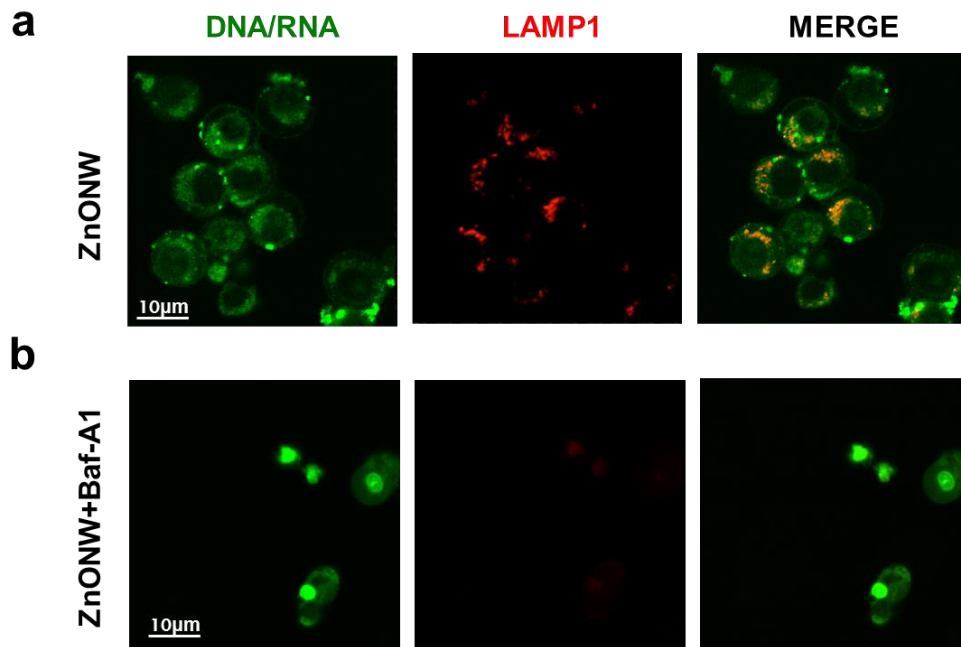
Figure 14: Inhibition of phagolysosome formation using Baf-A1 inhibitor.

LPS-primed BMDMs were stimulated with 25 µg/ml ZnONW for 3 h in the presence (b) or absence of Baf-A1 (a). Cells were stained with acridine orange for 30 min after ZnONWs exposure. Acridine orange stains the acidic vacuoles in the cells such as phagolysosome with orange to red color whereas DNA/RNA or cytoplasm of the cell with green color. Cells were visualized by Nikon A1 confocal microscopy. A minimum of five fields were captured for each sample in every experiment.
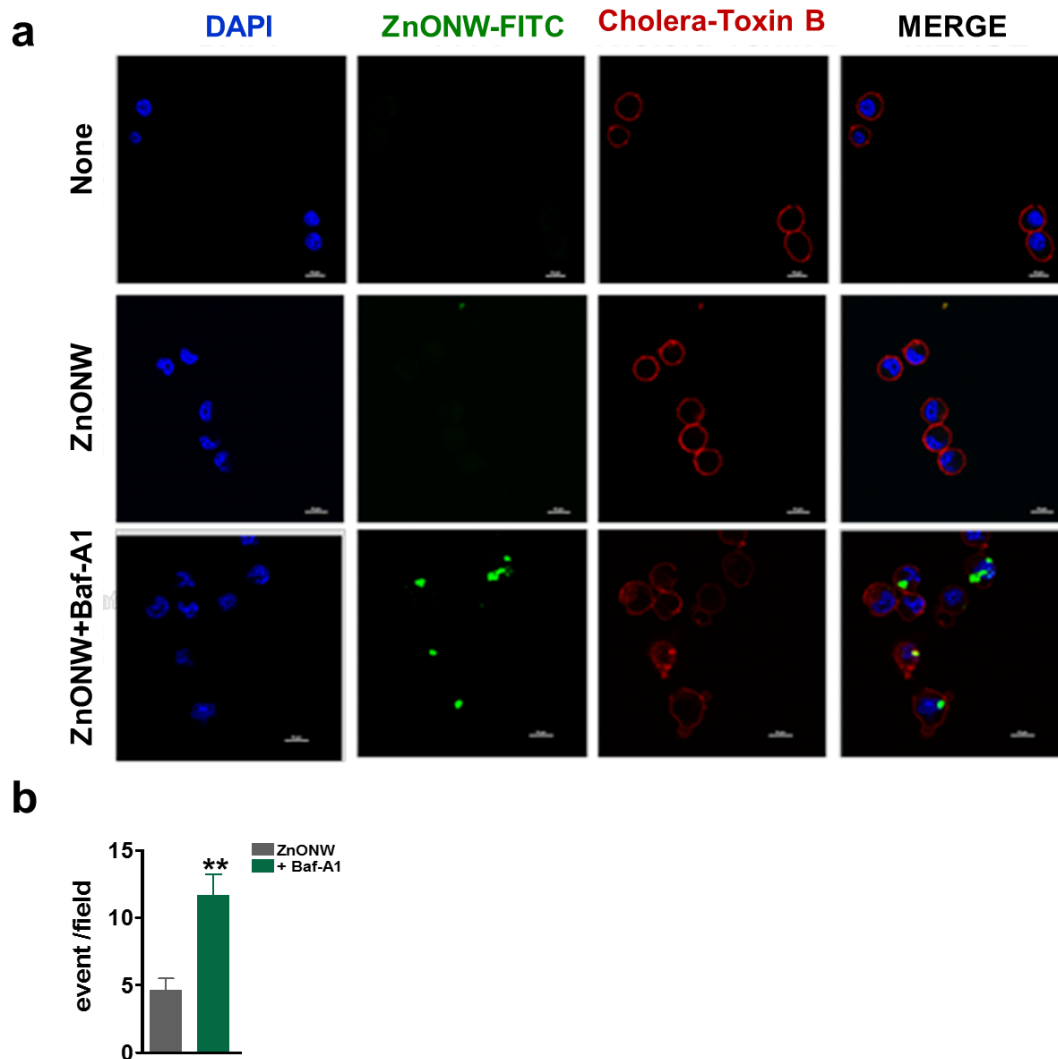
Figure 15: Cellular uptake of ZnONWs.

LPS-primed BMDM cells were stimulated with 30µg/ml FITC-ZnONW for 3h in the presence or absence of Baf-A1 (1µg/ml). Cells were stained with cholera-toxin B (red) and DAPI (blue) for 20min after fixation and visualized by Nikon A1 confocal microscopy (a). The density of intracellular ZnONW particles was calculated as number of particle events/ high power field as indicated in (b). Data represented is from one of the three experiments. Data are expressed as mean ± SE. **$p < 0.01$, ***$p < 0.001$ non-parametric-test.
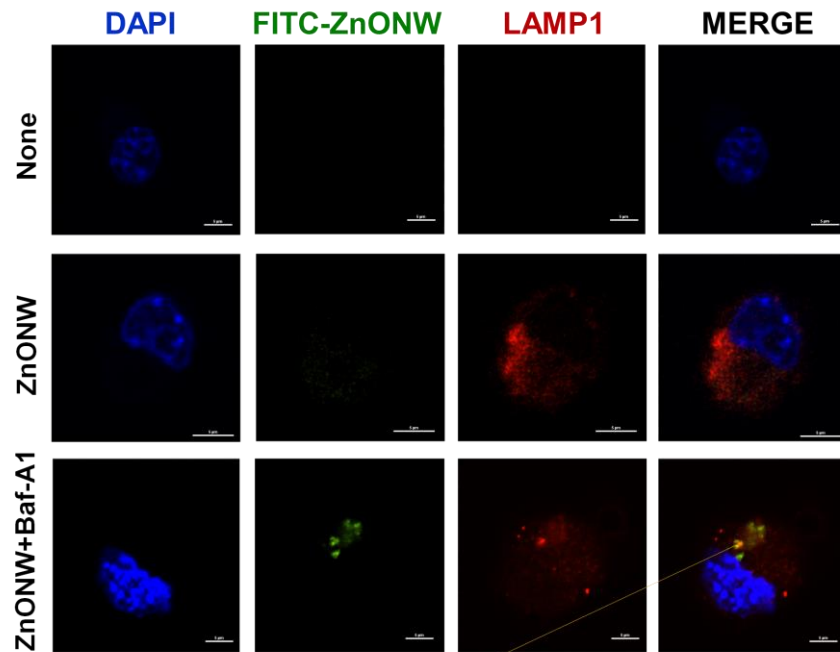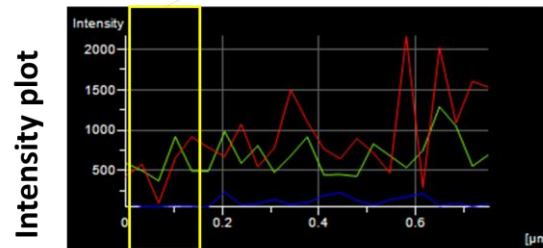
Figure 16: Sub-cellular localization of ZnONWs.

LPS-primed BMDM cells were stimulated with 30 μg/ml FITC-ZnONW for 3h in the presence or absence of Baf-A1 (1 μg/ml). After fixation and permeabilization, cells were stained with 1 μg/ml 1 μg/ml anti LAMP-1 antibody followed by Alexa 594 labeled antibody to visualize lysosomes (red) and DAPI (blue) (a). The intensity plot shows the overlapping of green and red signals (b).
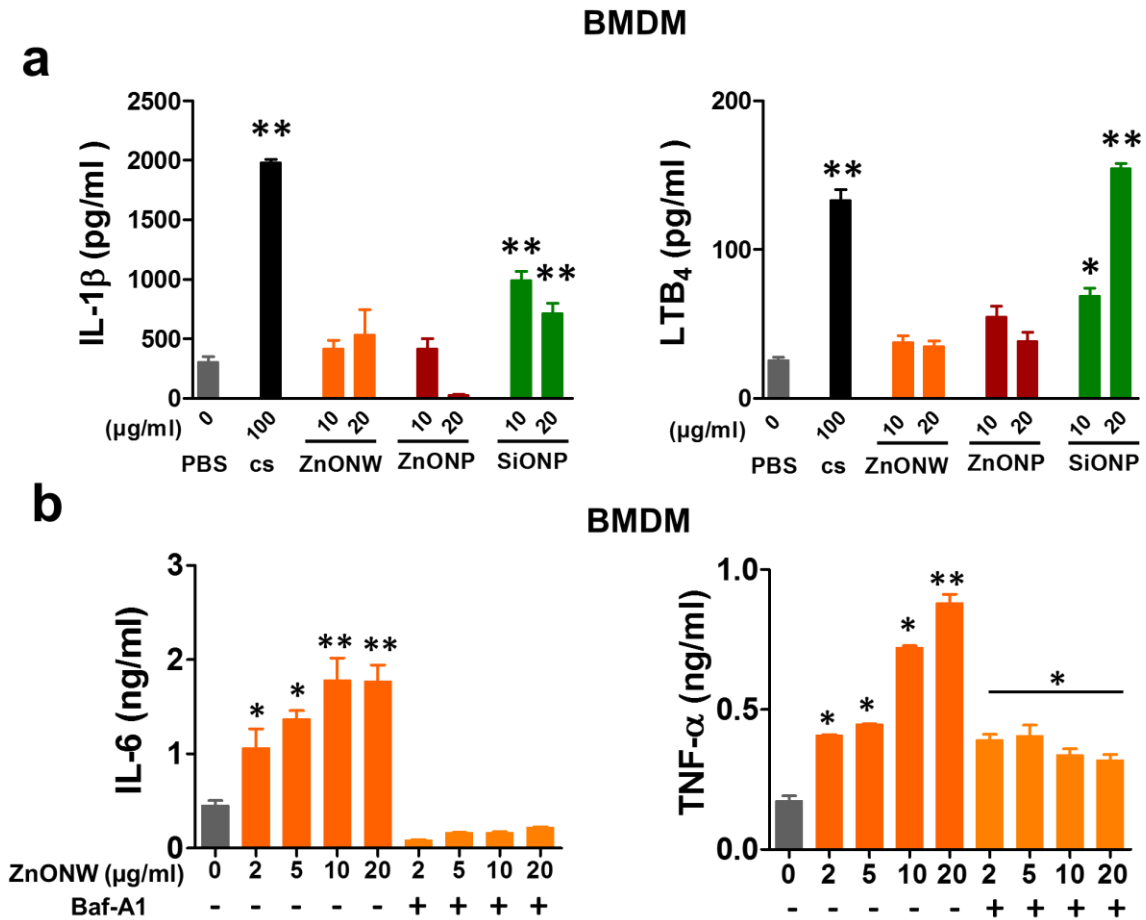
Figure 17: ZnONWs exposure induced the release of pro-inflammatory mediators by macrophages *in vitro*.

Pro-inflammatory cytokines levels from PBS or particles (ZnONP, ZnONW & SiONP) exposure in culture supernatants were analyzed using ELISA. IL-1β and LTB4 levels were measured in BMDMs exposed for 6hrs. Cells were primed with LPS (10ng/ml) for 3h and washed and then treated with ZnONW, ZnONP, SiONP or PBS (a). BMDMs cells were primed with LPS (10ng/ml) for 3h and washed then treated with or without Baf-A1. Then cells were treated with ZnONW or PBS for 6hrs, IL-6 and TNF-α levels were measured as indicated (b). Data represented is from one of the three experiments. Data are expressed as mean ± SE. **p< 0.01, ***p< 0.001 non-parametric-test.
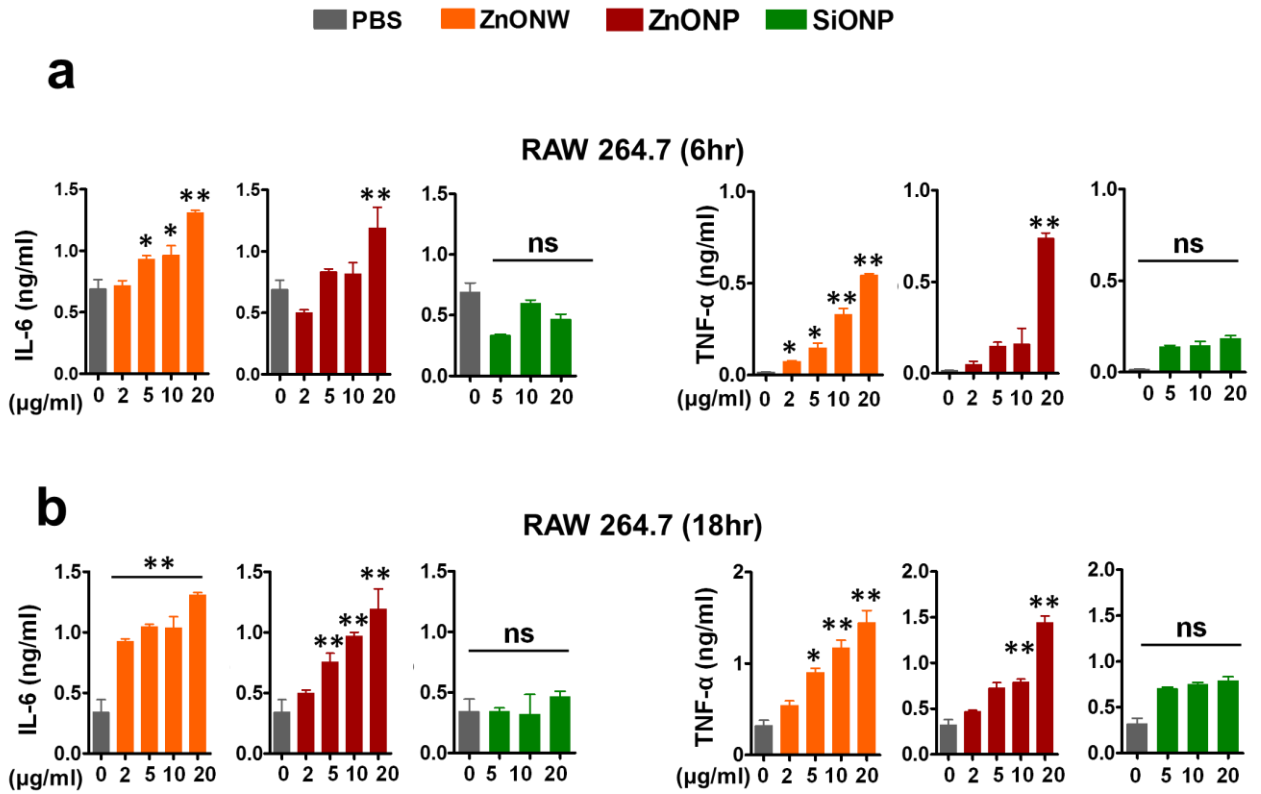
Figure 18: ZnONWs exposure induced the release of pro-inflammatory mediators by macrophages *in vitro*.

Pro-inflammatory cytokine levels from PBS or particles (ZnONP, ZnONW & SiONP) treated RAW264.7 cell culture supernatants were analyzed using ELISA. RAW 264.7 cells were stimulated with LPS (10 ng/ml) for 3h. Then cells were treated with ZnONW, ZnONP, SiONP or PBS for 6hrs (a) or 18 hrs (b) and the IL-6 and TNF-α levels were measured in the supernatants. Data represented is from one of the three experiments. Data are expressed as mean ± SE. **p< 0.01, ***p< 0.001 non-parametric-test.
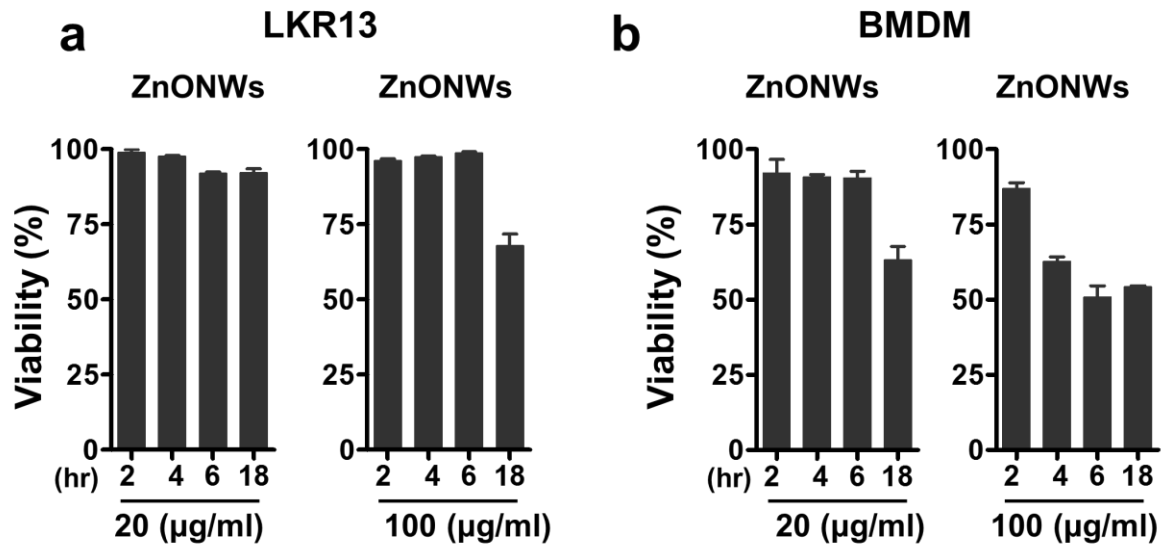
BMDM

a IL-6

b TNF-α
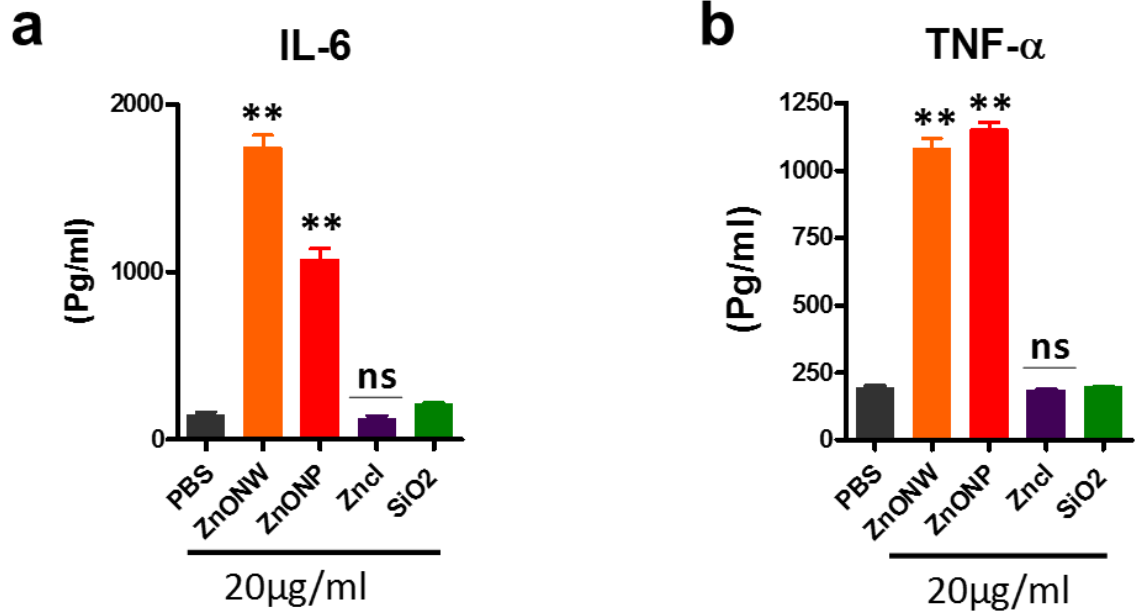
Figure 19: ZnCl₂ did not induced the release of IL-6 or TNF-α by macrophages *in vitro*.

BMDM cells were stimulated with LPS (10ng/ml) for 3h. Then cells were treated with ZnONW, ZnONP, ZnCL, SiONP or PBS for 6hrs, IL-6 (a) and TNF-α (b) levels were measured as indicated in the culture supernatants using ELISA. Data represented is from one of the three experiments. Data are expressed as mean ± SE. **p< 0.01, ***p< 0.001 non-parametric-test.
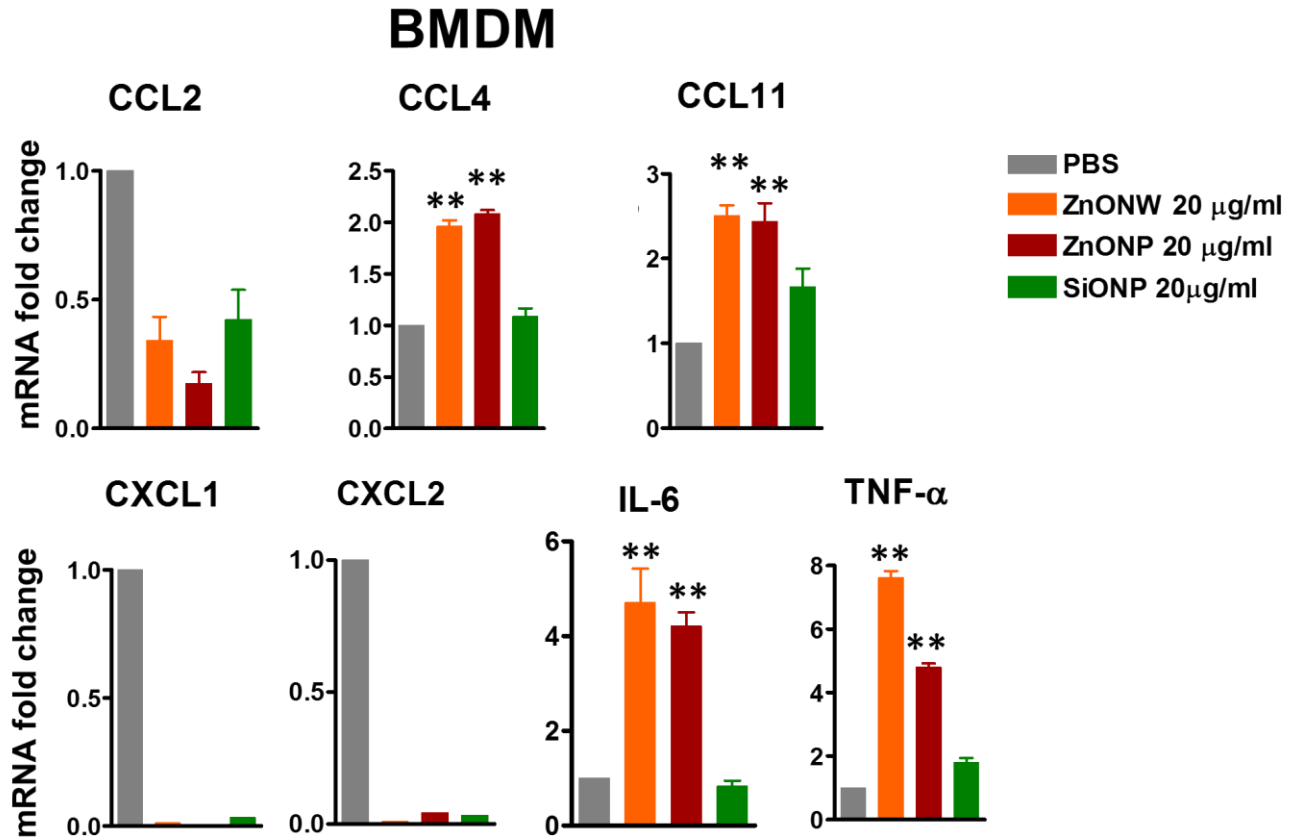
BMDM

**Figure 20: Inflammatory mediators induced by ZnONWs exposure.**

Cytokines and chemokines expression levels were analyzed in BMDM cells and LKR13 cells from PBS or particles treated cells using qRT-PCR. Various level of inflammatory genes mainly IL-6, TNF-α, CCL2, CCL4, CCL11, CXCL1 & CXCL2. (a) Cytokines and chemokines levels from BMDMs cells. (b) from LKR13 cells. Data represented is from one of the three experiments. Data are expressed as mean ± SE. **p< 0.01, ***p< 0.001 non-parametric-test.
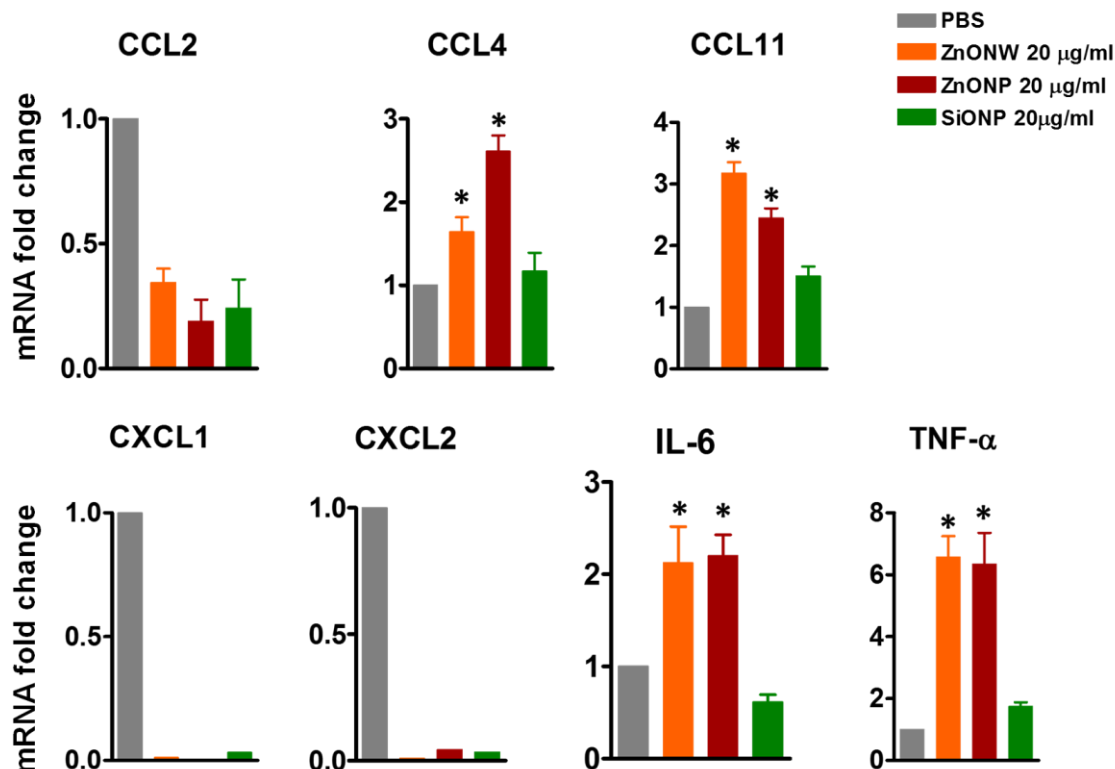
Figure 21: Expression levels of inflammatory marker induced by ZnONWs in RAW 264.7 cells.

Expression of cytokines and chemokines mRNA levels were analyzed in RAW 264.7 cells exposed to PBS or particles treated cells using qRT-PCR. Inflammatory marker IL-6, TNF-α, CCL2, CCL4, CCL11, CXCL1 and CXCL2. Data represented is from one of the three experiments. Data are expressed as mean ± SE. **p< 0.01, ***p< 0.001 non-parametric-test.
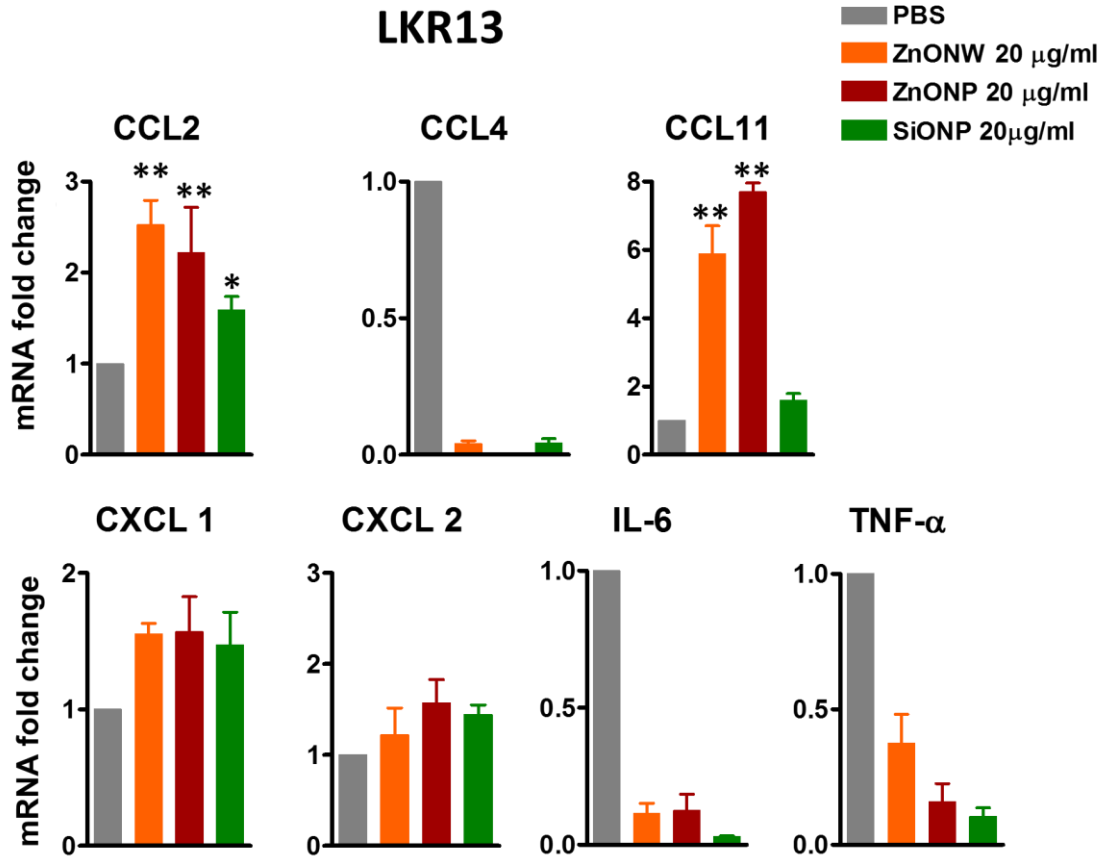
Figure 22: Inflammatory mediators induced by ZnONWs exposure.

Cytokines and chemokines levels were analyzed in LKR13 cells from PBS or particles treated cells using qRT-PCR. Various level of inflammatory genes mainly IL-6, TNF-α, CCL2, CCL4, CCL11, CXCL1 & CXCL2. Data represented is from one of the three experiments. Data are expressed as mean ± SE. **p< 0.01, ***p< 0.001 non-parametric-test.
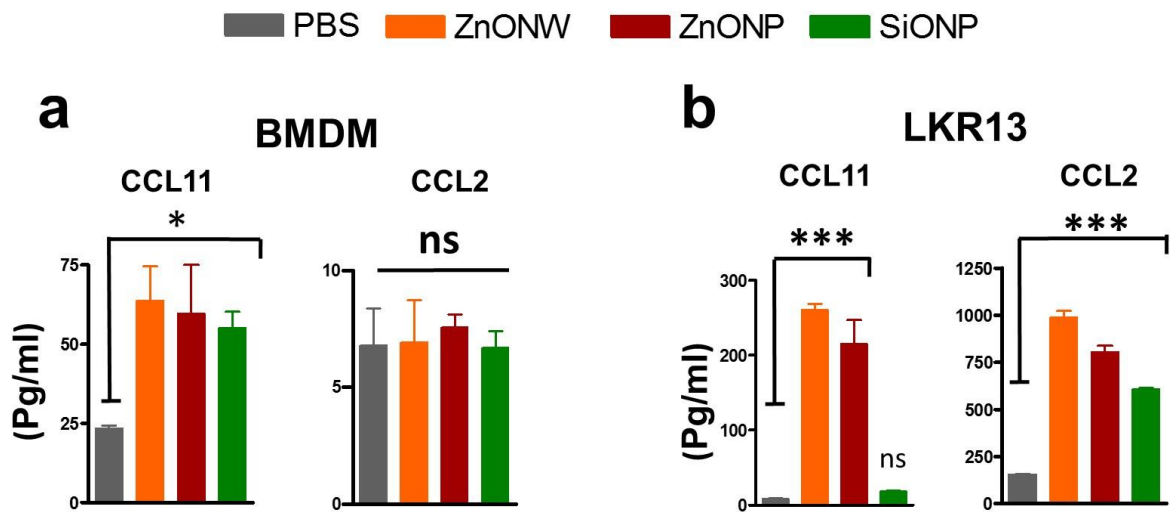
**Figure 23: CCL11 and CCL2 levels induced by ZnONWs in BMDMs and LKR13 cells.**

The levels of CCL11 and CCL2 proteins were determined in the culture supernatants from (a) BMDM and (b) LKR13 cells using ELISA. Data represented is from one of the three experiments. Data are expressed as mean ± SE. **p< 0.01, ***p< 0.001 non-parametric-test.

a

	DAPI	ZnONWs	Cholera-Toxin B	MERGE
None				
+Baf-A1				
+Baf-A1 +CytD				

b

BMDM

ZnONW (µg/ml)	0	2.5	5	10	20	2.5	5	10	20
CytD	-	-	-	-	-	+	+	+	+
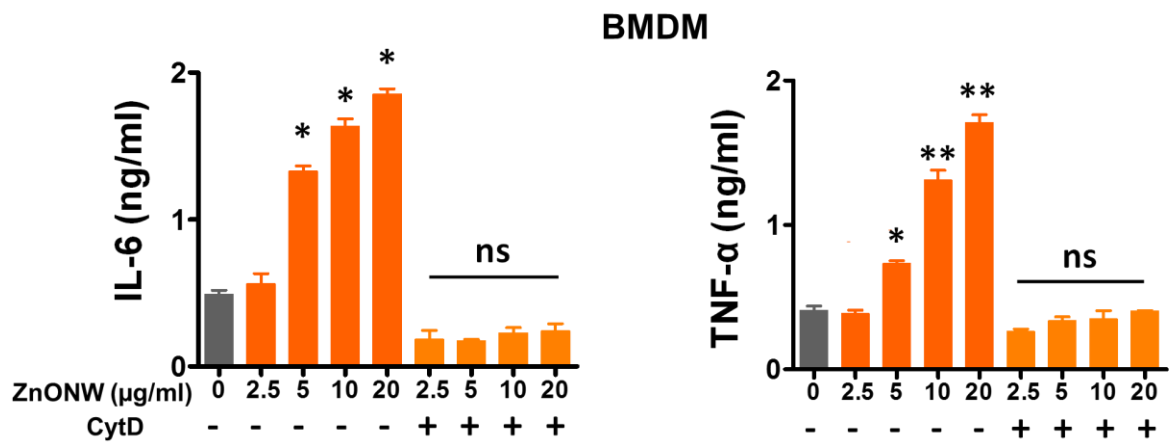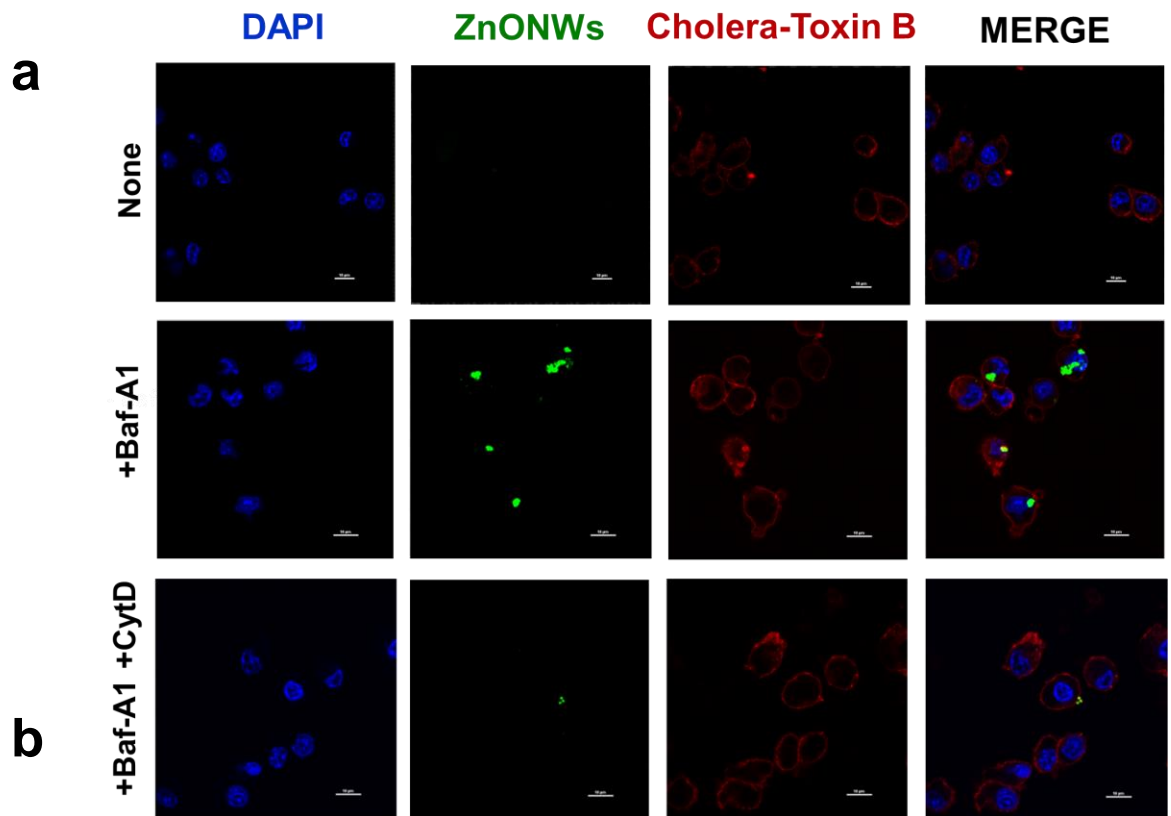
Figure 24: Phagocytosis is required for ZnONWs induced TNF-α and IL-6 production.

10 ng/ml LPS-primed BMDM cells were stimulated with 25 µg/ml FITC-ZnONW for 2h in the presence or absence of CytD (10µg/ml). Cells were stained with cholera-toxin B (red) and DAPI (blue) for 20 min after fixation and visualized by Nikon A1 confocal microscopy (a). BMDMs cells were primed with LPS (10ng/ml) for 3h and washed then treated with or without (1 µM) Baf-A1. Then cells were treated with ZnONW or PBS for 6hrs, IL-6 and TNF-α levels were measured as indicated (b). Data represented is from one of the three experiments. Data are expressed as mean ± SE. **p< 0.01, ***p< 0.001 non-parametric-test.

CHAPTER 5

# CONCLUSIONS

In the last two decades, with the advent of nanotechnology, the use of ENMs have become widespread due to their applicability in many areas including industry, agriculture, and medicine. ENMs are materials that were created and designed with specific shapes and sizes to produce new materials at nano-scale. The rapid development and the increase in use of ENMs in consumer products have created a gap and challenge through limited knowledge about the safe and sustainable use of ENMs. Previous studies indicated that some ENMs can be cytotoxic. Furthermore, some forms of ENMs can cross the blood-brain barrier inducing neurotoxicity, brain tissue damage, and inflammation [260]. However, the long-term consequences of exposure to most of these particles are unknown.

Zinc oxide (ZnO) has long been employed in many consumer products especially in sunscreen [225]. Despite the common use of ZnONP, the safety of these particles needs further investigation and the potential biological effects to humans are still unclear.

Moreover, the tremendous advancement in the field of nanotechnology has led to the emergence of new forms of ZnO ENMs called high aspect ratio ZnONW. These particles are being developed and introduced to the market with production rate estimated by millions of tons per year. The use of ZnONP is considered relatively safe, however with ZnONW, there is uncertainty about the safety of these ZnONW and their impact at the biological level. The rapid production of ZnONW pose a large of risk exposure for public and foundry workers.

Here in this study we found that ZnONW induces toxicity and cell death to BMDM, RAW267.4, and LKR13 cells. Significant toxicity was observed at 20 µg/ml of ZnONWs exposure for 18 hrs. However, at 100 µg/ml the cell viability is further reduced even at 4h of ZnONWs exposure. Based on previous studies done with ZnONP as mentioned in chapter 1, the toxicity is mainly due to the solubility of ZnONP inside the acidic vacuoles of the cells. We speculated that ZnONW induce toxicity similar to ZnONP since both ZnONW and ZnONP have the same chemical composition.

The uptake mechanisms of the ENMs largely depend on shape, size and physiochemical properties of the particles. Previous studies showed that cellular uptake of ENMs such as ZnONPs, gold nanoparticles, sliver nanoparticles, Iron oxide nanoparticles and carbon nanotubes is facilitated through different uptake mechanism based on the size of ENMs [67, 248-250, 260, 261]. ENMs that have size less than 10 nm cross cell membrane via direct diffusion or non-specific pathways. Clathrin, caveolae and/or scavenger receptor-mediated endocytic

pathways were found mainly with ENMs that have a size between 50- 150 nm. Larger ENMs (200-2000 nm) were believed to be internalize thorough phagocytosis pathway. Our studies showed that visible uptake of FITC-ZnONW aggregate with cells that were treated with Baf-A1. Based on the aggregate size we speculated that these FITC-ZnONW aggregate may be taken up by the actin-dependent endocytic pathways. Consistent with this notion, treatment with CytD completely blocked the uptake of FITC-ZnONW. These results indicated that phagocytosis appeared to be essential for uptake of ZnONW.

Direct contact through skin and airway exposure are the most common routes of exposure to ZnONW. This current study provided the first experimental evidence that ZnONW induce localized inflammation in a murine air-pouch model, resulting in a broad inflammatory response by infiltration of macrophages, eosinophils, and neutrophils: production of CCL11, CCL2, IL-6 and TNF-α. In contrast, intra-tracheal instillation of ZnONW in a healthy mouse without prior sensitization induced eosinophilic air-way inflammation and a tight and regulated inflammation in the lung by a massive influx in macrophages and eosinophils as well as remarkable increase in levels of CCL11, CCL2, IL-6 and TNF-α that are consistent with cell types infiltrated in the lung. The inflammatory response from ZnONW was distinct and different from SiONPs that induce neutrophilic inflammation both in lung and air-pouch.

To have a better understanding of this type of inflammation, the inflammatory mediators induced upon ZnONW exposure were investigated. Inflammasome (NLRP3) and IL-1β release are considered as common pathway

92

in which ENMs induce sterile inflammation [100]. Previous studies from table 2 above showed that some ENMs such as SiONP, CNT and TiONP induce the production IL-1β throw the activation of Inflammasome (NLRP3) pathway. On the other hand most of these studies did not investigated the possibility of endotoxin (LPS) contamination of ENMs, LPS contamination could lead to a misleading result since LPS could induce the activation of Inflammasome (NLRP3) pathway and production of IL-1β. Here, ZnONW was made endotoxin-free by baking at 200°C overnight to overcome the possibility of endotoxin (LPS) contamination. Earlier studies from our laboratory showed that crystalline silica exposure (CS) induced neutrophilic inflammation in the air pouch model with a significant increase in the levels of IL-1β and LTB4 [232]. This type of inflammation observed with the CS is linked to the lipidosome activation and LTB4 production as well as NLRP3 inflammasome pathway leading to caspase-1 activation [232]. ZnONW did not induce the production of IL-1β nor LTB4. Indication that ZnONW do not activate the inflammasome pathway. Instead ZnONW induce the production of IL-6 and TNF-α in a dose-dependent manner. Since IL-6 and TNF-α are produced after ZnONWs exposure, it appears that inflammation induced by ZnONWs is mediated via NF-Kβ pathway. IL-6 and TNF-α level were significantly reduced and after Baf-A1 and CytD treatment, suggesting that both the uptake and solubility of ZnONW essential for IL-6 and TNF-α. Moreover, exposure of BMDM to ZnONW induced the production of CCL11 while LKR13 cells induced both CCL11 and CCL2. The production of these chemokines and cytokines were consistent with our previous findings to

the cell types recruited in the site of exposure in lung and air-pouch mouse model.

ZnONP toxicity was linked to the solubility of the particles under acidic conditions in the cell. However, pre-treatment of BMDMs with Baf-A1 did not result of IL-6 or TNF-α production upon ZnONW exposure. These results indicated that soluble zinc ions were mediating the production of these cytokines. In addition, treatment of BMDMs with $ZnCl_2$ was not sufficient for the production of pro-inflammatory cytokines, suggesting that the uptake of ZnONW and their dissolution within the phagolysosome compartment is required for the activation and production of IL-6 and TNF-α.

Studying the potential negative health implications for ZnONW exposure in animal models might give an insight to the possible adverse outcome for exposure to these particles and other ENMs that have similar properties.
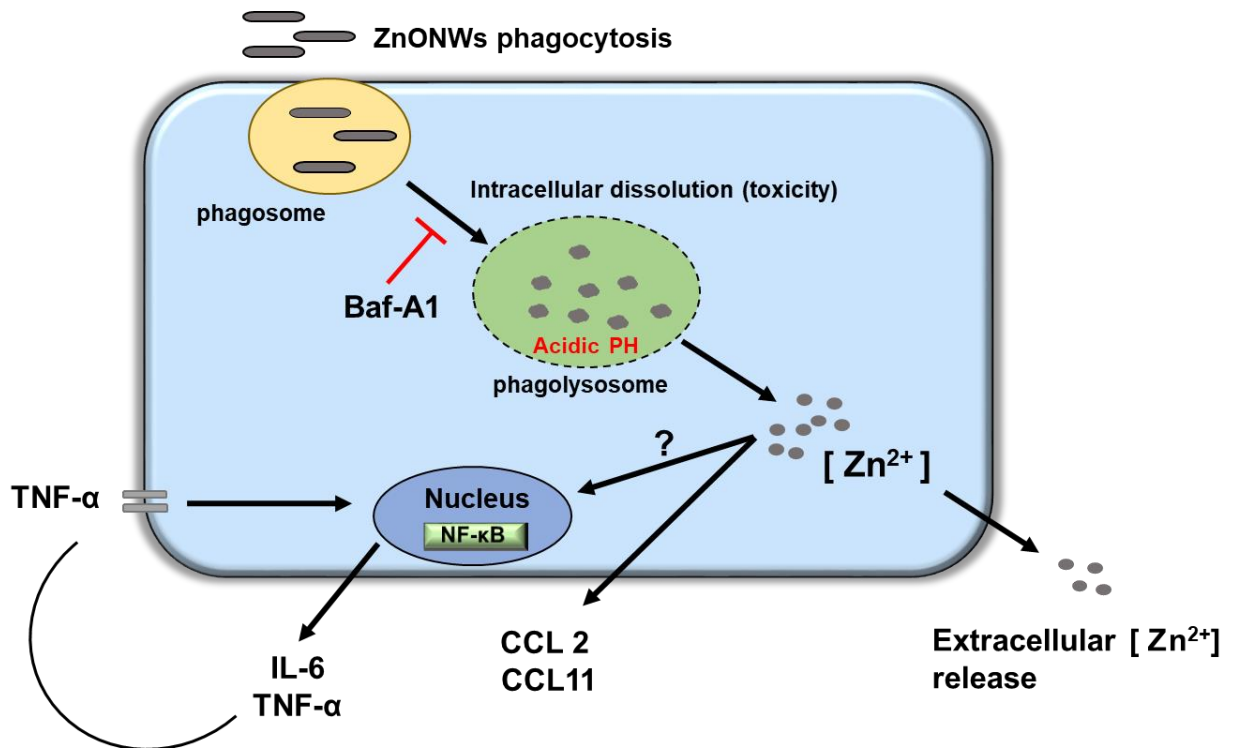
Figure 25: Graphical summary.

Cells take up ZnONW by phagocytosis process. During phagosome maturation pH drops and ZnONWs starts to dissolve. The intracellular dissolution leads to an increase of the Zn ion concentration and lysosomal destabilization, leading to toxicity and production of IL-6 and TNF-α, CCL2, and CCL11. Blocking the acidification of phagolysosome with Baf-A1 prevents the production of these cytokines.

FUTURE DIRECTIONS

This dissertation studied the potential toxicity and inflammatory effects of ZnONW in a murine mouse model and cultured cells. Although this study outlines only the biological consequences for exposure to ZnONW in vivo and ex-vivo, it raises important issues and questions that are needs to be addressed and worth investigation.

Studies presented here indicated that ZnONW induce toxicity and cell death to different cell lines. Toxicity of ENMs depends on both the physical and chemical properties. Moreover, very little is known and understood about the mechanisms of ENM toxicity in mammalian cells lines. The fact that ZnONW have sensitive dissolution points in the acidic aqueous conditions in the cells, and ZnO dissolution has been shown to play a role in the acute or chronic toxicity, the novel 1D morphology of ZnONW could lead to a different toxicological profile. Therefore, future studies could be aimed at understanding the impacts of the physical properties of ZnONW on toxicity.

Confocal microscopy images revealed that ZnONW inside the cells were taken up as aggregated in presence of Baf-A1 and not as a single individual particle. However, we do not know whether this aggression can be reversed or how long these can be persisting or how they could activate an inflammatory cascade. Thus, mechanistic studies need to be conducted to investigate ZnONW' immunomodulatory effects.

In our previous study, crystalline silica (CS) induced sterile inflammation through the activation of NLRP3- inflammasome pathway and the production of

IL-1β and LTB$_4$. Based on our results here, ZnONW induced sterile inflammatory responses in lung and air-pouch mouse models that were qualitatively and quantitatively distinct from CS and SiONP. ZnONW induced the recruitments of eosinophils and macrophages as well as the production of CCL2, CCL11 and IL-6, and TNF-α. Previous studies with ZnONP revealed that pulmonary exposure to ZnONP induce the recruitment of neutrophils in lung. However, here in this study, ZnONW did not induce the infiltration of neutrophil in the lung; this could be explained by either the overwhelming cellular infiltration or that ZnONW' shape elicit a different response than ZnONP.

The cellular basis of the production of these chemokine and cytokines was investigated. We demonstrated the importance of LKR13 cells in the production of CCL11 and CCL2, with BMDMs and RAW 264.7 cells as the main source for IL-6 and TNF-α and its contribution to the production of CCL11. However, the actual sequence of the production of these chemokines and cytokines remains unknown. Future experiments could be aimed at understanding how this inflammatory pathway initiates and the molecular pathways involved need to be examined using inhibitors of phagocytosis and assessed using Western Blotting techniques.

Lastly, this study could reveal important information about sterile inflammatory effects of ZnONW which could apply to similar ENMs that may have similar physical or chemical characteristics to ZnONW.

REFERENCES

1. Schug, T.T., et al., *ONE Nano: NIEHS's strategic initiative on the health and safety effects of engineered nanomaterials.* Environ Health Perspect, 2013. **121**(4): p. 410-4.

2. Wang, X., S.P. Reece, and J.M. Brown, *Immunotoxicological impact of engineered nanomaterial exposure: mechanisms of immune cell modulation.* Toxicol Mech Methods, 2013. **23**(3): p. 168-77.

3. Donaldson, K., et al., *The pulmonary toxicology of ultrafine particles.* J Aerosol Med, 2002. **15**(2): p. 213-20.

4. Duffin, R., N.L. Mills, and K. Donaldson, *Nanoparticles-a thoracic toxicology perspective.* Yonsei Med J, 2007. **48**(4): p. 561-72.

5. Oberdorster, G., E. Oberdorster, and J. Oberdorster, *Nanotoxicology: An emerging discipline evolving from studies of ultrafine particles.* Environmental Health Perspectives, 2005. **113**(7): p. 823-839.

6. U.S. Environmental Protection Agency, O.o.R.a. and Development:, *Air quality criteria for particulate matter.* Washington, D.C.;, 1994(3 600/P-95-001cF.).

7. Griffin, S., et al., *Natural Nanoparticles: A Particular Matter Inspired by Nature.* Antioxidants (Basel), 2017. **7**(1).

8. Gubala, V., et al., *Engineered nanomaterials and human health: Part 1. Preparation, functionalization and characterization (IUPAC Technical Report).* Pure and Applied Chemistry, 2018. **90**(8): p. 1283-1324.

9. Schwerha, J.J., *Fantastic voyage and opportunities of engineered nanomaterials: What are the potential risks of occupational exposures?* Journal of Occupational and Environmental Medicine, 2010. **52**(9): p. 943-946.

10. *<Engineered Nanoparticles in Consumer Products- Understanding a New Ingredient.pdf>.*

11. Wise, K. and M. Brasuel, *The current state of engineered nanomaterials in consumer goods and waste streams: the need to develop nanoproperty-quantifiable sensors for monitoring engineered nanomaterials.* Nanotechnol Sci Appl, 2011. **4**: p. 73-86.

12. Contado, C., *Nanomaterials in consumer products: a challenging analytical problem.* Front Chem, 2015. **3**: p. 48.

13. Calzolai, L., D. Gilliland, and F. Rossi, *Measuring nanoparticles size distribution in food and consumer products: a review.* Food Addit Contam Part A Chem Anal Control Expo Risk Assess, 2012. **29**(8): p. 1183-93.

14. Michel, K., et al., *Risk assessment of amorphous silicon dioxide nanoparticles in a glass cleaner formulation.* Nanotoxicology, 2013. **7**(5): p. 974-88.

15. Lu, P.J., et al., *Analysis of titanium dioxide and zinc oxide nanoparticles in cosmetics.* J Food Drug Anal, 2015. **23**(3): p. 587-594.

16. Randviir, E.P., D.A.C. Brownson, and C.E. Banks, *A decade of graphene research: production, applications and outlook.* Materials Today, 2014. **17**(9): p. 426-432.

17. Cha, C., et al., *Carbon-based nanomaterials: multifunctional materials for biomedical engineering.* ACS Nano, 2013. **7**(4): p. 2891-7.

18. Wang, Z., et al., *Carbon nanomaterials-based electrochemical aptasensors.* Biosens Bioelectron, 2016. **79**: p. 136-49.

19. Roco, M.C., *International perspective on government nanotechnology funding in 2005.* Journal of Nanoparticle Research, 2005. **7**(6): p. 707-712.

20. Inshakova, E. and O. Inshakov, *World market for nanomaterials: structure and trends*. Vol. 129. 2017. 02013.

21. Yokel, R.A. and R.C. Macphail, *Engineered nanomaterials: exposures, hazards, and risk prevention.* J Occup Med Toxicol, 2011. **6**: p. 7.

22. Nowack, B., et al., *Meeting the Needs for Released Nanomaterials Required for Further Testing-The SUN Approach.* Environmental Science & Technology, 2016. **50**(6): p. 2747-2753.

23. Bour, A., et al., *Environmentally relevant approaches to assess nanoparticles ecotoxicity: a review.* J Hazard Mater, 2015. **283**: p. 764-77.

24. Gottschalk, F., T. Sun, and B. Nowack, *Environmental concentrations of engineered nanomaterials: review of modeling and analytical studies.* Environ Pollut, 2013. **181**: p. 287-300.

25. Hunt, G., et al., *Towards a Consensus View on Understanding Nanomaterials Hazards and Managing Exposure: Knowledge Gaps and Recommendations.* Materials (Basel), 2013. **6**(3): p. 1090-1117.

26. Lazareva, A. and A.A. Keller, *Estimating Potential Life Cycle Releases of Engineered Nanomaterials from Wastewater Treatment Plants.* Acs Sustainable Chemistry & Engineering, 2014. **2**(7): p. 1656-1665.

27. Cornelis, G., et al., *Fate and Bioavailability of Engineered Nanoparticles in Soils: A Review.* Critical Reviews in Environmental Science and Technology, 2014. **44**(24): p. 2720-2764.

28. Garner, K.L. and A.A. Keller, *Emerging patterns for engineered nanomaterials in the environment: a review of fate and toxicity studies.* Journal of Nanoparticle Research, 2014. **16**(8).

29. Baalousha, M., et al., *Modeling nanomaterial fate and uptake in the environment: current knowledge and future trends.* Environmental Science-Nano, 2016. **3**(2): p. 323-345.

30. Gottschalk, F. and B. Nowack, *The release of engineered nanomaterials to the environment.* Journal of Environmental Monitoring, 2011. **13**(5): p. 1145-1155.

31. Keller, A.A. and A. Lazareva, *Predicted Releases of Engineered Nanomaterials: From Global to Regional to Local.* Environmental Science & Technology Letters, 2014. **1**(1): p. 65-70.

32. Sun, T.Y., et al., *Dynamic Probabilistic Modeling of Environmental Emissions of Engineered Nanomaterials.* Environmental Science & Technology, 2016. **50**(9): p. 4701-4711.

33. Garner, K.L., S. Suh, and A.A. Keller, *Assessing the Risk of Engineered Nanomaterials in the Environment: Development and Application of the nanoFate Model.* Environmental Science & Technology, 2017. **51**(10): p. 5541-5551.

34. Handy, R.D., et al., *Ecotoxicity test methods for engineered nanomaterials: Practical experiences and recommendations from the bench.* Environmental Toxicology and Chemistry, 2012. **31**(1): p. 15-31.

35. Tourinho, P.S., et al., *Metal-based nanoparticles in soil: Fate, behavior, and effects on soil invertebrates.* Environmental Toxicology and Chemistry, 2012. **31**(8): p. 1679-1692.

36.   Nowack, B., *Chemistry. Nanosilver revisited downstream.* Science, 2010. **330**(6007): p. 1054-5.

37.   Maurer-Jones, M.A., et al., *Toxicity of engineered nanoparticles in the environment.* Anal Chem, 2013. **85**(6): p. 3036-49.

38.   Farrera, C. and B. Fadeel, *It takes two to tango: Understanding the interactions between engineered nanomaterials and the immune system.* Eur J Pharm Biopharm, 2015. **95**(Pt A): p. 3-12.

39.   Chou, C.C., et al., *Single-walled carbon nanotubes can induce pulmonary injury in mouse model.* Nano Letters, 2008. **8**(2): p. 437-445.

40.   Fujita, K., et al., *Gene expression profiles in rat lung after inhalation exposure to C60 fullerene particles.* Toxicology, 2009. **258**(1): p. 47-55.

41.   Geiser, M., et al., *The role of macrophages in the clearance of inhaled ultrafine titanium dioxide particles.* Am J Respir Cell Mol Biol, 2008. **38**(3): p. 371-6.

42.   Herzog, E., et al., *SWCNT suppress inflammatory mediator responses in human lung epithelium in vitro.* Toxicol Appl Pharmacol, 2009. **234**(3): p. 378-90.

43.   Hutter, E., et al., *Microglial response to gold nanoparticles.* ACS Nano, 2010. **4**(5): p. 2595-606.

44.   Li, X., et al., *Silica-induced TNF-alpha and TGF-beta1 expression in RAW264.7 cells are dependent on Src-ERK/AP-1 pathways.* Toxicol Mech Methods, 2009. **19**(1): p. 51-8.

45.   Morishige, T., et al., *Titanium dioxide induces different levels of IL-1beta production dependent on its particle characteristics through caspase-1 activation mediated by reactive oxygen species and cathepsin B.* Biochem Biophys Res Commun, 2010. **392**(2): p. 160-5.

46.   Muller, L., et al., *Oxidative stress and inflammation response after nanoparticle exposure: differences between human lung cell monocultures and an advanced three-dimensional model of the human epithelial airways.* J R Soc Interface, 2010. **7 Suppl 1**: p. S27-40.

47.   Niwa, Y., et al., *Inhalation exposure to carbon black induces inflammatory response in rats.* Circ J, 2008. **72**(1): p. 144-9.

48.   Park, Y.H., et al., *Assessment of dermal toxicity of nanosilica using cultured keratinocytes, a human skin equivalent model and an in vivo model.* Toxicology, 2010. **267**(1-3): p. 178-181.

49.   Yanagisawa, R., et al., *Titanium dioxide nanoparticles aggravate atopic dermatitis-like skin lesions in NC/Nga mice.* Exp Biol Med (Maywood), 2009. **234**(3): p. 314-22.

50.   Ye, S.F., et al., *ROS and NF-kappaB are involved in upregulation of IL-8 in A549 cells exposed to multi-walled carbon nanotubes.* Biochem Biophys Res Commun, 2009. **379**(2): p. 643-8.

51.   Bondarenko, O., et al., *Toxicity of Ag, CuO and ZnO nanoparticles to selected environmentally relevant test organisms and mammalian cells in vitro: a critical review.* Archives of Toxicology, 2013. **87**(7): p. 1181-1200.

52.   Vandebriel, R.J. and W.H. De Jong, *A review of mammalian toxicity of ZnO nanoparticles.* Nanotechnol Sci Appl, 2012. **5**: p. 61-71.

53.   Barua, S. and S. Mitragotri, *Challenges associated with Penetration of Nanoparticles across Cell and Tissue Barriers: A Review of Current Status and Future Prospects.* Nano Today, 2014. **9**(2): p. 223-243.

54.   Dukhin, S.S. and M.E. Labib, *Convective diffusion of nanoparticles from the epithelial barrier toward regional lymph nodes.* Advances in Colloid and Interface Science, 2013. **199**: p. 23-43.

55.   Lucchini, R.G., et al., *Neurological impacts from inhalation of pollutants and the nose-brain connection.* Neurotoxicology, 2012. **33**(4): p. 838-41.

56.   Madl, A.K., et al., *Nanoparticles, lung injury, and the role of oxidant stress.* Annu Rev Physiol, 2014. **76**: p. 447-65.

57.   Ryman-Rasmussen, J.P., J.E. Riviere, and N.A. Monteiro-Riviere, *Penetration of intact skin by quantum dots with diverse physicochemical properties.* Toxicological Sciences, 2006. **91**(1): p. 159-165.

58.   Glista-Baker, E.E., et al., *Nickel Nanoparticles Enhance Platelet-Derived Growth Factor-Induced Chemokine Expression by Mesothelial Cells via Prolonged Mitogen-Activated Protein Kinase Activation.* American Journal of Respiratory Cell and Molecular Biology, 2012. **47**(4): p. 552-561.

59.   Guidetti, G.F., et al., *Nanoparticles induce platelet activation in vitro through stimulation of canonical signalling pathways.* Nanomedicine-Nanotechnology Biology and Medicine, 2012. **8**(8): p. 1329-1336.

60.   Radomski, A., et al., *Nanoparticle-induced platelet aggregation and vascular thrombosis.* Br J Pharmacol, 2005. **146**(6): p. 882-93.

61.   Zhu, M.T., et al., *Particokinetics and extrapulmonary translocation of intratracheally instilled ferric oxide nanoparticles in rats and the potential health risk assessment.* Toxicol Sci, 2009. **107**(2): p. 342-51.

62.   Ruenraroengsak, P., et al., *Respiratory epithelial cytotoxicity and membrane damage (holes) caused by amine-modified nanoparticles.* Nanotoxicology, 2012. **6**(1): p. 94-108.

63.   Mao, Z., et al., *Titanium dioxide nanoparticles alter cellular morphology via disturbing the microtubule dynamics.* Nanoscale, 2015. **7**(18): p. 8466-75.

64.   Nguyen, K.C., et al., *Mitochondrial Toxicity of Cadmium Telluride Quantum Dot Nanoparticles in Mammalian Hepatocytes.* Toxicol Sci, 2015. **146**(1): p. 31-42.

65.   Alarifi, S., D. Ali, and S. Alkahtani, *Nanoalumina induces apoptosis by impairing antioxidant enzyme systems in human hepatocarcinoma cells.* International Journal of Nanomedicine, 2015. **10**.

66.   Avalos, A., et al., *Cytotoxicity and ROS production of manufactured silver nanoparticles of different sizes in hepatoma and leukemia cells.* Journal of Applied Toxicology, 2014. **34**(4): p. 413-423.

67.   Fahmy, B. and S.A. Cormier, *Copper oxide nanoparticles induce oxidative stress and cytotoxicity in airway epithelial cells.* Toxicology in Vitro, 2009. **23**(7): p. 1365-1371.

68.   Manke, A., L. Wang, and Y. Rojanasakul, *Mechanisms of nanoparticle-induced oxidative stress and toxicity.* Biomed Res Int, 2013. **2013**: p. 942916.

69.   Park, E.J. and K. Park, *Oxidative stress and pro-inflammatory responses induced by silica nanoparticles in vivo and in vitro.* Toxicology Letters, 2009. **184**(1): p. 18-25.

70.   Risom, L., P. Moller, and S. Loft, *Oxidative stress-induced DNA damage by particulate air pollution.* Mutation Research-Fundamental and Molecular Mechanisms of Mutagenesis, 2005. **592**(1-2): p. 119-137.

71.   Sarkar, A., M. Ghosh, and P.C. Sil, *Nanotoxicity: Oxidative Stress Mediated Toxicity of Metal and Metal Oxide Nanoparticles.* Journal of Nanoscience and Nanotechnology, 2014. **14**(1): p. 730-743.

72.   Stern, S.T., P.P. Adiseshaiah, and R.M. Crist, *Autophagy and lysosomal dysfunction as emerging mechanisms of nanomaterial toxicity.* Particle and Fibre Toxicology, 2012. **9**.

73.   Gatoo, M.A., et al., *Physicochemical properties of nanomaterials: implication in associated toxic manifestations.* Biomed Res Int, 2014. **2014**: p. 498420.

74. Hemmerich, P.H. and A.H. von Mikecz, *Defining the subcellular interface of nanoparticles by live-cell imaging.* PLoS One, 2013. **8**(4): p. e62018.

75. Huo, S., et al., *Ultrasmall gold nanoparticles as carriers for nucleus-based gene therapy due to size-dependent nuclear entry.* ACS Nano, 2014. **8**(6): p. 5852-62.

76. Nel, A., et al., *Toxic potential of materials at the nanolevel.* Science, 2006. **311**(5761): p. 622-627.

77. Zhang, S., H. Gao, and G. Bao, *Physical Principles of Nanoparticle Cellular Endocytosis.* ACS Nano, 2015. **9**(9): p. 8655-71.

78. De Jong, W.H., et al., *Particle size-dependent organ distribution of gold nanoparticles after intravenous administration.* Biomaterials, 2008. **29**(12): p. 1912-9.

79. Talamini, L., et al., *Influence of Size and Shape on the Anatomical Distribution of Endotoxin-Free Gold Nanoparticles.* ACS Nano, 2017. **11**(6): p. 5519-5529.

80. Zhao, Y., et al., *Interaction of mesoporous silica nanoparticles with human red blood cell membranes: size and surface effects.* ACS Nano, 2011. **5**(2): p. 1366-75.

81. Favi, P.M., et al., *Shape and surface effects on the cytotoxicity of nanoparticles: Gold nanospheres versus gold nanostars.* J Biomed Mater Res A, 2015. **103**(11): p. 3449-62.

82. Hamilton, R.F., et al., *Particle length-dependent titanium dioxide nanomaterials toxicity and bioactivity.* Part Fibre Toxicol, 2009. **6**: p. 35.

83. Ispas, C., et al., *Toxicity and developmental defects of different sizes and shape nickel nanoparticles in zebrafish.* Environ Sci Technol, 2009. **43**(16): p. 6349-56.

84. Kong, B., et al., *Experimental considerations on the cytotoxicity of nanoparticles.* Nanomedicine (Lond), 2011. **6**(5): p. 929-41.

85. Porter, D.W., et al., *Differential mouse pulmonary dose and time course responses to titanium dioxide nanospheres and nanobelts.* Toxicol Sci, 2013. **131**(1): p. 179-93.

86. Zhao, X.X., et al., *Cytotoxicity of hydroxyapatite nanoparticles is shape and cell dependent.* Archives of Toxicology, 2013. **87**(6): p. 1037-1052.

87. El Badawy, A.M., et al., *Surface charge-dependent toxicity of silver nanoparticles.* Environ Sci Technol, 2011. **45**(1): p. 283-7.

88. Schaeublin, N.M., et al., *Surface charge of gold nanoparticles mediates mechanism of toxicity.* Nanoscale, 2011. **3**(2): p. 410-20.

89. Liu, Y.X., et al., *Intracellular dynamics of cationic and anionic polystyrene nanoparticles without direct interaction with mitotic spindle and chromosomes.* Biomaterials, 2011. **32**(32): p. 8291-8303.

90. Huhn, D., et al., *Polymer-coated nanoparticles interacting with proteins and cells: focusing on the sign of the net charge.* ACS Nano, 2013. **7**(4): p. 3253-63.

91. Alexis, F., et al., *Factors affecting the clearance and biodistribution of polymeric nanoparticles.* Mol Pharm, 2008. **5**(4): p. 505-15.

92. Muller, K.H., et al., *pH-dependent toxicity of high aspect ratio ZnO nanowires in macrophages due to intracellular dissolution.* ACS Nano, 2010. **4**(11): p. 6767-79.

93. Yang, H., et al., *Comparative study of cytotoxicity, oxidative stress and genotoxicity induced by four typical nanomaterials: the role of particle size, shape and composition.* J Appl Toxicol, 2009. **29**(1): p. 69-78.

94. Rock, K.L., et al., *The sterile inflammatory response.* Annu Rev Immunol, 2010. **28**: p. 321-42.

95. Alsaleh, N.B. and J.M. Brown, *Immune responses to engineered nanomaterials: current understanding and challenges.* Curr Opin Toxicol, 2018. **10**: p. 8-14.

96. Leso, V., L. Fontana, and I. Iavicoli, *Nanomaterial exposure and sterile inflammatory reactions.* Toxicol Appl Pharmacol, 2018. **355**: p. 80-92.

97.   Akira, S., S. Uematsu, and O. Takeuchi, *Pathogen recognition and innate immunity.* Cell, 2006. **124**(4): p. 783-801.

98.   Fadeel, B., *Clear and present danger? Engineered nanoparticles and the immune system.* Swiss Med Wkly, 2012. **142**: p. w13609.

99.   Baron, L., et al., *The NLRP3 inflammasome is activated by nanoparticles through ATP, ADP and adenosine.* Cell Death & Disease, 2015. **6**.

100.   Hamilton, R.F., et al., *NLRP3 inflammasome activation in murine alveolar macrophages and related lung pathology is associated with MWCNT nickel contamination.* Inhalation Toxicology, 2012. **24**(14): p. 995-1008.

101.   Liang, X., et al., *Reactive oxygen species trigger NF-kappaB-mediated NLRP3 inflammasome activation induced by zinc oxide nanoparticles in A549 cells.* Toxicol Ind Health, 2017. **33**(10): p. 737-745.

102.   Ruiz, P.A., et al., *Titanium dioxide nanoparticles exacerbate DSS-induced colitis: role of the NLRP3 inflammasome.* Gut, 2017. **66**(7): p. 1216-1224.

103.   Yazdi, A.S., et al., *Nanoparticles activate the NLR pyrin domain containing 3 (Nlrp3) inflammasome and cause pulmonary inflammation through release of IL-1alpha and IL-1beta.* Proc Natl Acad Sci U S A, 2010. **107**(45): p. 19449-54.

104.   Jiang, J., J. Pi, and J. Cai, *The Advancing of Zinc Oxide Nanoparticles for Biomedical Applications.* Bioinorg Chem Appl, 2018. **2018**: p. 1062562.

105.   Kent, P., G. Aldous, and M. Blake, *Titanium dioxide and zinc oxide nanoparticles in sunscreen formulations: A study of the post production particle size distribution of particles in a range of commercial emulsion variants.* Australasian Journal of Dermatology, 2010. **51**: p. A31-A31.

106.   Kolodziejczak-Radzimska, A. and T. Jesionowski, *Zinc Oxide-From Synthesis to Application: A Review.* Materials (Basel), 2014. **7**(4): p. 2833-2881.

107.   Sahoo, S., et al., *Effect of zinc oxide nanoparticles as cure activator on the properties of natural rubber and nitrile rubber.* Journal of Applied Polymer Science, 2007. **105**(4): p. 2407-2415.

108.   Newman, M.D., M. Stotland, and J.I. Ellis, *The safety of nanosized particles in titanium dioxide- and zinc oxide-based sunscreens.* J Am Acad Dermatol, 2009. **61**(4): p. 685-92.

109.   Hatamie, A., et al., *Zinc Oxide Nanostructure-Modified Textile and Its Application to Biosensing, Photocatalysis, and as Antibacterial Material.* Langmuir, 2015. **31**(39): p. 10913-10921.

110.   Xiao, F.X., et al., *Spatially branched hierarchical ZnO nanorod-TiO2 nanotube array heterostructures for versatile photocatalytic and photoelectrocatalytic applications: towards intimate integration of 1D-1D hybrid nanostructures.* Nanoscale, 2014. **6**(24): p. 14950-61.

111.   Khan, M.A.M., et al., *Influences of Co doping on the structural and optical properties of ZnO nanostructured.* Applied Physics a-Materials Science & Processing, 2010. **100**(1): p. 45-51.

112.   Zhang, Z.Y. and H.M. Xiong, *Photoluminescent ZnO Nanoparticles and Their Biological Applications.* Materials, 2015. **8**(6): p. 3101-3127.

113.   Malizia, R., et al., *Zinc deficiency and cell-mediated and humoral autoimmunity of insulin-dependent diabetes in thalassemic subjects.* Journal of Pediatric Endocrinology & Metabolism, 1998. **11**: p. 981-984.

114.   Rasmussen, J.W., et al., *Zinc oxide nanoparticles for selective destruction of tumor cells and potential for drug delivery applications.* Expert Opin Drug Deliv, 2010. **7**(9): p. 1063-77.

115. Ilves, M., et al., *Topically applied ZnO nanoparticles suppress allergen induced skin inflammation but induce vigorous IgE production in the atopic dermatitis mouse model.* Particle and Fibre Toxicology, 2014. **11**.

116. Li, J.Q., et al., *ZnO nanoparticles act as supportive therapy in DSS-induced ulcerative colitis in mice by maintaining gut homeostasis and activating Nrf2 signaling.* Scientific Reports, 2017. **7**.

117. Nagajyothi, P.C., et al., *Antioxidant and anti-inflammatory activities of zinc oxide nanoparticles synthesized using Polygala tenuifolia root extract.* Journal of Photochemistry and Photobiology B-Biology, 2015. **146**: p. 10-17.

118. Rajakumar, G., et al., *Green approach for synthesis of zinc oxide nanoparticles from Andrographis paniculata leaf extract and evaluation of their antioxidant, anti-diabetic, and anti-inflammatory activities.* Bioprocess Biosyst Eng, 2018. **41**(1): p. 21-30.

119. Wiegand, C., et al., *Skin-protective effects of a zinc oxide-functionalized textile and its relevance for atopic dermatitis.* Clin Cosmet Investig Dermatol, 2013. **6**: p. 115-21.

120. Xia, T., et al., *Dietary ZnO nanoparticles alters intestinal microbiota and inflammation response in weaned piglets.* Oncotarget, 2017. **8**(39): p. 64878-64891.

121. Yao, S.L., et al., *Antibacterial activity and inflammation inhibition of ZnO nanoparticles embedded TiO2 nanotubes.* Nanotechnology, 2018. **29**(24).

122. Kuschner, W.G., et al., *Pulmonary responses to purified zinc oxide fume.* J Investig Med, 1995. **43**(4): p. 371-8.

123. Kuschner, W.G., et al., *Early pulmonary cytokine responses to zinc oxide fume inhalation.* Environ Res, 1997. **75**(1): p. 7-11.

124. Rohrs, L.C., *Metal-fume fever from inhaling zinc oxide.* AMA Arch Ind Health, 1957. **16**(1): p. 42-7.

125. Fine, J.M., et al., *Metal fume fever: Characterization of clinical and plasma IL-6 responses in controlled human exposures to zinc oxide fume at and below the threshold limit value.* Journal of Occupational and Environmental Medicine, 1997. **39**(8): p. 722-726.

126. Ray, P.D., B.W. Huang, and Y. Tsuji, *Reactive oxygen species (ROS) homeostasis and redox regulation in cellular signaling.* Cell Signal, 2012. **24**(5): p. 981-90.

127. Bishop, G.M., R. Dringen, and S.R. Robinson, *Zinc stimulates the production of toxic reactive oxygen species (ROS) and inhibits glutathione reductase in astrocytes.* Free Radic Biol Med, 2007. **42**(8): p. 1222-30.

128. Song, W., et al., *Role of the dissolved zinc ion and reactive oxygen species in cytotoxicity of ZnO nanoparticles.* Toxicol Lett, 2010. **199**(3): p. 389-97.

129. Wiseman, D.A., et al., *Alterations in zinc homeostasis underlie endothelial cell death induced by oxidative stress from acute exposure to hydrogen peroxide.* Am J Physiol Lung Cell Mol Physiol, 2007. **292**(1): p. L165-77.

130. Chen, J.K., et al., *Particulate nature of inhaled zinc oxide nanoparticles determines systemic effects and mechanisms of pulmonary inflammation in mice.* Nanotoxicology, 2015. **9**(1): p. 43-53.

131. Guo, D., et al., *Reactive oxygen species-induced cytotoxic effects of zinc oxide nanoparticles in rat retinal ganglion cells.* Toxicol In Vitro, 2013. **27**(2): p. 731-8.

132. Yu, K.N., et al., *Zinc oxide nanoparticle induced autophagic cell death and mitochondrial damage via reactive oxygen species generation.* Toxicol In Vitro, 2013. **27**(4): p. 1187-95.

133. Attia, H., H. Nounou, and M. Shalaby, *Zinc Oxide Nanoparticles Induced Oxidative DNA Damage, Inflammation and Apoptosis in Rat's Brain after Oral Exposure.* Toxics, 2018. **6**(2).

134. Lenz, A.G., et al., *Inflammatory and Oxidative Stress Responses of an Alveolar Epithelial Cell Line to Airborne Zinc Oxide Nanoparticles at the Air-Liquid Interface: A Comparison with Conventional, Submerged Cell-Culture Conditions.* Biomed Research International, 2013.

135. Roy, R., et al., *Zinc oxide nanoparticles induce apoptosis by enhancement of autophagy via PI3K/Akt/mTOR inhibition.* Toxicol Lett, 2014. **227**(1): p. 29-40.

136. Sharma, V., D. Anderson, and A. Dhawan, *Zinc oxide nanoparticles induce oxidative DNA damage and ROS-triggered mitochondria mediated apoptosis in human liver cells (HepG2).* Apoptosis, 2012. **17**(8): p. 852-870.

137. Sharma, V., et al., *Induction of oxidative stress, DNA damage and apoptosis in mouse liver after sub-acute oral exposure to zinc oxide nanoparticles.* Mutat Res, 2012. **745**(1-2): p. 84-91.

138. Roy, R., et al., *Toll-like receptor 6 mediated inflammatory and functional responses of zinc oxide nanoparticles primed macrophages.* Immunology, 2014. **142**(3): p. 453-64.

139. Chang, H., et al., *Involvement of MyD88 in zinc oxide nanoparticle-induced lung inflammation.* Experimental and Toxicologic Pathology, 2013. **65**(6): p. 887-896.

140. Wu, W.D., et al., *Phosphorylation of p65 Is Required for Zinc Oxide Nanoparticle-Induced Interleukin 8 Expression in Human Bronchial Epithelial Cells.* Environmental Health Perspectives, 2010. **118**(7): p. 982-987.

141. Roy, R., et al., *Mechanism of uptake of ZnO nanoparticles and inflammatory responses in macrophages require PI3K mediated MAPKs signaling.* Toxicol In Vitro, 2014. **28**(3): p. 457-67.

142. Singh, N., et al., *NanoGenotoxicology: the DNA damaging potential of engineered nanomaterials.* Biomaterials, 2009. **30**(23-24): p. 3891-914.

143. Hackenberg, S., et al., *Genotoxic effects of zinc oxide nanoparticles in nasal mucosa cells are antagonized by titanium dioxide nanoparticles.* Mutat Res Genet Toxicol Environ Mutagen, 2017. **816-817**: p. 32-37.

144. Ickrath, P., et al., *Time-Dependent Toxic and Genotoxic Effects of Zinc Oxide Nanoparticles after Long-Term and Repetitive Exposure to Human Mesenchymal Stem Cells.* Int J Environ Res Public Health, 2017. **14**(12).

145. Pati, R., et al., *Zinc-Oxide Nanoparticles Exhibit Genotoxic, Clastogenic, Cytotoxic and Actin Depolymerization Effects by Inducing Oxidative Stress Responses in Macrophages and Adult Mice.* Toxicol Sci, 2016. **150**(2): p. 454-72.

146. Heim, J., et al., *Genotoxic effects of zinc oxide nanoparticles.* Nanoscale, 2015. **7**(19): p. 8931-8.

147. Uzar, N.K., et al., *Zinc oxide nanoparticles induced cyto- and genotoxicity in kidney epithelial cells.* Toxicol Mech Methods, 2015. **25**(4): p. 334-9.

148. Mann, E.E., et al., *Changes in cardiopulmonary function induced by nanoparticles.* Wiley Interdiscip Rev Nanomed Nanobiotechnol, 2012. **4**(6): p. 691-702.

149. Cheng, W.Y., et al., *An integrated imaging approach to the study of oxidative stress generation by mitochondrial dysfunction in living cells.* Environ Health Perspect, 2010. **118**(7): p. 902-8.

150. Lee, S.J., K.S. Cho, and J.Y. Koh, *Oxidative injury triggers autophagy in astrocytes: the role of endogenous zinc.* Glia, 2009. **57**(12): p. 1351-61.

151. Kim, Y.H., et al., *Alveolar Epithelial Cell Injury Due to Zinc Oxide Nanoparticle Exposure.* American Journal of Respiratory and Critical Care Medicine, 2010. **182**(11): p. 1398-1409.

152. Mihai, C., et al., *Intracellular accumulation dynamics and fate of zinc ions in alveolar epithelial cells exposed to airborne ZnO nanoparticles at the air-liquid interface.* Nanotoxicology, 2015. **9**(1): p. 9-22.

153. Cho, W.S., et al., *Progressive severe lung injury by zinc oxide nanoparticles; the role of Zn2+ dissolution inside lysosomes.* Part Fibre Toxicol, 2011. **8**: p. 27.

154. Huang, K.L., et al., *Zinc oxide nanoparticles induce eosinophilic airway inflammation in mice.* J Hazard Mater, 2015. **297**: p. 304-12.

155. Jacobsen, N.R., et al., *Acute and subacute pulmonary toxicity and mortality in mice after intratracheal instillation of ZnO nanoparticles in three laboratories.* Food Chem Toxicol, 2015. **85**: p. 84-95.

156. Wang, D., et al., *Acute toxicological effects of zinc oxide nanoparticles in mice after intratracheal instillation.* Int J Occup Environ Health, 2017. **23**(1): p. 11-19.

157. Adamcakova-Dodd, A., et al., *Toxicity assessment of zinc oxide nanoparticles using sub-acute and sub-chronic murine inhalation models.* Particle and Fibre Toxicology, 2014. **11**.

158. Gosens, I., et al., *Comparative hazard identification by a single dose lung exposure of zinc oxide and silver nanomaterials in mice.* PLoS One, 2015. **10**(5): p. e0126934.

159. Jain, S., et al., *Pulmonary fibrotic response to inhalation of ZnO nanoparticles and toluene co-exposure through directed flow nose only exposure chamber.* Inhalation Toxicology, 2013. **25**(13): p. 703-713.

160. Yoo, J., et al., *Evaluation of Recovery from Acute Lung Injury Induced by Intratracheal Instillation of Zinc Oxide Nanoparticles.* Applied Ecology and Environmental Research, 2018. **16**(3): p. 3145-3157.

161. Zhang, Y., et al., *Immune responses during single and repeated murine endotracheal exposures of zinc oxide nanoparticles.* Nanoimpact, 2017. **7**: p. 54-65.

162. Baek, M., et al., *Pharmacokinetics, tissue distribution, and excretion of zinc oxide nanoparticles.* Int J Nanomedicine, 2012. **7**: p. 3081-97.

163. Esmaeillou, M., et al., *Toxicity of ZnO nanoparticles in healthy adult mice.* Environ Toxicol Pharmacol, 2013. **35**(1): p. 67-71.

164. Monse, C., et al., *Concentration-dependent systemic response after inhalation of nano-sized zinc oxide particles in human volunteers.* Part Fibre Toxicol, 2018. **15**(1): p. 8.

165. Saptarshi, S.R., A. Duschl, and A.L. Lopata, *Biological reactivity of zinc oxide nanoparticles with mammalian test systems: an overview.* Nanomedicine (Lond), 2015. **10**(13): p. 2075-92.

166. Xia, T., et al., *Dietary ZnO nanoparticles alters intestinal microbiota and inflammation response in weaned piglets.* Oncotarget, 2017. **8**(39): p. 64878-64891.

167. Ilinskaya, A.N. and M.A. Dobrovolskaia, *Immunosuppressive and anti-inflammatory properties of engineered nanomaterials.* Br J Pharmacol, 2014. **171**(17): p. 3988-4000.

168. Mogensen, T.H., *Pathogen recognition and inflammatory signaling in innate immune defenses.* Clinical Microbiology Reviews, 2009. **22**(2): p. 240–273.

169. Aderem, A. and D.M. Underhill, *Mechanisms of phagocytosis in macrophages.* Annu Rev Immunol, 1999. **17**: p. 593-623.

170. Roy, R., et al., *Cytotoxicity and uptake of zinc oxide nanoparticles leading to enhanced inflammatory cytokines levels in murine macrophages: comparison with bulk zinc oxide.* J Biomed Nanotechnol, 2011. **7**(1): p. 110-1.

171. Kawai, T. and S. Akira, *The role of pattern-recognition receptors in innate immunity: update on Toll-like receptors.* Nat Immunol, 2010. **11**(5): p. 373-84.

172. Davies, L.C. and P.R. Taylor, *Tissue-resident macrophages: then and now.* Immunology, 2015. **144**(4): p. 541-548.

173. Vlahos, R. and S. Bozinovski, *Role of alveolar macrophages in chronic obstructive pulmonary disease.* Frontiers in Immunology, 2014. **5**.

174. Holian, A., K. Kelley, and R.F. Hamilton, *Mechanisms Associated with Human Alveolar Macrophage Stimulation by Particulates.* Environmental Health Perspectives, 1994. **102**: p. 69-74.

175. Lin, C.D., et al., *Zinc oxide nanoparticles impair bacterial clearance by macrophages.* Nanomedicine (Lond), 2014. **9**(9): p. 1327-39.

176. Simon-Vazquez, R., et al., *Analysis of the activation routes induced by different metal oxide nanoparticles on human lung epithelial cells.* Future Science Oa, 2016. **2**(2).

177. Sahu, D., et al., *Nanosized zinc oxide induces toxicity in human lung cells.* ISRN Toxicol, 2013. **2013**: p. 316075.

178. Lenz, A.G., et al., *Inflammatory and oxidative stress responses of an alveolar epithelial cell line to airborne zinc oxide nanoparticles at the air-liquid interface: a comparison with conventional, submerged cell-culture conditions.* Biomed Res Int, 2013. **2013**: p. 652632.

179. Roy, R., et al., *Zinc oxide nanoparticles provide an adjuvant effect to ovalbumin via a Th2 response in Balb/c mice.* Int Immunol, 2014. **26**(3): p. 159-72.

180. Park, Y.M. and B.S. Bochner, *Eosinophil survival and apoptosis in health and disease.* Allergy Asthma Immunol Res, 2010. **2**(2): p. 87-101.

181. Acharya, K.R. and S.J. Ackerman, *Eosinophil granule proteins: form and function.* J Biol Chem, 2014. **289**(25): p. 17406-15.

182. Bandeira-Melo, C., et al., *Cutting edge: eotaxin elicits rapid vesicular transport-mediated release of preformed IL-4 from human eosinophils.* J Immunol, 2001. **166**(8): p. 4813-7.

183. Miyamasu, M., et al., *Chemotactic agonists induce cytokine generation in eosinophils.* J Immunol, 1995. **154**(3): p. 1339-49.

184. Spencer, L.A., et al., *Human eosinophils constitutively express multiple Th1, Th2, and immunoregulatory cytokines that are secreted rapidly and differentially.* Journal of Leukocyte Biology, 2009. **85**(1): p. 117-123.

185. Behm, C.A. and K.S. Ovington, *The role of eosinophils in parasitic helminth infections: insights from genetically modified mice.* Parasitol Today, 2000. **16**(5): p. 202-9.

186. Butterworth, A.E., *The eosinophil and its role in immunity to helminth infection.* Curr Top Microbiol Immunol, 1977. **77**: p. 127-68.

187. Barthel, S.R., et al., *Dissection of the hyperadhesive phenotype of airway eosinophils in asthma.* Am J Respir Cell Mol Biol, 2006. **35**(3): p. 378-86.

188. Kay, A.B., S. Phipps, and D.S. Robinson, *A role for eosinophils in airway remodelling in asthma.* Trends Immunol, 2004. **25**(9): p. 477-82.

189. Gouon-Evans, V., M.E. Rothenberg, and J.W. Pollard, *Postnatal mammary gland development requires macrophages and eosinophils.* Development, 2000. **127**(11): p. 2269-82.

190. Robertson, S.A., et al., *Cytokine-leukocyte networks and the establishment of pregnancy.* Am J Reprod Immunol, 1997. **37**(6): p. 438-42.

191. Hoshino, M., M. Takahashi, and N. Aoike, *Expression of vascular endothelial growth factor, basic fibroblast growth factor, and angiogenin immunoreactivity in asthmatic airways and its relationship to angiogenesis.* Journal of Allergy and Clinical Immunology, 2001. **107**(2): p. 295-301.

192. Puxeddu, A., et al., *Human peripheral blood eosinophils induce angiogenesis.* International Journal of Biochemistry & Cell Biology, 2005. **37**(3): p. 628-636.

193. Todd, R., et al., *The Eosinophil as a Cellular Source of Transforming Growth Factor-Alpha in Healing Cutaneous Wounds.* American Journal of Pathology, 1991. **138**(6): p. 1307-1313.

194. Jacobsen, E.A., et al., *Allergic pulmonary inflammation in mice is dependent on eosinophil-induced recruitment of effector T cells.* Journal of Experimental Medicine, 2008. **205**(3): p. 699-710.

195. Wang, H. and P. Weller, *Eosinophils mediate early alum adjuvant-elicited B cell priming and IgM production.* Clinical Immunology, 2008. **127**: p. S3-S3.

196. Chu, V.T., et al., *Eosinophils are required for the maintenance of plasma cells in the bone marrow.* Nat Immunol, 2011. **12**(2): p. 151-9.

197. Lehrer, R.I., et al., *Antibacterial properties of eosinophil major basic protein and eosinophil cationic protein.* J Immunol, 1989. **142**(12): p. 4428-34.

198. Linch, S.N., et al., *Mouse eosinophils possess potent antibacterial properties in vivo.* Infect Immun, 2009. **77**(11): p. 4976-82.

199. Persson, T., et al., *Bactericidal activity of human eosinophilic granulocytes against Escherichia coli.* Infect Immun, 2001. **69**(6): p. 3591-6.

200. Inoue, Y., et al., *Nonpathogenic, environmental fungi induce activation and degranulation of human eosinophils.* J Immunol, 2005. **175**(8): p. 5439-47.

201. Yoon, J., et al., *Innate antifungal immunity of human eosinophils mediated by a beta 2 integrin, CD11b.* J Immunol, 2008. **181**(4): p. 2907-15.

202. Cormier, S.A., et al., *Pivotal advance: Eosinophil infiltration of solid tumors is an early and persistent inflammatory host response.* Journal of Leukocyte Biology, 2006. **79**(6): p. 1131-1139.

203. Silva, L.R. and D. Girard, *Human eosinophils are direct targets to nanoparticles: Zinc oxide nanoparticles (ZnO) delay apoptosis and increase the production of the pro-inflammatory cytokines IL-1beta and IL-8.* Toxicol Lett, 2016. **259**: p. 11-20.

204. Kozak, W., et al., *IL-6 and IL-1 beta in fever - Studies using cytokine-deficient (knockout) mice.* Molecular Mechanisms of Fever, 1998. **856**: p. 33-47.

205. Kokkonen, H., et al., *Up-regulation of cytokines and chemokines predates the onset of rheumatoid arthritis.* Arthritis Rheum, 2010. **62**(2): p. 383-91.

206. Scheller, J., et al., *The pro- and anti-inflammatory properties of the cytokine interleukin-6.* Biochim Biophys Acta, 2011. **1813**(5): p. 878-88.

207. Ksontini, R., S.L. MacKay, and L.L. Moldawer, *Revisiting the role of tumor necrosis factor alpha and the response to surgical injury and inflammation.* Arch Surg, 1998. **133**(5): p. 558-67.

208. Genestra, M., *Oxyl radicals, redox-sensitive signalling cascades and antioxidants.* Cell Signal, 2007. **19**(9): p. 1807-19.

209. Chang, H., et al., *Involvement of MyD88 in zinc oxide nanoparticle-induced lung inflammation.* Exp Toxicol Pathol, 2013. **65**(6): p. 887-96.

210. Hanley, C., et al., *The Influences of Cell Type and ZnO Nanoparticle Size on Immune Cell Cytotoxicity and Cytokine Induction.* Nanoscale Res Lett, 2009. **4**(12): p. 1409-20.

211. Zhang, J.A., L. Patel, and K.J. Pienta, *Targeting Chemokine (C-C motif) Ligand 2 (CCL2) as an Example of Translation of Cancer Molecular Biology to the Clinic.* Molecular Biology of Cancer: Translation to the Clinic, 2010. **95**: p. 31-53.

212. Niu, J.L. and P.E. Kolattukudy, *Role of MCP-1 in cardiovascular disease: molecular mechanisms and clinical implications.* Clinical Science, 2009. **117**(3-4): p. 95-109.

213. Woo, H.M., et al., *Active spice-derived components can inhibit inflammatory responses of adipose tissue in obesity by suppressing inflammatory actions of macrophages and*

release of monocyte chemoattractant protein-1 from adipocytes. Life Sciences, 2007. **80**(10): p. 926-931.

214. Blanco-Alvarez, V.M., et al., *Prophylactic Subacute Administration of Zinc Increases CCL2, CCR2, FGF2, and IGF-1 Expression and Prevents the Long-Term Memory Loss in a Rat Model of Cerebral Hypoxia-Ischemia.* Neural Plast, 2015. **2015**: p. 375391.

215. Sahu, D., G.M. Kannan, and R. Vijayaraghavan, *Size-dependent effect of zinc oxide on toxicity and inflammatory potential of human monocytes.* J Toxicol Environ Health A, 2014. **77**(4): p. 177-91.

216. Jose, P.J., et al., *Eotaxin: a potent eosinophil chemoattractant cytokine detected in a guinea pig model of allergic airways inflammation.* J Exp Med, 1994. **179**(3): p. 881-7.

217. Humbles, A.A., et al., *Kinetics of eotaxin generation and its relationship to eosinophil accumulation in allergic airways disease: analysis in a guinea pig model in vivo.* J Exp Med, 1997. **186**(4): p. 601-12.

218. Li, D., et al., *Eotaxin protein and gene expression in guinea-pig lungs: constitutive expression and upregulation after allergen challenge.* Eur Respir J, 1997. **10**(9): p. 1946-54.

219. Conroy, D.M. and T.J. Williams, *Eotaxin and the attraction of eosinophils to the asthmatic lung.* Respiratory Research, 2001. **2**(3): p. 150-156.

220. Corrigan, C.J., *Eotaxin and asthma: some answers, more questions.* Clinical and Experimental Immunology, 1999. **116**(1): p. 1-3.

221. Saptarshi, S.R., et al., *Investigating the immunomodulatory nature of zinc oxide nanoparticles at sub-cytotoxic levels in vitro and after intranasal instillation in vivo.* J Nanobiotechnology, 2015. **13**: p. 6.

222. Murphy, F.A., et al., *Length-dependent retention of carbon nanotubes in the pleural space of mice initiates sustained inflammation and progressive fibrosis on the parietal pleura.* Am J Pathol, 2011. **178**(6): p. 2587-600.

223. Rydman EM, I.M., Koivisto AJ, Kinaret PA, Fortino V, Savinko TS, ... Alenius H. , *Inhalation of rod-like carbon nanotubes causes unconventional allergic airway inflammation. .* Particle And Fibre Toxicology, (2014). . **11, 48. doi:10.1186/s12989-014-0048-2**

224. Xia, T., et al., *Comparison of the mechanism of toxicity of zinc oxide and cerium oxide nanoparticles based on dissolution and oxidative stress properties.* ACS Nano, 2008. **2**(10): p. 2121-34.

225. Bonner, J.C., et al., *Interlaboratory evaluation of rodent pulmonary responses to engineered nanomaterials: the NIEHS Nano GO Consortium.* Environ Health Perspect, 2013. **121**(6): p. 676-82.

226. Saber, A.T., et al., *Particle-induced pulmonary acute phase response correlates with neutrophil influx linking inhaled particles and cardiovascular risk.* PLoS One, 2013. **8**(7): p. e69020.

227. Hackenberg, S. and N. Kleinsasser, *Dermal toxicity of ZnO nanoparticles: a worrying feature of sunscreen?* Nanomedicine (Lond), 2012. **7**(4): p. 461-3.

228. Monteiro-Riviere, N.A., et al., *Safety evaluation of sunscreen formulations containing titanium dioxide and zinc oxide nanoparticles in UVB sunburned skin: an in vitro and in vivo study.* Toxicol Sci, 2011. **123**(1): p. 264-80.

229. Cross, S.E., et al., *Human skin penetration of sunscreen nanoparticles: in-vitro assessment of a novel micronized zinc oxide formulation.* Skin Pharmacol Physiol, 2007. **20**(3): p. 148-54.

230. Lademann, J., et al., *Investigation of follicular penetration of topically applied substances.* Skin Pharmacol Appl Skin Physiol, 2001. **14 Suppl 1**: p. 17-22.

231. Zvyagin, A.V., et al., *Imaging of zinc oxide nanoparticle penetration in human skin in vitro and in vivo.* J Biomed Opt, 2008. **13**(6): p. 064031.

232. Hegde, B., et al., *Inflammasome-Independent Leukotriene B4 Production Drives Crystalline Silica-Induced Sterile Inflammation.* J Immunol, 2018. **200**(10): p. 3556-3567.

233. Hornung, V., et al., *Silica crystals and aluminum salts activate the NALP3 inflammasome through phagosomal destabilization.* Nature Immunology, 2008. **9**(8): p. 847-856.

234. Cho, W.S., et al., *Metal oxide nanoparticles induce unique inflammatory footprints in the lung: important implications for nanoparticle testing.* Environ Health Perspect, 2010. **118**(12): p. 1699-706.

235. Asgharian, B., et al., *Dosimetry of inhaled elongate mineral particles in the respiratory tract: The impact of shape factor.* Toxicol Appl Pharmacol, 2018. **361**: p. 27-35.

236. Rahman, L., et al., *Multi-walled carbon nanotube-induced genotoxic, inflammatory and pro-fibrotic responses in mice: Investigating the mechanisms of pulmonary carcinogenesis.* Mutat Res, 2017. **823**: p. 28-44.

237. Rola-Pleszczynski, M., S. Gouin, and R. Begin, *Asbestos-induced lung inflammation. Role of local macrophage-derived chemotactic factors in accumulation of neutrophils in the lungs.* Inflammation, 1984. **8**(1): p. 53-62.

238. Park, E.J., et al., *Pro-inflammatory and potential allergic responses resulting from B cell activation in mice treated with multi-walled carbon nanotubes by intratracheal instillation.* Toxicology, 2009. **259**(3): p. 113-21.

239. Larsen, S.T., et al., *Nano titanium dioxide particles promote allergic sensitization and lung inflammation in mice.* Basic Clin Pharmacol Toxicol, 2010. **106**(2): p. 114-7.

240. Lee, S., et al., *Nickel oxide nanoparticles can recruit eosinophils in the lungs of rats by the direct release of intracellular eotaxin.* Particle and Fibre Toxicology, 2016. **13**.

241. Rydman, E.M., et al., *Inhalation of rod-like carbon nanotubes causes unconventional allergic airway inflammation.* Particle and Fibre Toxicology, 2014. **11**.

242. Jeng, H.A. and J. Swanson, *Toxicity of metal oxide nanoparticles in mammalian cells.* J Environ Sci Health A Tox Hazard Subst Environ Eng, 2006. **41**(12): p. 2699-711.

243. Deng, X., et al., *Nanosized zinc oxide particles induce neural stem cell apoptosis.* Nanotechnology, 2009. **20**(11): p. 115101.

244. Wong, S.W., et al., *Toxicities of nano zinc oxide to five marine organisms: influences of aggregate size and ion solubility.* Anal Bioanal Chem, 2010. **396**(2): p. 609-18.

245. Huotari, J. and A. Helenius, *Endosome maturation.* EMBO J, 2011. **30**(17): p. 3481-500.

246. Zhang, J., et al., *Zinc oxide nanoparticles harness autophagy to induce cell death in lung epithelial cells.* Cell Death Dis, 2017. **8**(7): p. e2954.

247. Kang, B., et al., *Cell response to carbon nanotubes: size-dependent intracellular uptake mechanism and subcellular fate.* Small, 2010. **6**(21): p. 2362-6.

248. Kettler, K., et al., *Uptake of silver nanoparticles by monocytic THP-1 cells depends on particle size and presence of serum proteins.* J Nanopart Res, 2016. **18**(9): p. 286.

249. Kettler, K., et al., *Cellular uptake of nanoparticles as determined by particle properties, experimental conditions, and cell type.* Environmental Toxicology and Chemistry, 2014. **33**(3): p. 481-492.

250. Nativo, P., I.A. Prior, and M. Brust, *Uptake and intracellular fate of surface-modified gold nanoparticles.* Acs Nano, 2008. **2**(8): p. 1639-1644.

251. Oh, N. and J.H. Park, *Endocytosis and exocytosis of nanoparticles in mammalian cells.* Int J Nanomedicine, 2014. **9 Suppl 1**: p. 51-63.

252. Raynal, I., et al., *Macrophage endocytosis of superparamagnetic iron oxide nanoparticles - Mechanisms and comparison of Ferumoxides and Ferumoxtran-10.* Investigative Radiology, 2004. **39**(1): p. 56-63.

253. Dean, K.M., Y. Qin, and A.E. Palmer, *Visualizing metal ions in cells: an overview of analytical techniques, approaches, and probes.* Biochim Biophys Acta, 2012. **1823**(9): p. 1406-15.

254. Heng, B.C., et al., *Evaluation of the cytotoxic and inflammatory potential of differentially shaped zinc oxide nanoparticles.* Arch Toxicol, 2011. **85**(12): p. 1517-28.

255. Jeong, S.H., et al., *ZnO nanoparticles induce TNF-alpha expression via ROS-ERK-Egr-1 pathway in human keratinocytes.* J Dermatol Sci, 2013. **72**(3): p. 263-73.

256. Wu, Y. and B.P. Zhou, *TNF-alpha/NF-kappa B/Snail pathway in cancer cell migration and invasion.* British Journal of Cancer, 2010. **102**(4): p. 639-644.

257. Rosenberg, H.F., K.D. Dyer, and P.S. Foster, *Eosinophils: changing perspectives in health and disease.* Nat Rev Immunol, 2013. **13**(1): p. 9-22.

258. Bostrom, E.A., et al., *Increased Eotaxin and MCP-1 Levels in Serum from Individuals with Periodontitis and in Human Gingival Fibroblasts Exposed to Pro-Inflammatory Cytokines.* PLoS One, 2015. **10**(8): p. e0134608.

259. Penido, C., et al., *Inhibition of allergen-induced eosinophil recruitment by natural tetranortriterpenoids is mediated by the suppression of IL-5, CCL11/eotaxin and NFkappaB activation.* Int Immunopharmacol, 2006. **6**(2): p. 109-21.

260. Simko, M. and M.O. Mattsson, *Interactions Between Nanosized Materials and the Brain.* Current Medicinal Chemistry, 2014. **21**(37): p. 4200-4214.

261. Zhao, C.M. and W.X. Wang, *Size-dependent uptake of silver nanoparticles in Daphnia magna.* Environ Sci Technol, 2012. **46**(20): p. 11345-51.

ABBREVIATIONS

NM: Nanometer

ENMs: Engineered nanomaterials

ENPs: Engineered nanoparticles

TiO_2NP: Titanium dioxide nanoparticle

CeO_2NP: Cerium dioxide nanoparticle

Al_2O_3NP: Aluminum oxide nanoparticle

SiONP: Silicon dioxide nanoparticle

ZnONP: Zinc oxide nanoparticle

CNT: Carbon nanotubes

CS: Crystalline silica

ROS: Reactive oxygen species

DNA: Deoxyribonucleic acid

TWA: Time weighted average

STEL: short-term exposure limit

RNS: Reactive nitrogen species

DAMP: Damage-associated molecular patterns

HMGB-1: High mobility group box 1 protein

IL-1β: Interleukin-1beta

TNF-α: Tumor necrosis factor alpha

Nrf2: Nuclear factor (erythroid-derived 2)-like 2

MAPK: Mitogen activated protein kinase

NF-κB: Nuclear factor kappa-light-chain enhancer of activated B cells

iNOS: Inducible nitric oxide synthase

ERKs: Extracellular signal-related kinases

LDH: Lactate dehydrogenase

HOCl: Hypochlorous acid

ONOO−: Peroxynitrite

AM: Alveolar macrophages

HARN: High aspect ratio nanomaterials

PARP: Poly-ADP-ribose polymerase

TLR6: Toll-like receptor 6

OVA: Allergen ovalbumin

BALF: Bronchial alveolar lavage fluids

CRP: Acute phase proteins

SSR: Signal sequence receptor

PRP: Pattern recognition protein

SR: Scavenger receptor

MR: Mannose receptor

CR: Complement receptor

COPD: Chronic obstructive pulmonary diseases

NTHi: Haemophilus influenza

MBP: Major basic protein

EPO: Eosinophil peroxidase

EDN: Eosinophil-derived neurotoxin

H&E: Hematoxylin and eosin

Th2: T helper 2 cells

HMMs: Human monocyte macrophages

H_2O_2: Hydrogen peroxide

$O_2\cdot$ Superoxideanion

$OH\cdot$: Hydroxylradical

$^1O_2$: Singlet oxygen

MCP-1: Monocyte Chemoattractant protein 1

CCL11: Chemokine 11 or eosinophil chemotactic protein

BMDM: Bone marrow derived macrophage

RAW 264.7: Macrophage-like, Abelson leukemia virus cells

LKR13: Murine K-ras mutant lung adenocarcinoma cell line

LPS: Lipopolysaccharide

EE: Early endosome

LE: Late endosome

Baf-A1: Bafilomycin-A1

Cyt D: Cytocholasin D

MTT: Methylthiazol Tetrazolium Assay

CURRICULUM VITAE

Ruqaih Salem Alghsham

rsalgh01@louisville.edu   419-651-5002

EDUCATION

Ph.D., Microbiology and Immunology, University of Louisville, KY   2012-Present

M.S., Microbiology and Immunology, University of Louisville, KY   2014-2016

B.S., Clinical Laboratory Sciences, KAU, Jeddah, KSA   2004-2009

RESEARCH EXPERIENCE

Graduate Research Assistant   **2014-Present**

Department of Microbiology and Immunology, School of Medicine, University of Louisville

Dissertation Chair: Haribabu Boudduluri Ph.D.

Project: ZnONWs induce a distinct pattern of inflammation *in vivo* and *in vitro*.

- Performed in-vivo studies to investigate the potential biological effect of ZnONWs and ability to induce sterile inflammation.

- Performed ex-vivo studies to understand the cellular mechanisms activated in ZnONWs inducing sterile inflammation.

- Resolved technical problems associated with ex-vivo experiment related to nanoparticle physicochemical properties.

- Trained and supervised summer trainees in basic cell culture and immunology techniques

- Study contributes to understanding the interaction of ZnONWs with immune system and their potential to induce sterile inflammation.

TECHNICAL RESEARCH EXPERTISE

Mouse model of inflammation	Immunohistochemistry
Agarose gel electrophoresis	Subset isolation of leukocytes from peripheral blood
Polyacrylamide gel electrophoresis	H& E Staining
qRT-PCR	ELISA
Mammalian cell culture	Western blotting
Scientific Writing	Cytotoxicity assays
Primer design	GraphPad Prism
Microscopy	Multicolor flow-cytometry

PUBLICATIOS

Hegde B, Bodduluri SR, Satpathy SR, **Alghsham RS**, Jala VR, Uriarte SM, Chen D, Lawrenz MB, Haribabu B. Inflammasome independent leukotriene-B4 production drives crystalline silica induced sterile inflammation. J Immunol. 2018 Apr 2.pii:ji1701504.doi: 10.4049/jimmunol.1701504.

MANUSCRIPTS UNDER PREPARATION

Alghsham RS, Bodduluri SR, Satpathy SR, Hegde B, Jala VR, Sunkara M, Haribabu B. eosinophilic inflammation induce by ZnONWs in mouse animal model. Frontiers in immunology.

Conferences & symposiums

Leadership and communication skills workshop	2019
Critical thinking workshop	2019
Introduction to Academic leadership	2018
Research Louisville	2017
The American Association of Immunologists Conference	2017
Tutor training workshop	2011
5th Applied Medical Sciences Student's Meeting	2009
Laboratory total quality management	2009
Microbiology laboratory Day	2008
The Advance in Laboratory Medicine	2007

POSTER PRESENTATIONS

Alghsham RS, Satpathy SR, et. al. distinct inflammatory pathways induced by ZnONWs. Research! Louisville2016, Louisville, USA, September 2017

WORK EXPERIENCE

- Medical Technologist II at molecular diagnostic lab King Abdul-Aziz University hospital in Jeddah
- Medical Technologist II at immunology lab King Abdul-Aziz University Hospital in Jeddah
- Medical Technologist II at virology lab King Abdul-Aziz University Hospital in Jeddah
- Teaching assistant at Alqassim University from 2010 to 2015.
- Lecturer at Alqassim University from 2016 currant
- Vice president of women affair at university of Louisville Saudi student association 2016.

- Vice president of women affair at university of Louisville Saudi student association 2017.
- President of Louisville Saudi student association 2018.

HONORS AND AWARDS

- Award for dedication and outstanding effort as president of Saudi student association at university of Louisville (2018-2019).

- Award for dedication and outstanding effort as vice president of Saudi student association at university of Louisville (2017-2018).

- Award and recognition for valuable participation to the activities of the Saudi association at Louisville University (2017-2018).

- Award for dedication and outstanding effort as vice president of Saudi student association at university of Louisville (2016-2017).

- Best student of the year, ACCESS English program, university of Ashland, Ashland, OH (2013-2014).

- The intern of the year at King Abdul Aziz university hospital laboratories, Jeddah, KSA (2009-2010).

- Award for excellence from King Abdul-Aziz University (2007-2008).

- Award for excellence from King Abdul-Aziz University (2006-2007).

- Award for excellence from King Abdul-Aziz University (2005-2006).